



HAL
open science

Exploring the plasticity of the InhA substrate-binding site using new diaryl ether inhibitors

Rasoul Tamhaev, Emeline Grosjean, Hikmat Ahamed, Mélina Chebaiki, Deborah Recchia, Giulia Degiacomi, Maria Rosalia Pasca, Laurent Maveyraud, Lionel Mourey, Frédéric Rodriguez, et al.

► To cite this version:

Rasoul Tamhaev, Emeline Grosjean, Hikmat Ahamed, Mélina Chebaiki, Deborah Recchia, et al.. Exploring the plasticity of the InhA substrate-binding site using new diaryl ether inhibitors. *Bioorganic Chemistry*, 2024, 143, pp.107032. 10.1016/j.bioorg.2023.107032 . hal-04389877

HAL Id: hal-04389877

<https://hal.science/hal-04389877v1>

Submitted on 16 Oct 2024

HAL is a multi-disciplinary open access archive for the deposit and dissemination of scientific research documents, whether they are published or not. The documents may come from teaching and research institutions in France or abroad, or from public or private research centers.

L'archive ouverte pluridisciplinaire **HAL**, est destinée au dépôt et à la diffusion de documents scientifiques de niveau recherche, publiés ou non, émanant des établissements d'enseignement et de recherche français ou étrangers, des laboratoires publics ou privés.

Highlights

- Design and synthesis of new diaryl ether derivatives that target InhA.
- Bis-diaryl ethers with improved activity against the enzyme.
- Crystal structure of InhA-NAD⁺ in complex with the most potent compound.
- Structural analysis revealed the protein adaptability to relatively large inhibitors.
- Opening of the minor portal underlines molecular plasticity.

Exploring the plasticity of the InhA substrate-binding site using new diaryl ether inhibitors

Rasoul Tamhaev,^{a,b} Emeline Grosjean,^a Hikmat Ahamed,^a Mélina Chebaiki,^{a,b} Frédéric Rodriguez,^a Deborah Recchia,^c Giulia Degiacomi,^c Maria Rosalia Pasca,^c Laurent Maveyraud,^{b,*} Lionel Mourey,^{b,**} Christian Lherbet^{a,***}

^a Synthèse et Physico-Chimie de Molécules d'Intérêt Biologique (LSPCMIB), UMR 5068, CNRS, Université Toulouse III – Paul Sabatier (UT3), Toulouse, France

^b Institut de Pharmacologie et de Biologie Structurale (IPBS), Université de Toulouse, CNRS, Université Toulouse III – Paul Sabatier (UT3), Toulouse, France.

^c Department of Biology and Biotechnology “Lazzaro Spallanzani”, University of Pavia, 27100 Pavia, Italy.

* Corresponding author.

** Corresponding author.

*** Corresponding author.

Email addresses laurent.maveyraud@ipbs.fr (L. Maveyraud), lionel.mourey@ipbs.fr (L. Mourey), christian.lherbet@univ-tlse3.fr (C. Lherbet).

Keywords: tuberculosis, InhA, minor portal, inhibitors, diaryl ethers, X-ray crystallography

Abstract

Tuberculosis (TB), caused by *Mycobacterium tuberculosis* (Mtb), remains a worldwide scourge with more than 10 million people affected yearly. Among the proteins essential for the survival of Mtb, InhA has been and is still clinically validated as a therapeutic target. A new family of diaryl ethers has been designed with the ambition of fully occupying the InhA substrate-binding site. Thus, eleven compounds, featuring three pharmacophores within the same molecule, were synthesized. One of them, compound **21**, showed good inhibitory activity against InhA. The crystal structure of compound **21** in complex with InhA/NAD⁺ showed how the molecule fills the substrate-binding site as well as the minor portal of InhA. This study represents a further step towards the design of new inhibitors of InhA.

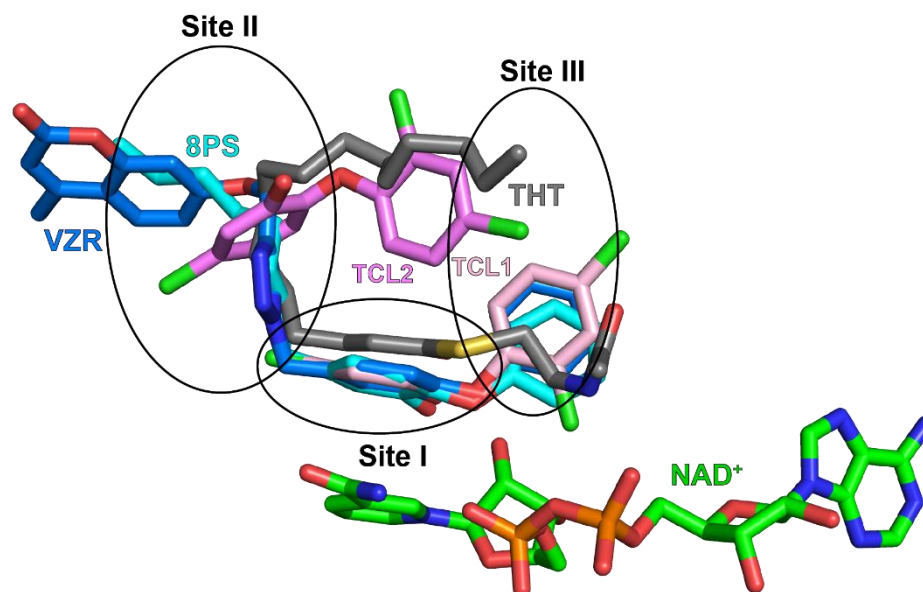
1. Introduction

According to the recent World Health Organization (WHO) report, Tuberculosis (TB) caused by *Mycobacterium tuberculosis* (Mtb) affects nearly 10 million people each year worldwide and remains one of the leading causes of death due to a single infectious agent [1]. Emergence of multidrug-resistant (MDR) and of extensively drug-resistant (XDR) TB augurs for a growing incidence, leading to an increasing number of victims. In the last 60 years, no new anti-TB drugs have been approved by the US-FDA for MDR-TB treatment with the exception of bedaquiline, delamanid and pretomanid, for which resistances are already emerging [2]. Therefore, there is a real need for new drugs capable of eradicating TB.

Mycobacteria present a unique cell wall that acts as a barrier to antibiotics. Biosynthetic pathways of cell wall components, such as mycolic acids, are very attractive targets for the development of antitubercular drugs. In that respect, enzymes belonging to the type II Fatty Acid Synthesis (FAS-II) system required for the mycolic acid biosynthesis are essential for mycobacterial survival [3]. As such, they represent privileged targets for the discovery of new anti-TB drugs [4]. Among them, InhA catalyzes the reduction by the cofactor NADH of the double bond at position 2 of growing *trans*-2-enoyl-ACP substrates. InhA is the primary target of isoniazid (INH), a first-line anti-TB drug and one of the most effective compounds to treat TB. INH acts as a prodrug requiring activation by KatG, a catalase-peroxidase, to generate the adduct INH-NAD that inhibits InhA [5, 6]. Since the beginning of the clinical use of INH, resistances to this antibiotic have been observed, mainly through mutations in the activating enzyme KatG [7] and less commonly in InhA. Consequently, the discovery of direct inhibitors of InhA that do not require pre-activation by KatG is crucial. Only a limited set of potent direct inhibitors with activity against INH-resistant and wild-type strains of Mtb have been identified [8]. These include triclosan (TCL), a highly effective broad-spectrum diaryl ether antibacterial agent, and its analogues, some of which have shown promising activities against InhA [9-14].

The substrate-binding site of InhA can be divided in three distinct sites as illustrated in **Figure 1** [15, 16]. Site I corresponds to the catalytic site. Site II corresponds to a hydrophobic pocket where sits the aliphatic chain of the substrate, as exemplified by the structure of InhA/NAD⁺ with a C16 fatty acyl substrate analogue (ligand ID THT in PDB 1BVR, chain A) [6]. Site III is solvent-exposed and narrows the size of the entrance of the protein at the so-called major portal. It is noteworthy that in the X-ray structure reported for the InhA/NAD⁺/TCL complex (ligand ID TCL in PDB 1P45, chain A), two molecules of TCL were found to bind within the substrate-binding site of InhA [17] (**Figure 1**). One TCL molecule (TCL1) occupies site I and part of site III and shows close contacts with the cofactor and with Tyr158, which belongs together with Phe149 and Lys165 to the catalytic triad of InhA. The second TCL molecule (TCL2) binds to the hydrophobic pocket defined by site II. The presence of these

two TCL molecules was recently exploited to develop macrocyclic or dimeric, TCL-based, bis-diaryl ether inhibitors of InhA (**Figure 2**). For instance, we reported the synthesis of macrocyclic diaryl ether analogues such as compound M01 that showed an IC₅₀ inhibitory activity of 4.6 μM [18]. On the other hand, Chetty *et al.* designed and synthesized a series of flexible di-triclosan analogues, which displayed InhA inhibition also in the micromolar range (Cpd2 and Cpd38, **Figure 2**) [19, 20]. A more rigid acyclic bis-diaryl ether derivative (Cpd6I, **Figure 2**) showed a similar inhibitory activity against InhA [21]. It is worth mentioning that another part of the protein, the minor portal located behind site II, has been little exploited until now. This site was recently targeted through the design of coumarin diaryl ethers that are highly effective against both InhA and mycobacterial growth (e.g. Cpd7b, ligand ID VZR in PDB 8OTN, chain D; **Figures 1 and 2**) [22]. This site may also be targeted, although in a lesser extent, by alkyl chains grafted onto TCL (e.g. compound 8PP, ligand ID 8PS in PDB 2B37, chain D; **Figures 1 and 2**) [12-14, 23]. Thus, several choices of pharmacophore groups can be used to occupy the different sites defining the substrate-binding site of InhA. Following this line, we report here on the design, synthesis and characterization of new InhA inhibitors incorporating within the same molecule two diaryl ether moieties and an alkyl chain grafted on a nitrogen atom (**Figure 2**). The high-resolution structure of the most potent compound revealed a previously unseen occupation



of the active site with maximum opening of the minor portal.

Figure 1. Overlaid X-ray structures of TCL1 and TCL2 (respectively pink and magenta, PDB 1P45:A), 8PS (cyan, PDB 2B37:A), VZR (blue, 8OTN:D), and THT (grey, 1BVR:A) binding to InhA in the presence of NAD⁺ (green). The substrate binding site is divided in three sites i.e site I, site II and site III (after [15, 16]).

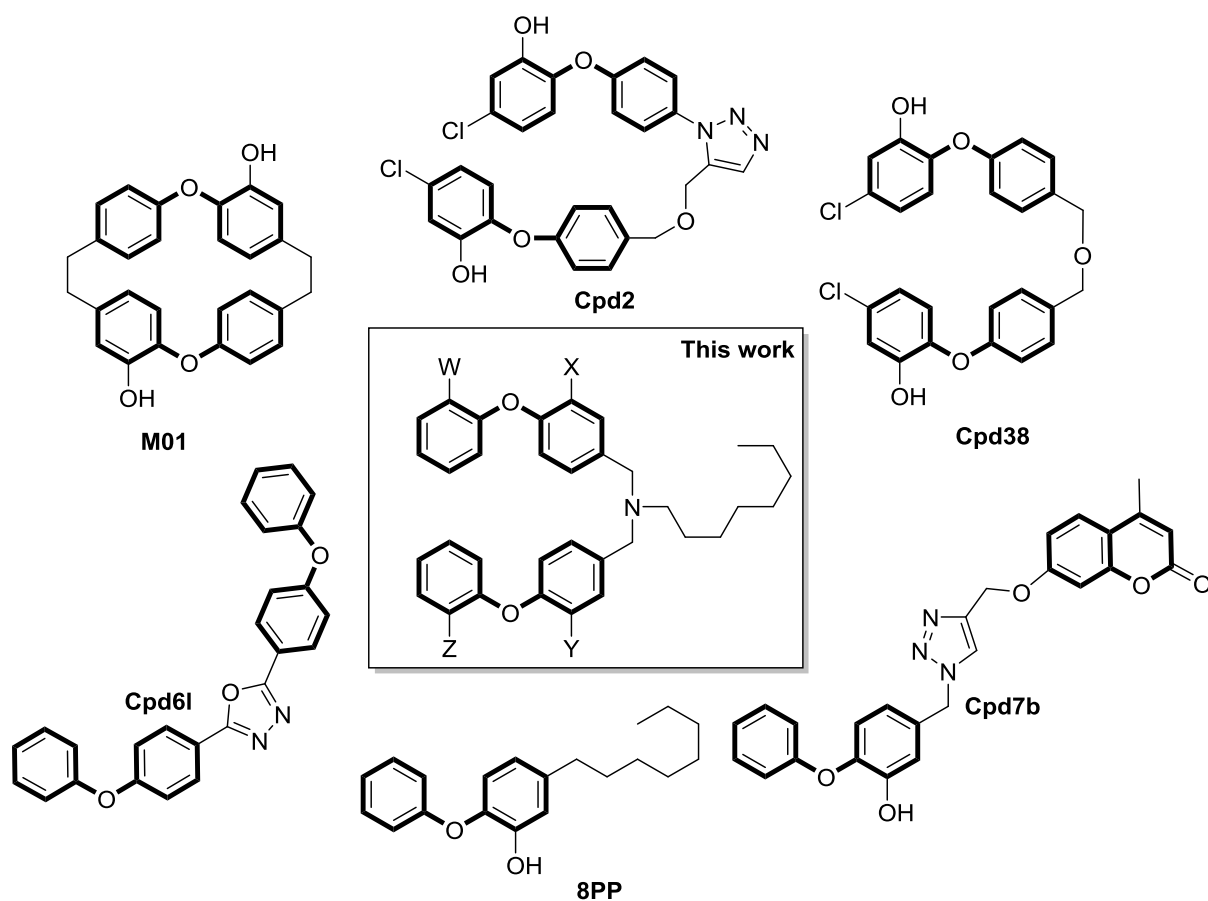
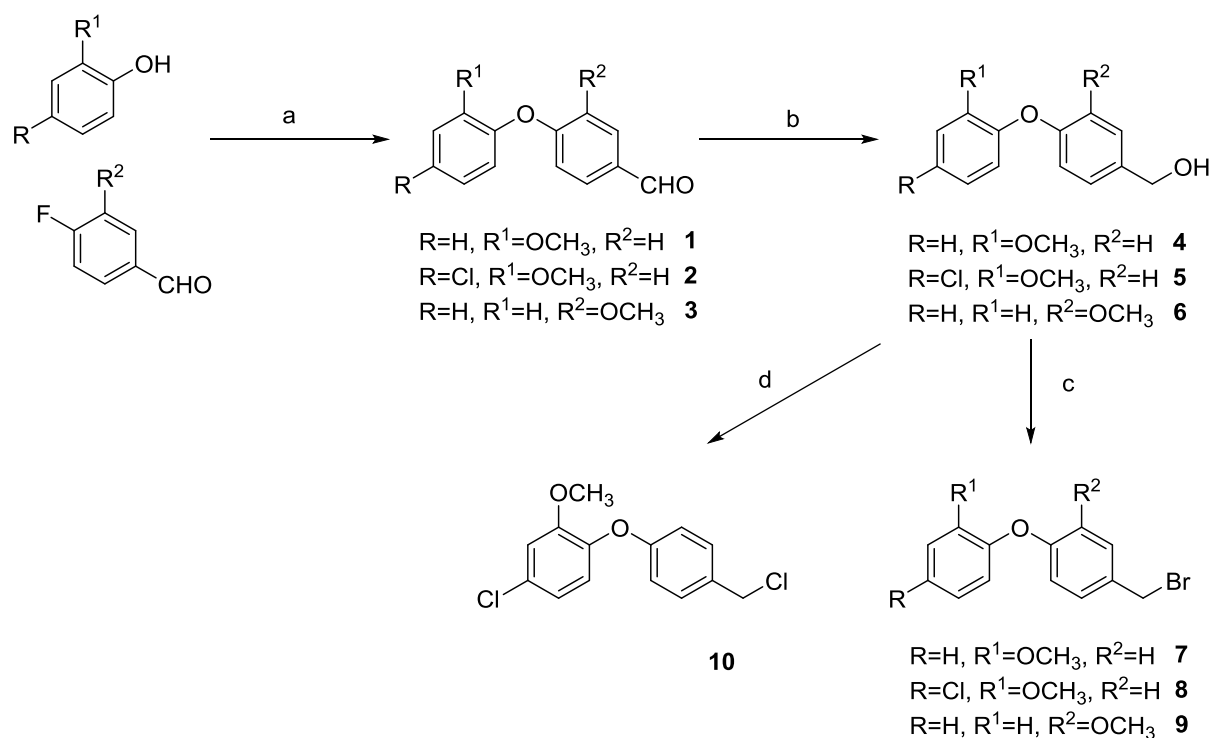


Figure 2. Bis-diaryl ether inhibitors of InhA.

2. Results and discussion

2.1. Synthesis of the molecules

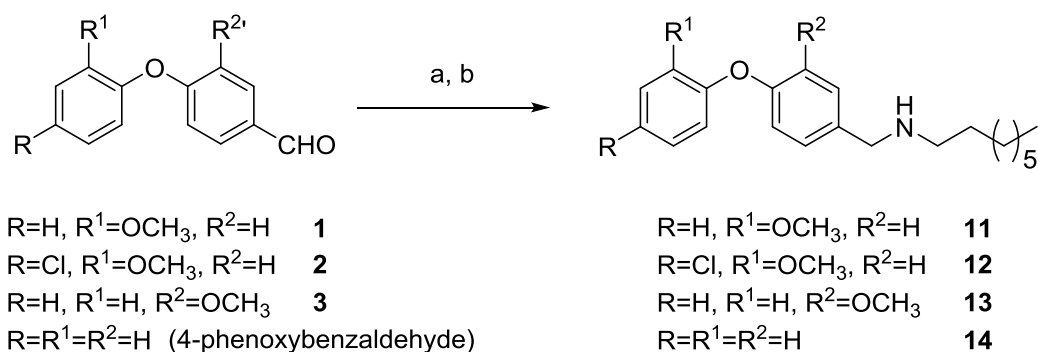
The synthetic routes of bis-diaryl ether compounds and their analogues are depicted in **Schemes 1-6**.



(a) K_2CO_3 , DMF, 120 °C, 66-91%; (b) $NaBH_4$, MeOH, 89-92%; (c) CBr_4/PPh_3 , CH_2Cl_2 , 70-88%; (d) $MsCl$, Et_3N , CH_2Cl_2 , 67% (from **5**).

Scheme 1. Synthesis of the precursors **1-10**.

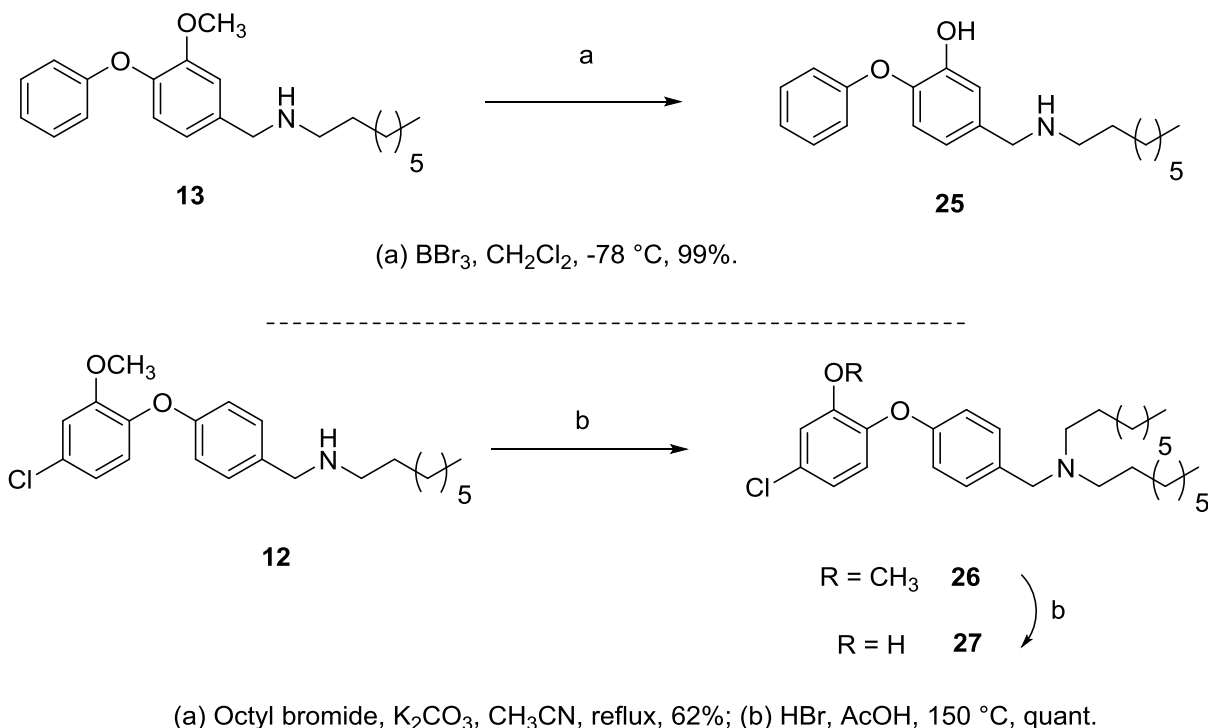
The initial steps start with the synthesis of the various precursors, i.e. aldehydes **1**, **2** and **3** and halides **7-9** and **10** (Scheme 1). Condensation of differently substituted phenols with 4-fluorobenzaldehyde affords diaryl ethers **1**, **2** and **3** in good yields, which were subsequently reduced using $NaBH_4$. The resulting alcohols were treated with triphenylphosphine/carbon tetrabromide or mesyl chloride to afford the bromide or chloride derivatives **7**, **8**, **9** and **10**.



(a) Octylamine, CH_2Cl_2 ; (b) $NaBH_4$, MeOH/EtOH

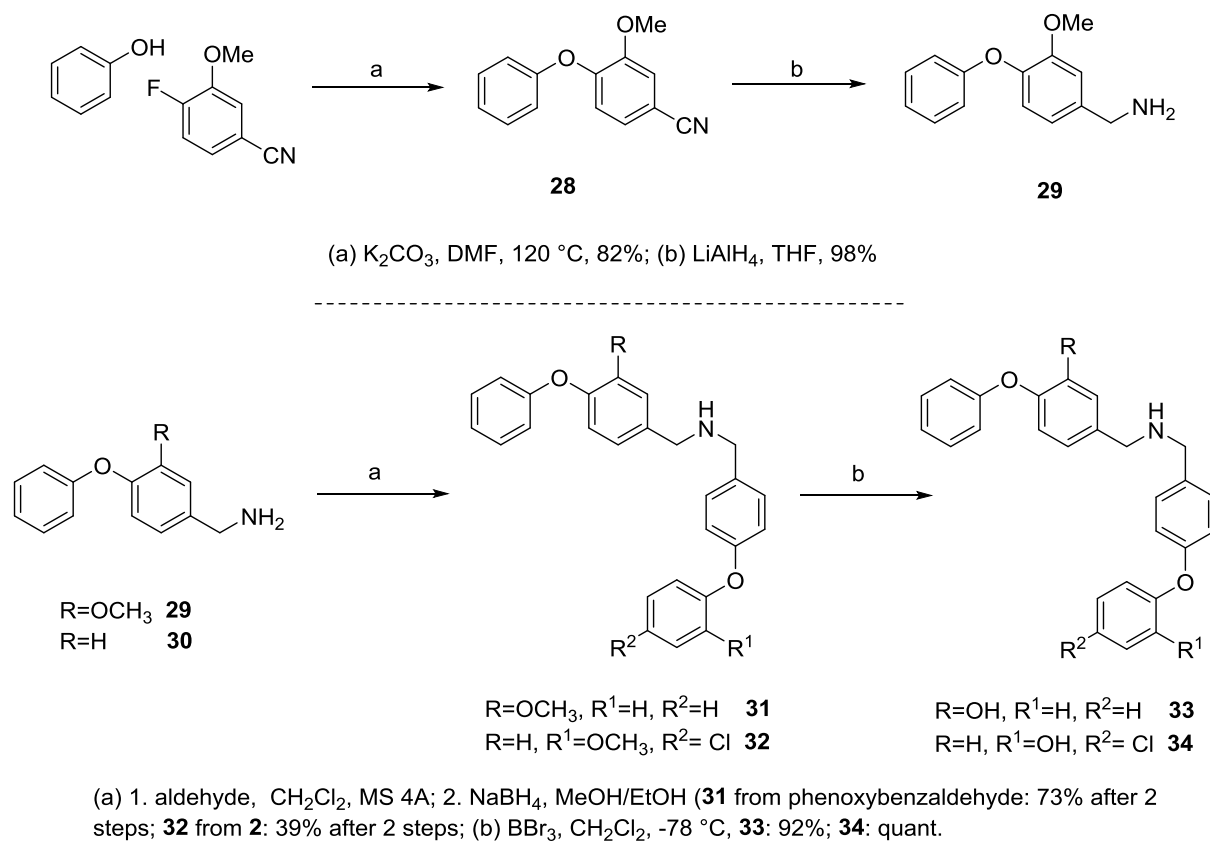
Scheme 2. Synthesis of the precursors **11-14**.

In order to synthesize diaryl ether **15**, octylamine was treated with bromide derivative **8** using potassium carbonate as base (**Scheme 3**). Various substituted diaryl ether derivatives **17-20** were synthesized by condensing compounds **8** or **9** with secondary amines **11**, **13** and **14** using the same conditions. Each bis-diaryl ether molecule was demethylated using hydrogen bromide in acetic acid under reflux (**Scheme 3**). For these molecules, the reaction with HBr/AcOH by comparison with BBr₃ has the merit of being much cleaner and above all reproducible. Nevertheless, secondary amine derivative **25** was synthesized in one-step from **13** using BBr₃ at low temperature.



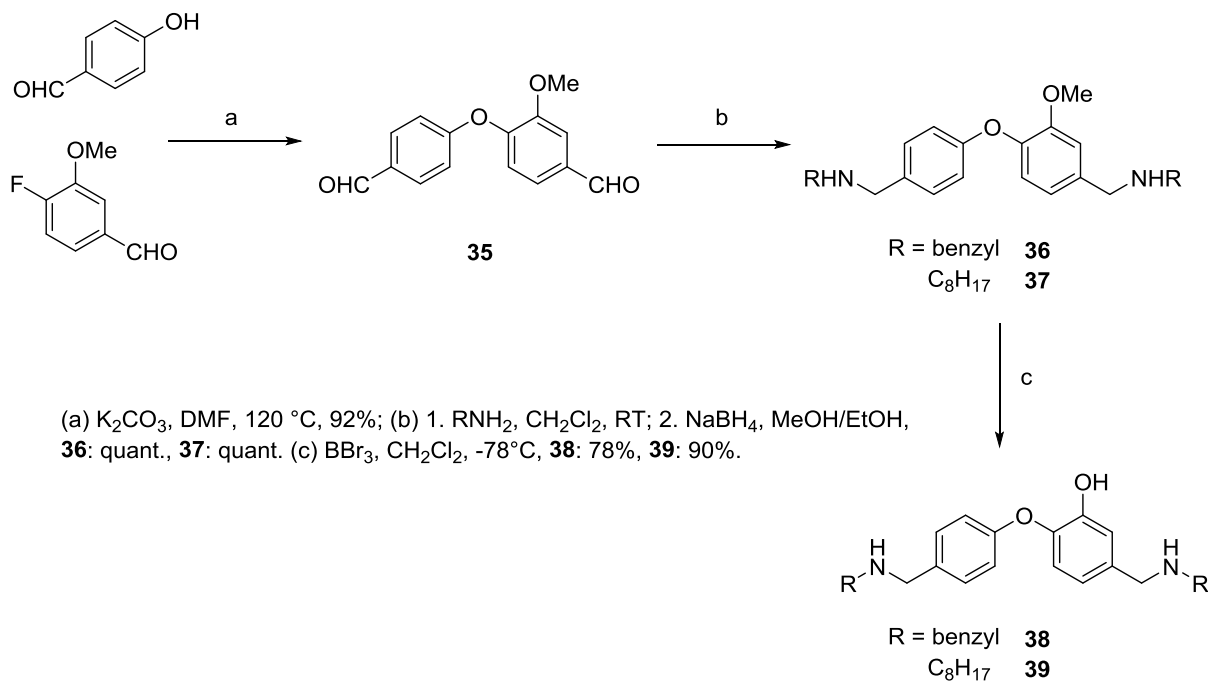
Scheme 4. Synthesis of derivatives **25** and **27**.

In addition to mono-alkylated bis-diaryl ether derivatives listed above, miscellaneous analogs or truncated compounds such as **27**, **33** and **34** have been synthesized to verify their ability to inhibit the InhA protein. Bis-C₈-alkylated amine **27** was synthesized from compound **12** and octyl bromide after demethylation in good yield (**Scheme 4**). Compounds **33** and **34**, deprived of alkyl chain, have also been synthesized to determine the impact of this chain on recognition by InhA. To this end, compounds **31** and **32** were synthesized by reductive amination of amines **29** and **30** in the presence of 4-phenoxybenzaldehyde and aldehyde **2**, respectively, in good yields (**Scheme 5**). Final compounds **33** and **34** were obtained after demethylation using BBr₃ in excellent yields.



Scheme 5. Synthesis of diaryl ether compounds **33** and **34**.

Two bifunctionalized diaryl ethers **38** and **39** were synthesized in two steps from aldehyde **35** (**Scheme 6**). Unlike the other molecules shown above, these molecules have two secondary amines containing either a benzyl or an octyl group.

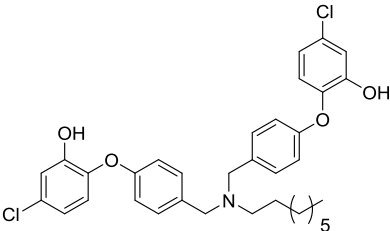
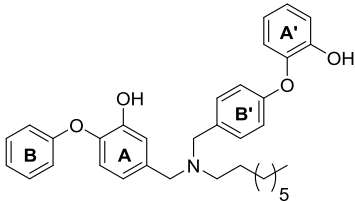
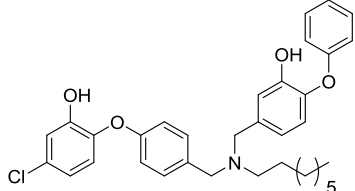


Scheme 6. Synthesis of compounds **38** and **39**.

2.2. InhA inhibition assay

The inhibition activity of synthesized compounds was investigated via a well-known procedure [24]. Initial velocities were measured at fixed concentrations of NADH (250 μM), dodecenoyl Coenzyme A (DDCoA, 50 μM) and inhibitors as a first screening (50 μM). The reactions were initiated by the addition of InhA enzyme. Triclosan was used as a control. As shown in **Table 1**, compound **21** showed the best inhibitory activity with IC_{50} of 0.70 μM , making it one of the most efficient derivatives bearing two diaryl ethers as compared to previous studies [19, 20]. Surprisingly, comparing compounds **22** and **21**, the presence of a chlorine atom on the aromatic leads to a significant decrease in inhibitory activity. If a hydroxyl group is absent as found in compound **24**, compared to compound **21**, a decrease in affinity was observed with an IC_{50} of 1.82 μM . This may be due to the loss of a hydrogen bond with a residue of InhA. Bis-diaryl ether derivative **33** bearing no alkyl chain showed an IC_{50} of 1.38 μM while the same compound with a different hydroxyl positioning and bearing a chloride atom displays no capacity to inhibit InhA.

Table 1. Structure and inhibitory activity of diaryl ether derivatives toward InhA enzyme and Mtb H37Rv strain.

ID molecules	Molecules	% inhibition at 50 μM	IC_{50} (μM)	MIC_{90} ($\mu\text{g/mL}$)
16		28	ND ^a	10
21 (EG1-57)		100 (91% at 5 μM)	0.70 \pm 0.07	20
22		28 (at 5 μM) ^b	ND ^a	20

23		43	ND ^a	>40
24		100 (80% at 5 μM)	1.82 ± 0.21	ND ^a
25		30 (at 5 μM) ^b	ND ^a	5
27		41	ND ^a	10
33		91 (at 15 μM) ^b	1.38 ± 0.07	ND
34		NI ^c	ND ^a	5
38		<5	ND ^a	10
39		62	ND ^a	2.5
Triclosan (TCL)		98	ND ^a	ND ^a

^aND, not determined; ^bNot soluble at 50 μM; ^cNI, no inhibition.

2.3. Inhibition of mycolic acid biosynthesis in *Mtb* H37Rv

Compounds were screened against *Mtb* strain H37Rv by determining the minimum inhibitory concentrations (MIC). Results are reported in **Table 1**. As a general trend, most of the compounds showed poor antimycobacterial activities with MIC values in the range of 10 to > 40 μg/mL. Among diaryl ether derivatives, **34** and **39** showed the best inhibitory activity with MIC of 5 and 2.5 μg/mL, respectively. The best inhibitor **21** of the enzyme InhA was poorly active against *Mtb* with a MIC of 20 μg/mL.

2.4. *In silico* studies of compound **21**

As designed, compound **21** consists of three fragments: two diaryl ethers and one C8-alkyl chain. Each of these three fragments may bind into the TCL1 or the TCL2 site as shown in **Figure 1**. Therefore, molecular docking of compound **21** to InhA was performed to gain insights into the possible binding modes. The structure of InhA in complex with NAD⁺ and compound PT70 (2-(*o*-tolylxy)-5-hexylphenol, ligand ID TCU in PDB 2X22, chain A, hereafter 2X22:A), in which the minor portal is opened, was chosen, offering more space in the vicinity of the protein substrate-binding site. The most realistic complex of compound **21** with InhA/NAD⁺ was selected on the basis of docking scores and similarities (or compliance) with X-ray crystal structure complexes of InhA with known inhibitors. After docking, the best poses show that compound **21** is able to dock with one diaryl ether group within the TCL1-binding site (site I) in the major portal and the other diaryl ether in the minor portal. For the first diaryl ether, typical π -stacking interactions between the hydroxyl-substituted (A) ring and the nicotinamide ring of the cofactor as well as hydrogen bonding between the hydroxyl moiety of the A ring and the 2-hydroxyl group of the cofactor and hydroxyl group of Tyr158 are observed as found for other complexes with diaryl ethers. The other diaryl ether expands in the minor portal with a higher degree of fluctuation, covering the entire binding site surface of site II. The corresponding poses can be classified in two clusters, H+ and B+, which share the same values of docking scores (**Figure 3**). In the case of the H+ set, the second diaryl ether is in the upper part of the minor portal and the alkyl chain in the lower part. In the case of the B+ set, the relative position of the alkyl chain and diaryl ether is inverted (i.e. with the alkyl chain in the upper part of the minor portal). Interestingly, the position of the nitrogen atom is conserved in the two sets.

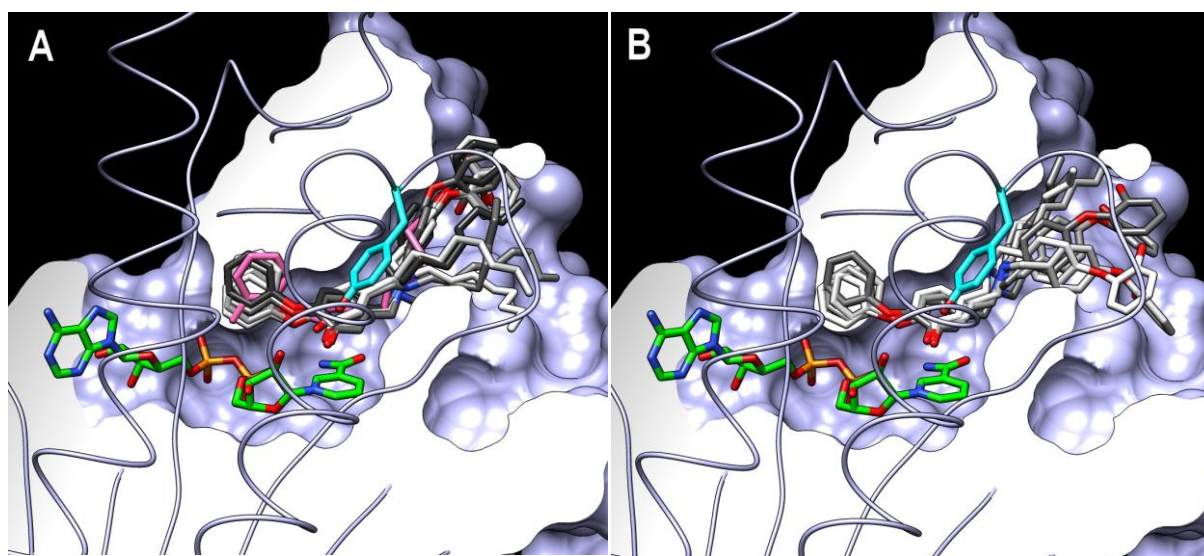


Figure 3. Best docking poses of compound **21** to the InhA structure (PDB 2X22, chain A). A. Fluctuation of type H+ (alkyl chain down). B. Fluctuation of type B+ (alkyl chain up). The different poses of compound **21** are shown

as different shades of gray. Compound PT70 (ligand ID TCU, hot pink) and NAD⁺ (green) of 2X22:A (light blue surface) are shown.

2.5. X-ray structure of the *InhA*/NAD⁺/**21** complex

To gain further insight into protein-ligand interactions, we succeeded in obtaining the X-ray structure of the complex of compound **21**, the best diaryl ether derivatives (in terms of IC₅₀) in our series, with *InhA* and NAD⁺ (PDB code 8OTL). Crystals were obtained in the presence of PEG 4000 after successive incubation of the protein with the cofactor then with compound **21**. They belong to space group $C222_1$ with 6 molecules in the asymmetric unit and diffracted X-rays to a maximum resolution of 2.1 Å. Clear electron density was visible in the substrate-binding site of *InhA* that allows for unambiguous positioning of the cofactor and the ligand. The latter was observed in only one of the six molecules of the asymmetric unit (**Figure 4**), a quite common feature when considering structures of *InhA*/NAD(H)/ligand complexes obtained in $C2_1$ and $C222_1$ space groups available in the PDB. In all 6 chains of the asymmetric unit, the NAD⁺ molecules adopt strictly the same position and canonical conformation observed in other deposited *InhA* structures. Differences are observed for the so-called “substrate-binding loop” (SBL, residues 192-226 encompassing helices H6 and H7) where H6 adopts an open conformation in the unpopulated chains (**Figure 4A**) and a closed conformation in the only one chain bearing the ligand (**Figure 4B**). Furthermore, the Phe149 and Tyr158 side chains are in the so-called *out* and *in* conformation, respectively, in the populated molecule but adopt various, and even alternate, *in/out* orientations in the molecules that only contains the cofactor (**Figure 4**).

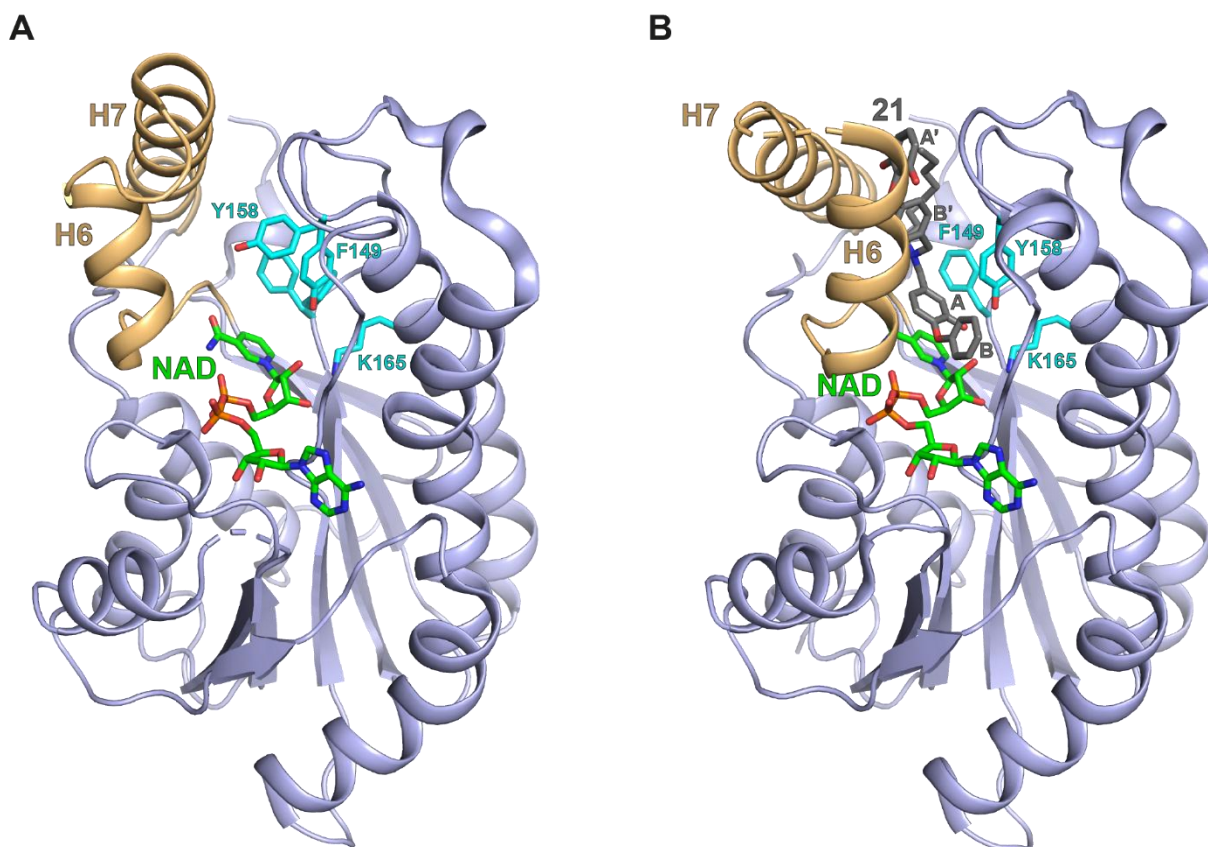


Figure 4. X-ray structure of the InhA/NAD⁺/21 complex. **A.** Five of the six molecules making up the crystal have no bound ligand (only 8OTL:A is shown). **B.** Bound ligand in the sixth molecule (8OTL:F). Cartoon representation showing the difference in the conformation of the SBL loop (residues 192-226, orange), with helix H6 from open to closed. The NAD⁺ (green), the ligand (gray) and the side chains of the catalytic triad Phe149-Tyr158-Lys165 (cyan) are shown as sticks. In the non-populated molecules, the side chains of Phe149 and Tyr158 adopt alternative in/out conformations whereas in the ligand complex, Phe149 and Tyr158 side chains are out and in, respectively

As found in other InhA-diaryl ether structures, the hydroxyl-substituted ring A of **21** is stacked with the NAD⁺ nicotinamide and its hydroxyl moiety makes hydrogen bonds with the hydroxyl group of Tyr158 and the 2'-hydroxyl group of NAD⁺ (**Figure 5A**). Two additional hydrogen bonds are formed between the hydroxyl group of the other hydroxyl-substituted ring of **21** (i.e. A'), which adopts two alternate conformations rotated by 180°, and either the main-chain oxygen atom of Ile202 or the side-chain nitrogen atom of Gln214 (**Figure 5B**). Another polar contact might be formed between the protein and the ligand through a cation- π interaction involving the Phe149 side chain and the nitrogen atom of **21**, which would require protonation of the amine (**Figure 5C**). In addition to polar contacts, binding of **21** occurs through numerous, i.e. 80 in total, non-bonded contacts involving the cofactor and protein residues. Among top contributors, number of contacts in parentheses, are found NAD⁺ (28), Tyr158 (8), Ile202 (7), and Gln214 (5). Other contacts involved Gly96 (3), Phe97 (3), Gly104 (1), Phe149 (3), Met155 (1), Pro156 (2), Ala157 (3), Met161 (4), Lys165 (1), Pro193 (1), Ala198 (3), Met199 (1), Val203 (2), Val206 (2), Leu218 (1), and Trp222 (1). From the ligand perspective, 64%

(51) of these contacts involve the AB diphenyl ether (**Figure 5A**), 23% (19) the A'B' diphenyl ether (**Figure 5B**), 4% (3) the benzylic CH₂ groups, and 9% (7) the alkyl chain (**Figure 5C**).

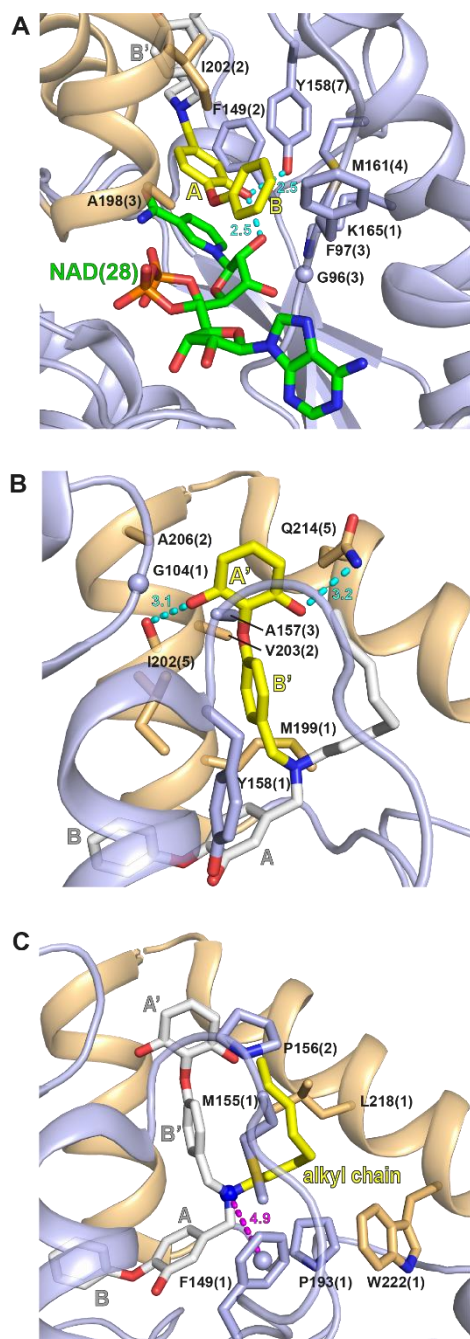


Figure 5. Detailed interactions of compound **21** with InhA/NAD⁺. Three different zooms are shown that correspond to **A**. The AB diaryl ether. **B**. The A'B' diaryl ether. Both observed orientations of cycle A' are shown. **C**. The alkyl chain. The protein is shown as cartoon using the same color scheme as in Figure 4. In each panel, the considered part of the ligand is in yellow while the remaining part is in light gray. The cofactor is in green. Protein residues involved in defining the inhibitor-binding pocket are shown as sticks and labeled with their number of non-bonded contacts with the ligand given in parentheses. Hydrogen bonds are displayed as cyan dotted lines. The putative cation- π interaction is shown as magenta dotted lines. Distances are indicated.

Comparison of docking and crystallographic binding poses shows similar conformations for the AB diaryl ether and the nitrogen (**Figure 6**). Beyond nitrogen, in the direction of the minor portal, significant differences are observed with the alkyl chain and the A'B' diaryl ether mainly due to a very different opening of the minor portal in the 2X22:A vs. 8OTL:F structures.

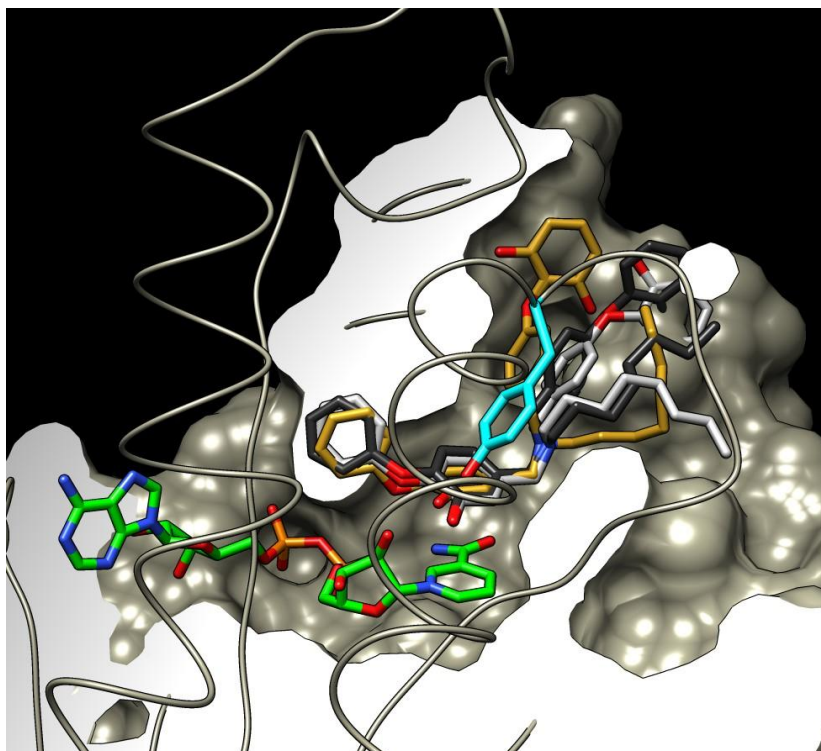


Figure 6. Comparison of the two best docking poses (black, grey) with the crystallographic conformation (orange) of compound **21** in 8OTL:F (gray surface). The side chain of Tyr258 and NAD⁺ are shown in cyan and green, respectively.

2.6. *Compared analysis of the functional and structural effect of InhA complexation to alkyl diaryl ethers*

Compound **21** has 6.6 fold improved IC₅₀ compared to macrocyclic diaryl ether analogues such as compound M01 (0.7 μM vs. 4.6 μM) [18]. This might be explained by the fact that the latter are rigid molecules although more flexible bis-diaryl ether analogues have also been shown to display InhA inhibition in the micromolar range [20, 21]. However, the difference in inhibition of both protein activity and Mtb growth between the alkyl bis-diaryl ether compound **21** and smaller alkyl diaryl ethers, which display IC₅₀ values up to 10 times lower (at nearby InhA concentrations, i.e. 50 and 100 nM, **Table 2**), is quite striking. To try to rationalize these differences, we compared the crystallographic structures of the corresponding complexes in terms of both the number of hydrogen bonds/non-bonded contacts and minor portal opening (**Table 2** and **Figure 7**). For instance, compound **21** makes two more hydrogen bonds with the protein (alternating between either the main-chain oxygen atom of Ile202 or the side-chain nitrogen atom of Gln214 and the hydroxyl group on the A' ring) than alkyl diaryl ethers and as many non-bonded contacts with InhA and NAD⁺ as the alkyl diaryl ether compound (8PP), which bears an octyl chain. Another major difference is the wider opening of the minor portal in the structure of the complex with **21** compared to alkyl diaryl ethers (**Figure 7**). Indeed, the alkyl part of compound **21** extends towards the minor portal in a manner

reminiscent of what has been observed for coumarin diaryl ethers [22], and opening is further accentuated by the presence of the A'B' diaryl ether.

Table 2. Structure and properties of diaryl ether analogues bearing an alkylated chain.

PDB:chain	Compound name (PDB ligand ID)	Structure	IC ₅₀ (nM)	MIC (µg/ mL)	N° H-bonds	N° non-bonded contacts ^a	Ref.
8OTL:F	21 (VZE)		700 ^b	20	4	80:28-52	This work
2B36:A	5PP (5PP)		17 ^c	1	2	47:28-19	[14]
2B37:D	8PP (8PS)		5 ^c	1.9	2	83:38-45	[14]
2X23:G	PT70 (TCU)		50.3 ^d	3.1	2	70:34-36	[12]
4OHU:A	PT92 (2TK)		10 ^e	3.1	2	61:28-33	[13, 23]
4OIM:A	PT119 (JUS)		235.6 ^d	2.5	2	72:31-41	[13]
4OXN:B	PT155 (1S5)		ND ^f	ND	3	63:30-33	[23]
4OXY:B	PT10 (1TN)		182 ^d	12.5	2	67:32-35	[23]
4OYR:C	PT91 (1US)		49.5 ^d	1.6	2	59:31-28	[23]

^a Total number: with cofactor-with protein, determined using the LigPlot+ program [25]. InhA concentration: ^b50 nM, ^c1 nM, ^d100 nM and ^e20nM. ^fND, not determined.

3. Conclusions

Over the past decade, InhA has been demonstrated as a promising target and various types of inhibitors have been identified that bind to the substrate site. In the present study, the substrate-binding site was exploited by designing bis-diaryl ether molecules bearing a chain reminiscent of the substrate. A series of eleven alkyl bis-diaryl ether derivatives were synthesized and one of them displayed nanomolar inhibitory activity against the enzyme. The X-ray structure of the corresponding complex with InhA and NAD⁺ was obtained. This structure revealed the protein adaptability to a relatively large inhibitor and the observed opening of the minor portal underlines its plasticity. Such an opening of the minor portal raises the question of whether it could act as an entry/exit gate for compounds (substrates and/or inhibitors).

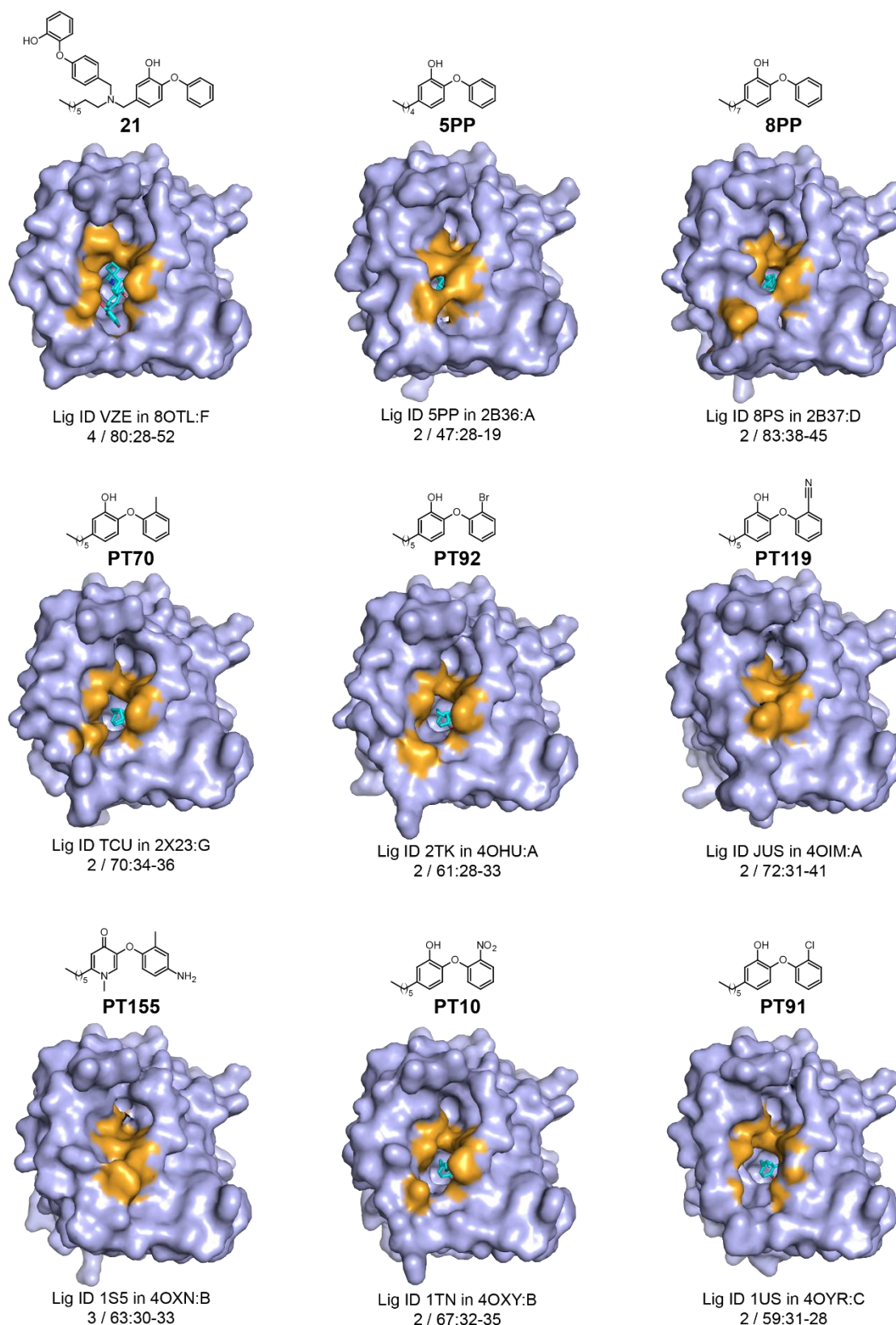


Figure 7. Effect of alkyl diaryl ether binding on minor portal opening. In each panel, the chemical structure and compound name (upper lines) and PDB identifiers as well as the number of hydrogen bonds and the number of (total:with cofactor/with protein) non-bonded contacts (lower lines) are given. The protein molecular surface is represented in lightblue. Residues interacting with compound **21** are displayed in orange on all structures, which are represented in the same orientation.

4. Experimental section

4.1. Chemistry

All commercial reagents were purchased from Sigma-Aldrich or Alfa Aesar and were used without further purification. CH_2Cl_2 and *N,N*-dimethylformamide were purified over a solvent purification system. Proton and carbon nuclear magnetic resonance (^1H NMR and ^{13}C NMR) spectra were recorded on Bruker advance (300 MHz/75 MHz or 500 MHz/125 MHz) spectrometers. Chemical shifts were recorded in parts per million (ppm, δ) relative to the corresponding deuterated solvent (7.26 ppm and 77.0 ppm for CDCl_3). ^1H NMR splitting patterns are designated as singlet (s), doublet (d), triplet (t) and multiplet (m) or broad (b). Coupling constants (J) are reported in hertz (Hz). High-resolution mass spectrometry (HRMS) was performed on a Thermo-Finnigan MAT 95 XL instrument. Analytical thin-layer chromatography (TLC) was carried out on Merck 60 F254 pre-coated silica gel plates (0.2 mm thickness). Visualization was accomplished by UV irradiation at 254 nm. Flash column chromatography was performed on a Puriflash from Interchim or Combiflash from Serlabo.

General procedure for the aromatic substitution (compounds 1-3).

Phenol (1 eq) and 4-fluorobenzaldehyde (1.1-1.2 eq) were dissolved in *N,N*-dimethylformamide (20 mL). To this mixture, add K_2CO_3 (2.5 eq) and heat to 120 °C. After 18 h of stirring, the mixture was concentrated under reduced pressure. The resulting residue was diluted with ethyl acetate and washed with water. The combined organic layers are washed with brine, dried over MgSO_4 , filtered, and concentrated under reduced pressure. The product was purified by flash chromatography to afford the desired diaryl ether derivative.

General procedure for the reduction of aldehydes (compounds 4-6).

Sodium borohydride (2-4 eq) was added to a stirred solution of aldehyde derivative (1 eq) in methanol (10 mL) at 4 °C. The mixture was stirred 30 minutes at this temperature and then overnight at room temperature. Once the reaction was complete, the reaction mixture was concentrated under reduced pressure and diluted with ethyl acetate. The organic layer was washed with water and brine, dried over MgSO_4 , filtered, and concentrated under reduced pressure to afford the desired compound. No further purification step was necessary.

General procedure for the bromation of alcohol derivatives (compounds 7-9).

To a solution of alcohol derivative (1 eq) solubilized in dichloromethane (10 mL), were added carbon tetrabromide (1.25-1.5 eq) and triphenylphosphine (1.4-2 eq) at 4 °C. Then, the reaction mixture was stirred at room temperature for 24 h. The solvent was evaporated under reduced pressure and ethyl

acetate was added. The reaction mixture was washed with water (3×). The organic layer was washed with brine, dried over MgSO₄, filtered, and concentrated under reduced pressure to give the crude compound which was purified by flash chromatography.

General procedure for the reductive amination (compounds 11-14).

Octylamine (1 eq) was added to a solution of aldehyde (1 eq) in 50 mL anhydrous dichloromethane with molecular sieves. The reaction mixture was stirred overnight at room temperature. Molecular sieves were removed by filtration and the solution was concentrated *in vacuo*. The residue was diluted with methanol/ethanol (1/1, 50 mL) and sodium borohydride (3 eq) was slowly added to the ice-cooled solution. Once the reaction was complete as seen by TLC, saturated solution of NH₄Cl was added and the resulting solution was concentrated *in vacuo*. Ethyl acetate was added and the organic layer was washed with water and brine, dried over MgSO₄, filtered, and concentrated under reduced pressure to give the desired compound. No further purification was needed.

General procedure of demethylation (compounds 16, 21-24).

CH₃COOH (1 mL) and HBr 48% (1 mL) were added to the methoxybenzene derivative (0.162-0.322 mmol). The mixture was stirred at 150 °C for 5 h. Then a NaHCO₃ sat aqueous solution was added slowly and was extracted with ethyl acetate. The combined organic layers were washed with water, dried over MgSO₄, filtered, and concentrated *in vacuo* to give the desired compound.

4-(2-Methoxyphenoxy)benzaldehyde (1) [26].

The product **1** was synthesized as described in the general procedure for aromatic substitution with guaiacol (500 mg, 4 mmol) and 4-fluorobenzaldehyde (600 mg, 4.8 mmol). Purification by flash chromatography (linear gradient petroleum ether/ethyl acetate: 95/5 to 90/10) gave compound **1** as a lightly yellow oil (75%, 0.801 g). *R_f* = 0.27 (petroleum ether/ethyl acetate: 9/1). ¹H NMR (300 MHz, CDCl₃) δ 9.90 (s, 1H, CHO); 7.85 – 7.78 (m, 2H, ArH); 7.28 – 7.19 (m, 1H, ArH); 7.10 (dd, *J* = 7.9, 1.8 Hz, 1H, ArH); 7.06 – 6.95 (m, 4H, ArH); 3.79 (s, 3H, OCH₃); ¹³C NMR (75 MHz, CDCl₃) δ 190.8; 163.5; 151.6; 142.8; 131.8; 130.8; 126.4; 122.5; 121.3; 116.2; 113.0; 55.8.

4-(4-Chloro-2-methoxyphenoxy)benzaldehyde (2) [19].

The product **2** was synthesized as described previously in the general procedure for aromatic substitution with 4-chloro-2-methoxyphenol (0.700 g, 4.4 mmol) and 4-fluorobenzaldehyde (0.657 g, 5.3 mmol) and K₂CO₃ (1.22 g, 8.8 mmol). Purification by flash chromatography (petroleum ether and ethyl acetate: 9/1) gave compound **2** as a white powder. Yield: 91% (1.050 g). *R_f* = 0.65 (petroleum ether/EtOAc: 80/20). ¹H NMR (300 MHz, CDCl₃) δ 9.91 (s, 1H, ArCHO); 7.90 – 7.77 (m, 2H, ArH); 7.10 –

6.92 (m, 5H, ArH); 3.78 (s, 3H, OCH₃); NMR ¹³C (75 MHz, CDCl₃): δ 190.9; 163.3; 152.4; 141.7; 132.0; 131.5; 131.3; 123.4; 121.3; 116.3; 113.8; 56.3.

3-Methoxy-4-phenoxybenzaldehyde (3).

The product **3** was synthesized as described previously in the general procedure for aromatic substitution with phenol (1 g, 10.6 mmol) and 4-fluoro-3-methoxybenzaldehyde (1.8 g, 11.7 mmol) and K₂CO₃ (3.68 g, 26.3 mmol). Purification by flash chromatography (linear gradient petroleum ether/ethyl acetate: 95/5 to 80/20) gave compound **3** as a light beige oil (66%, 0.212 g). *R*_f = 0.26 (petroleum ether/EtOAc: 9/1). ¹H NMR (300 MHz, CDCl₃) δ 9.88 (s, 1H, CHO), 7.52 (d, *J* = 1.9 Hz, 1H, ArH), 7.40 – 7.32 (m, 3H, ArH), 7.20 – 7.13 (m, 1H, ArH), 7.07 – 7.01 (m, 2H, ArH), 6.91 (d, *J* = 8.2 Hz, 1H, ArH), 3.94 (s, 3H, OCH₃); ¹³C NMR (75 MHz, CDCl₃) δ 190.8; 155.7; 152.1; 150.9; 132.1; 129.9; 125.7; 124.3; 119.9; 117.7; 110.5; 56.0.

(4-(2-Methoxyphenoxy)phenyl)methanol (4).

The product **4** was synthesized as described in the general procedure for aldehyde reduction with compound **1** (330 mg, 1.45 mmol) and sodium borohydride (219 mg, 5.8 mmol) to give compound **4** as a lightly yellow oil (89%, 0.229 g). *R*_f = 0.47 (petroleum ether/ethyl acetate: 7/3). ¹H NMR (300 MHz, CDCl₃) δ 7.31 – 7.26 (m, 2H, ArH), 7.14 (ddd, *J* = 8.2, 7.0, 2.0 Hz, 1H, ArH), 7.05 – 6.95 (m, 2H, ArH), 6.95 – 6.90 (m, 3H, ArH), 4.62 (s, 2H, ArCH₂OH), 3.83 (s, 3H, OCH₃); ¹³C NMR (75 MHz, CDCl₃) δ 157.5; 151.3; 144.9; 134.9; 128.5; 124.9; 121.0; 121.0; 117.1; 112.8; 64.9; 55.9; HRMS (DCI/CH₄, [M]⁺) Calculated for C₁₄H₁₄O₃: 230.0943. Found: 230.0944.

(4-(4-Chloro-2-methoxyphenoxy)phenyl)methanol (5) [20].

The product **5** was synthesized as described in the general procedure for aldehyde reduction with compound **2** (600 mg, 2.29 mmol), sodium borohydride (183 mg, 4.83 mmol) to give compound **5** as a white solid (99%, 0.632 g). *R*_f = 0.16 (petroleum ether/ethyl acetate: 8/2). ¹H NMR (300 MHz, CDCl₃) δ 7.24 – 7.18 (m, 2H, ArH); 6.97 (m, 1H, ArH); 6.91 – 6.79 (m, 4H, ArH); 4.51 (s, 2H, CH₂OH); 3.75 (s, 3H, OCH₃); 3.40 (b, 1H, OH); ¹³C NMR (75 MHz, CDCl₃) δ 156.9; 151.7; 143.5; 135.2; 129.5; 128.4; 121.6; 120.7; 118.9; 113,3 (C2); 64,2 (C13); 55,9 (C14); HRMS (DCI-CH₄, [M]⁺) Calculated for C₁₄H₁₃O₃Cl: 264.0553. Found: 264.0557.

(3-Methoxy-4-phenoxyphenyl)methanol (6).

The product **6** was synthesized as described in the general procedure for aldehyde reduction with compound **3** (500 mg, 2.191 mmol) and sodium borohydride (249 mg, 6.57 mmol) to give **6** as a

white solid (92%, 464 mg). ^1H NMR (300 MHz, CDCl_3) δ 7.36 – 7.25 (m, 2H, ArH), 7.10 – 7.01 (m, 2H, ArH), 6.99 – 6.86 (m, 4H, ArH), 4.68 (s, 2H, Ar- CH_2), 3.84 (s, 3H, OCH_3); ^{13}C NMR (75 MHz, CDCl_3) δ 157.8; 151.5; 144.4; 137.6; 129.5; 122.5; 120.9; 119.5; 117.1; 111.5; 65.1; 55.9; HRMS (DCI- CH_4 , $[\text{M}]^+$) Calculated for $\text{C}_{14}\text{H}_{14}\text{O}_3$: 230.0943. Found: 230.0948.

1-(4-(Bromomethyl)phenoxy)-2-methoxybenzene (7).

The compound **7** was synthesized as described in the general procedure for bromation with compound **4** (299 mg, 1.3 mmol), carbon tetrabromide (539 mg, 1.625 mmol) and triphenylphosphine (477 mg, 1.82 mmol). Purification on silica with petroleum ether and ethyl acetate (9:1) gave compound **7** as a yellow oil (76%, 0.293 g). R_f = 0.65 (petroleum ether/ethyl acetate: 9/1). ^1H NMR (300 MHz, CDCl_3) δ 7.36 – 7.27 (m, 2H, ArH); 7.17 (ddd, J = 8.2, 7.2, 1.9 Hz, 1H, ArH); 7.01 (dd, J = 8.0, 1.7 Hz, 2H, ArH); 6.97 – 6.93 (m, 1H, ArH); 6.91 – 6.85 (m, 2H, ArH); 4.50 (s, 2H, Ar- CH_2); 3.82 (s, 3H, OCH_3); ^{13}C NMR (75 MHz, CDCl_3) δ 158.2; 151.6; 144.3; 131.5; 130.4; 125.3; 121.6; 121.1; 116.9; 112.8; 55.9; 33.6; HRMS (DCI- CH_4 , $[\text{M}]^+$) Calculated for $\text{C}_{14}\text{H}_{13}\text{O}_2\text{Br}$: 292.0099. Found: 292.0110.

1-(4-(Bromomethyl)phenoxy)-4-chloro-2-methoxybenzene (8) [27].

The compound **8** was synthesized as described in the general procedure for bromation with compound **5** (0.632 g, 2.41 mmol), carbon tetrabromide (1.199 g, 3.615 mmol) and triphenyl phosphine (0.948 g, 3.615 mmol). Purification on silica with petroleum ether and ethyl acetate (9:1) gave the desired compound **8** as a white solid (70%, 0.547 g). R_f = 0.79 (petroleum ether/ethyl acetate: 80/20). ^1H NMR (300 MHz, CDCl_3) δ 7.34 – 7.29 (m, 2H, ArH); 6.99 (m, 1H, ArH); 6.92 (m, 2H, ArH); 6.87 (m, 2H, ArH); 4.40 (s, 2H, Ar CH_2); 3.70 (s, 3H, OCH_3); ^{13}C NMR (75 MHz, CDCl_3) δ 157.9; 152.1; 142.9; 131.9; 130.5; 130.1; 122.4; 120.9; 116.9; 113.5; 56.1; 33.5; HRMS (DCI- CH_4 , $[\text{M}]^+$) Calculated for $\text{C}_{14}\text{H}_{12}\text{O}_2\text{ClBr}$: 325.9709. Found: 325.9706.

4-(Bromomethyl)-2-methoxy-1-phenoxybenzene (9).

The compound **9** was synthesized as described in the general procedure for bromation with compound **6** (230 mg, 1 mmol), carbon tetrabromide (497 mg, 1.5 mmol) and triphenylphosphine (525 mg, 2 mmol). Purification on silica with petroleum ether and ethyl acetate (9:1) gave **9** as a lightly pink oil (88%, 0.257 g). R_f = 0.67 (petroleum ether/ethyl acetate: 9/1). ^1H NMR (300 MHz, CDCl_3) δ 7.36 – 7.28 (m, 2H, ArH), 7.12 – 7.03 (m, 2H, ArH), 7.01 – 6.88 (m, 4H, ArH), 4.51 (s, 2H, Ar- CH_2), 3.86 (s, 3H, OCH_3); ^{13}C NMR (75 MHz, CDCl_3) δ 157.3; 151.1; 145.4; 133.9; 129.5; 122.8; 121.6;

120.3; 117.5; 113.3; 55.9; 33.6; HRMS (DCI/CH₄, [M]⁺) Calculated for C₁₄H₁₃O₂Br: 292.0099. Found: 292.0102.

4-Chloro-1-(4-chloromethyl)phenoxy)-2-methoxybenzene (10).

The product **10** was synthesized as described previously [20]. Briefly, to a ice-cooled solution of **5** (498 mg, 1.88 mmol) solubilized dichloromethane (15 mL) under argon, was added triethylamine (0.626 mL, 4.51 mmol). After 5 min of stirring, methanesulfonyl chloride (0.175 mL, 2.26 mmol) was added dropwise. The reaction mixture was stirred at room temperature for 23 h. Then the organic solution was washed with water and brine, dried over MgSO₄, filtered, and concentrated in vacuo. Purification by flash chromatography (linear gradient petroleum ether/ethyl acetate: 90/10 to 30/70) gave **10** as a white solid (67%, 0.356 g). *R_f* = 0.78 (petroleum ether/ethyl acetate: 9/1). ¹H NMR (300 MHz, CDCl₃) δ 7.35 – 7.28 (m, 2H, ArH), 7.02 – 6.99 (m, 1H, ArH), 6.93 (d, *J* = 2.0 Hz, 2H, ArH), 6.92 – 6.86 (m, 2H, ArH), 4.56 (s, 2H, ArCH₂); 3.79 (s, 3H, OCH₃); ¹³C NMR (75 MHz, CDCl₃) δ 157.8; 151.5; 144.4; 137.6; 129.5; 122.5; 120.9; 119.5; 117.1; 111.5; 65.1; 55.9; ¹³C NMR (75 MHz, CDCl₃) δ 157.8; 152.0; 143.0; 131.5; 130.0; 122.2; 120.8; 116.7; 113.3; 56.0; 45.8; HRMS (DCI/CH₄, [M]⁺) Calculated for C₁₄H₁₂O₂Cl₂: 282.0214. Found: 282.0216.

N-(4-(2-Methoxyphenoxy)benzyl)octan-1-amine (11).

The product **11** was synthesized as described in the general procedure for reductive amination with compound **1** (158 mg, 0.692 mmol), octylamine (0.115 mL, 0.692 mmol) and sodium borohydride (78.5 mg, 2.076 mmol) to give **11** as a beige solid (quant., 0.250 g). *R_f* = 0.13 (100 % ethyl acetate). ¹H NMR (300 MHz, CDCl₃) δ 7.48 – 7.39 (m, 2H, ArH), 7.13 (ddd, *J* = 8.8, 6.2, 2.9 Hz, 1H, ArH), 7.01 – 6.94 (m, 1H, ArH), 6.93 – 6.84 (m, 4H, ArH), 3.92 (s, 2H, ArCH₂), 3.76 (s, 3H), 2.80 – 2.55 (m, 2H, NHCH₂), 1.83 – 1.66 (m, 2H, NHCH₂-CH₂), 1.34 – 1.15 (m, 10H, CH₂ alkyl), 0.89 – 0.76 (m, 3H, CH₃ alkyl). ; ¹³C NMR (75 MHz, CDCl₃) δ 158.7; 151.5; 143.9; 131.; 125.4; 125.37; 121.6; 121.1; 116.9; 112.8; 55.8; 50.3; 46.2; 31.6; 29.0; 28.97; 26.80; 26.5; 22.4; 14.0; HRMS (ESI, [M+H]⁺) Calculated for C₂₂H₃₂NO₂: 342.2433. Found: 342.2436.

N-(4-(4-Chloro-2-methoxyphenoxy)benzyl)octan-1-amine (12).

The product **12** was synthesized as described in the general procedure for reductive amination with compound **2** (0.240 g, 0.914 mmol), octylamine (0.118 g, 9.136 mmol) and sodium borohydride (0.104 g, 2.749 mmol) to afford **12** (quant., 343 mg). *R_f* = 0.15 (petroleum ether/ethyl acetate: 6/4). ¹H NMR (300 MHz, CDCl₃) δ 7.29 – 7.20 (m, 2H, ArH); 6.95 (t, *J* = 1.3 Hz, 1H, ArH); 6.89 – 6.83 (m, 4H, ArH); 3.79 (s, 3H, OCH₃); 3.74 (s, 2H, Ar-CH₂); 2.61 (t, *J* = 7.3 Hz, 2H, NCH₂); 1.58 – 1.43 (m, 2H, NCH₂-

CH₂); 1.35 – 1.18 (m, 10H, CH₂ alkyl); 0.91 – 0.82 (m, 3H, CH₃ alkyl) ; ¹³C NMR (75 MHz, CDCl₃) δ 156.5; 151.8; 143.9; 134.3; 129.5; 129.4; 121.4; 120.7; 117.1; 113.2; 56.0; 53.1; 49.2; 31.7; 29.7; 29.4; 29.2; 27.2; 22.6; 14.0; HRMS (ESI, [M+H]⁺) Calculated for C₂₂H₃₁ClNO₂: 376.2043. Found: 376.2045.

N-(3-Methoxy-4-phenoxybenzyl)octan-1-amine (13).

The product was synthesized as described in the general procedure for reductive amination with 3-methoxy-4-phenoxybenzaldehyde **3** (507 mg, 2.2 mmol), octylamine (287 mg, 2.2 mmol) and sodium borohydride (6.67 mmol) to give **13** as a white solid (quant., 0.756 g). *R_f* = 0.11 (petroleum ether/ethyl acetate: 7/3). ¹H NMR (300 MHz, CDCl₃) δ 8.69 (s, 1H, CH₂-NH-CH₂); 7.49 (d, *J* = 2.0 Hz, 1H, ArH); 7.31 – 7.23 (m, 2H, ArH); 7.10 – 7.01 (m, 1H, ArH); 6.96 (dd, *J* = 8.1, 2.0 Hz, 1H, ArH); 6.93 – 6.83 (m, 3H, ArH); 4.02 (s, 2H, Ar-CH₂); 3.91 (s, 3H, OCH₃); 2.83 – 2.68 (m, 2H, NH-CH₂ alkyl); 1.91 – 1.74 (m, 2H, NHCH₂-CH₂ alkyl); 1.40 – 1.12 (m, 10H, CH₂ alkyl); 0.92 – 0.76 (m, 3H, CH₃ alkyl); ¹³C NMR (75 MHz, CDCl₃) δ 156.7; 151.3; 146.2; 129.4; 126.4; 122.9; 122.6; 119.7; 117.7; 114.3; 56.2; 50.3; 45.8; 31.5; 28.9; 28.8; 26.6; 25.9; 22.4; 13.8; HRMS (ESI, [M+H]⁺) Calculated for C₂₂H₃₂NO₂: 342.2433. Found: 342.2434.

N-(4-Phenoxybenzyl)octan-1-amine (14).

The product **14** was synthesized as described in the general procedure for reductive amination with commercially available 4-phenoxybenzaldehyde (0.400 g, 2.02 mmol), octylamine (0.261 g, 2.02 mmol) and sodium borohydride (0.229 g, 6.06 mmol) to afford **14** as a lightly yellow oil (quant., 0.628 g). *R_f* = 0.13 (100 % ethyl acetate). ¹H NMR (300 MHz, CDCl₃) δ 8.62 (br, 2H); 7.56 – 7.47 (m, 2H, ArH); 7.35 – 7.27 (m, 2H, ArH); 7.15 – 7.08 (m, 1H, ArH); 7.00 – 6.92 (m, 4H, ArH); 3.97 (s, 2H, Ar-CH₂-NH-); 2.79 – 2.66 (m, 2H, NH-CH₂); 1.88 – 1.69 (m, 2H, NH-CH₂-CH₂); 1.38 – 1.13 (m, 10H, CH₂ alkyl); 0.89 – 0.78 (m, 3H, CH₃ alkyl); ¹³C NMR (75 MHz, CDCl₃) δ 157.4; 156.2; 134.7; 129.7; 123.1; 118.9; 118.7; 53.2; 49.2; 31.8; 29.7; 29.5; 29.2; 27.3; 22.6; 14.1; HRMS (ESI, [M+H]⁺) Calculated for C₂₁H₃₀NO: 312.2327. Found: 312.2329.

N,N-Bis(4-(4-chloro-2-methoxyphenoxy)benzyl)octan-1-amine (15).

To a solution of compound **8** (150 mg, 0.46 mmol, 2.1 eq) in acetonitrile (10 mL), were added octylamine (30 mg, 0.22 mmol, 1 eq) and K₂CO₃ (95 mg, 0.69 mmol, 3.1 eq). The mixture was stirred overnight at reflux under inert gas (argon). The reaction mixture was concentrated and ethyl acetate was added. The organic solution was washed with water, dried over MgSO₄, filtered, and concentrated in vacuo. Purification by flash chromatography (linear gradient dichloromethane/methanol: 100/0 to 80/20) gave **15** as a yellow oil (76%, 0.108 g), *R_f* = 0.9

(dichloromethane/methanol: 97/3). ^1H NMR (300 MHz, CDCl_3) δ 7.28 (m, 4H, ArH); 6.98 (m, 2H, ArH); 6.91 – 6.85 (m, 8H, ArH); 3.83 (s, 6H, 2 OCH_3); 3.50 (s, 4H, 2 ArCH_2); 2.40 (t, $J = 7.2$ Hz, 2H, NCH_2); 1.25 (m, 12H, CH_2 alkyl); 0.88 (m, 3H CH_3 alkyl); ^{13}C NMR (75 MHz, CDCl_3): δ 156.5; 152.0; 144.2; 134.5; 130.1; 129.4; 121.5; 120.9; 117.1; 113.4; 57.6; 56.2; 53.4; 31.9; 29.5; 29.4; 27.4; 26.9; 22.8; 14.2; HRMS (ESI, $[\text{M}+\text{H}]^+$) Calculated for $\text{C}_{36}\text{H}_{42}\text{Cl}_2\text{NO}_4$: 622.2491. Found: 622.2502.

***N,N*-Bis(4-(4-chloro-2-hydroxyphenoxy)benzyl)octan-1-amine (16).**

The product **16** was synthesized as described in the general procedure of demethylation with compound **15** (100 mg, 0.162 mmol) to give **16** as a white powder (95%, 0.090 g). $R_f = 0.69$ (dichloromethane/methanol: 9/1). ^1H NMR (300 MHz, CDCl_3) δ 7.32 (m, 4H, ArH); 7.05 (dd, $J = 1.9$ Hz ; 0.8 Hz, 2H, ArH); 6.93 (m, 4H, ArH); 6.79 (m, 4H, ArH); 4.39 (br, 2H, 2 OH); 3.56 (s, 4H, 2 ArHCH_2); 2.44 (t, $J = 7.2$ Hz, 2H, NCH_2); 1.29 – 1.17 (m, 12H, CH_2 alkyl); 0.87 (m, 3H, CH_3 alkyl), ^{13}C NMR (75 MHz, CDCl_3) δ 155.6; 148.3; 142.5; 130.6; 129.5; 120.6; 119.8; 117.8; 116.8; 57.5; 53.4; 32.0; 29.9; 29.5; 29.4; 27.4; 22.8; 14.3; C_q missing. HRMS (DCI- CH_4 , $[\text{M}]^+$) Calculated for $\text{C}_{34}\text{H}_{37}\text{NO}_4\text{Cl}_2$: 593.2100. Found: 593.2098.

***N*-(3-Methoxy-4-phenoxybenzyl)-*N*-(4-(2-methoxyphenoxy)benzyl)octan-1-amine (17).**

Compounds **9** (144 mg, 0.49 mmol) and **11** (167 mg, 0.49 mmol) were dissolved in acetonitrile (10 mL). K_2CO_3 (169 mg, 1.225 mmol) was slowly added and the reaction mixture was stirred at reflux under argon overnight. The solvent was removed in vacuo and ethyl acetate was added. The organic solution was washed with water, dried over MgSO_4 , filtered, and concentrated in vacuo. Purification by flash chromatography (linear gradient petroleum ether/ethyl acetate: 100/0 to 90/10) gave **22** as a colorless oil (40%, 0.109 g). $R_f = 0.53$ (petroleum ether/ethyl acetate with few drops of ammonia solution). ^1H NMR (300 MHz, CDCl_3) δ 7.31 – 7.24 (m, 4H, ArH); 7.12 (ddd, $J = 8.2, 7.0, 2.0$ Hz, 1H, ArH); 7.07 – 7.00 (m, 2H, ArH); 7.00 – 6.96 (m, 1H, ArH); 6.96 – 6.93 (m, 2H, ArH); 6.93 – 6.86 (m, 6H, ArH); 3.84 (s, 3H, OCH_3); 3.82 (s, 3H, OCH_3); 3.53 (s, 4H, $\text{Ar-CH}_2\text{N}$); 2.43 (t, $J = 7.2$ Hz, 2H, NCH_2 -alkyl); 1.55 – 1.47 (m, 2H, NCH_2CH_2); 1.30 – 1.19 (m, 10H, CH_2 alkyl); 0.91 – 0.81 (m, 3H, CH_3 alkyl); ^{13}C NMR (75 MHz, CDCl_3) δ 158.1; 156.7; 151.4; 151.2; 145.3; 143.5; 137.1; 134.0; 129.8; 129.4; 124.6; 122.2; 121.1; 121.0; 120.8; 120.6; 117.0; 113.0; 112.8; 58.0; 57.7; 56.0; 55.9; 53.5; 31.8; 29.4; 29.3; 27.3; 27.0; 22.6; 14.1; HRMS (ESI, $[\text{M}+\text{H}]^+$) Calculated for $\text{C}_{36}\text{H}_{44}\text{NO}_4$: 554.3270. Found: 554.3280.

***N*-(4-(4-Chloro-2-methoxyphenoxy)benzyl)-*N*-(3-methoxy-4-phenoxybenzyl)octan-1-amine (18).**

Compounds **10** (155 mg, 0.55 mmol) and **13** (187 mg, 0.55 mmol) were solubilized in acetonitrile (10 mL) under argon. K_2CO_3 (1.37 mmol) was slowly added and the reaction mixture was stirred at reflux

overnight under argon. The solvent was removed in vacuo and ethyl acetate was added. The organic solution was washed with water, dried over MgSO_4 , filtered, and concentrated in vacuo. Purification with flash chromatography (linear gradient petroleum ether/EtOAc: 95/5 to 90/10) gave **19** as a lightly yellow oil (33%, 0.107 g). $R_f = 0.35$ (petroleum ether/EtOAc; 9/1). ^1H NMR (300 MHz, CDCl_3) δ 7.32 – 7.25 (m, 4H, ArH); 7.07 – 7.04 (m, 1H, ArH); 7.04 – 7.00 (m, 1H, ArH); 6.98 (t, $J = 1.3$ Hz, 1H, ArH); 6.97 – 6.92 (m, 2H, ArH); 6.91 – 6.87 (m, 6H, ArH); 3.83 (s, 3H, OCH_3); 3.83 (s, 3H, OCH_3); 3.53 (s, 4H, Ar- CH_2); 2.50 – 2.37 (m, 2H, NCH_2 alkyl); 1.60 – 1.45 (m, 2H, $\text{NCH}_2\text{-CH}_2$ alkyl); 1.33 – 1.23 (m, 10H, CH_2 alkyl); 0.92 – 0.84 (m, 4H, CH_3 alkyl); ^{13}C NMR (75 MHz, CDCl_3) δ 158.1; 156.3; 151.8; 151.2; 144.1; 143.5; 137.1; 134.4; 129.9; 129.4; 129.3; 122.2; 121.4; 120.9; 120.8; 120.6; 117.0; 116.9; 113.3; 112.9; 58.0; 57.6; 56.1; 55.9; 53.5; 31.8; 29.4; 29.3; 27.3; 27.0; 22.6; 14.1. HRMS (ESI, $[\text{M}+\text{H}]^+$) Calculated for $\text{C}_{36}\text{H}_{43}\text{ClNO}_4$: 588.2881. Found: 558.2882.

***N*-(4-(4-Chloro-2-methoxyphenoxy)benzyl)-*N*-(4-phenoxybenzyl)octan-1-amine (19).**

Compounds **8** (142.6 mg, 0.46 mmol) and **14** (150 mg; 0.46 mmol) were dissolved in acetonitrile (10 mL) and K_2CO_3 (158.2 mg, 1.14 mmol) was added. The reaction mixture was stirred at reflux for 24 h. The solvent was removed in vacuo and ethyl acetate was added. The organic solution was washed with water, dried over MgSO_4 , filtered, and concentrated in vacuo. Purification by flash chromatography (linear gradient (dichloromethane/methanol: 100/0 to 97/3)) gave **19** as a yellow oil (74%, 0.191 g). $R_f = 0.8$ (dichloromethane/methanol: 97/3). ^1H NMR (300 MHz, CDCl_3) δ 7.39 – 7.32 (m, 6H, ArH); 7.12 (m, 1H, ArH); 7.07 – 6.98 (m, 5H, ArH); 6.96 – 6.92 (m, 4H, ArH); 3.85 (s, 3H, OCH_3); 3.57 (s, 4H, Ar CH_2); 2.47 (t, $J = 7.1$ Hz, 2H, NCH_2 alkyl); 1.64 – 1.27 (m, 10H, CH_2 alkyl); 0.94 (m, 3H, CH_3 alkyl); ^{13}C NMR (75 MHz, CDCl_3) δ 157.5; 156.5; 156.0; 151.9; 144.2; 135.0; 134.5; 130.1; 130.0; 129.7; 129.4; 123.1; 121.5; 120.9; 118.7; 117.0; 113.4; 57.7; 56.2; 53.4; 32.0; 29.5; 29.4; 27.4; 27.0; 22.8; 14.2; HRMS (ESI, $[\text{M}+\text{H}]^+$) Calculated for $\text{C}_{35}\text{H}_{41}\text{ClNO}_3$: 558.2775. Found: 558.2770.

***N*-(3-methoxy-4-phenoxybenzyl)-*N*-(4-phenoxybenzyl)octan-1-amine (20).**

To a solution of compound **14** (95.6 mg, 0.3 mmol) dissolved in acetonitrile (10 mL), compound **9** (90.2 mg, 0.3 mmol) and K_2CO_3 (106 mg, 0.76 mmol) were added. The mixture was refluxed for 21 h under argon. The solvent was removed in vacuo, ethyl acetate was added, and the organic mixture was washed with water (3X) and brine, dried over MgSO_4 , filtered, and concentrated in vacuo. Purification by flash chromatography (linear gradient petroleum ether with 0.5 % ammonia solution/ethyl acetate: 100/0 to 80/20) gave **20** as a yellow oil (97%, 154.6 mg). $R_f = 0.37$ (petroleum ether/ethyl acetate with few drops of ammonia solution; 9/1). ^1H NMR (300 MHz, CDCl_3): δ 7.41 – 7.27 (m, 6H, ArH); 7.17 – 7.09 (m, 2H, ArH); 7.08 – 7.01 (m, 4H, ArH); 7.01 – 6.98 (m, 2H, ArH); 6.98 –

6.93 (m, 3H, ArH); 3.87 (s, 3H, OCH₃); 3.60 (s, 4H, Ar-CH₂-N); 2.50 (t, J = 7.1 Hz, 2H, N-CH₂ alkyl); 1.67 – 1.52 (m, 2H, NHCH₂-CH₂); 1.42 – 1.23 (m, 10H, CH₂ alkyl); 0.99 – 0.87 (m, 3H, CH₃ alkyl). ¹³C NMR (75 MHz, CDCl₃) δ 158.1; 157.4; 155.9; 151.2; 143.5; 137.0; 134.8; 130.0; 129.6; 129.4; 123.0; 122.2; 120.9; 120.6; 118.64; 118.59; 117.0; 112.9; 58.0; 57.7; 55.8; 53.5; 31.8; 29.4; 29.3; 27.3; 27.0; 22.6; 14.1; HRMS (DCI-CH₄, [M+H]⁺) Calculated for C₃₅H₄₂NO₃: 524.3165. Found: 524.3158.

5-(((4-(2-Hydroxyphenoxy)benzyl)(octyl)amino)methyl)-2-phenoxyphenol (21).

To a solution of compound **17** (100 mg, 0.18 mmol) in dry dichloromethane, boron tribromide (0.54 mL, 0.54 mmol) was slowly added at -80 °C under argon. The reaction mixture was stirred at -80 °C for 1 h then for 4 h at room temperature. The reaction was quenched with cold water at 4 °C followed by a saturated NaHCO₃ (aq) solution. The aqueous solution was extracted with dichloromethane (3 ×). Combined organic layers were dried over MgSO₄, filtered, and concentrated *in vacuo*. Purification by flash chromatography (linear gradient dichloromethane/methanol/ammonia solution: 99.5/0/0.5 to 95/5) gave **21** as a lightly yellow oil (71%, 0.068 g). *R_f* = 0.22 (dichloromethane/methanol: 97/3 with few drops of ammonia solution). ¹H NMR (300 MHz, CDCl₃) δ 7.38 – 7.29 (m, 4H, ArH), 7.14 – 7.07 (m, 2H, ArH), 7.05 – 7.01 (m, 3H, ArH), 7.01 – 6.94 (m, 3H, ArH), 6.90 – 6.79 (m, 4H, ArH), 3.53 (s, 2H, Ar-CH₂-N), 3.49 (s, 2H, Ar-CH₂-N), 2.49 – 2.36 (m, 2H, NCH₂), 1.60 – 1.43 (m, 2H, CH₂ alkyl), 1.35 – 1.13 (m, 10H, CH₂ alkyl), 0.93 – 0.82 (m, 3H, CH₃ alkyl); ¹³C NMR (75 MHz, CDCl₃) δ 157.0; 155.5; 147.4; 147.2; 143.7; 142.0; 137.0; 135.3; 130.1; 129.8; 124.5; 123.4; 120.7; 120.5; 118.7; 118.6; 117.7; 116.3; 116.1; 57.7; 57.6; 53.4; 31.9; 29.4; 29.3; 27.3; 26.9; 22.6; 14.1; HRMS (ESI, [M+H]⁺) Calculated for C₃₄H₄₀NO₄: 526.2957. Found: 526.2957.

5-Chloro-2-(4-(((3-hydroxy-4-phenoxybenzyl)(octyl)amino)methyl)phenoxy)phenol (22).

The product **22** was synthesized as described in the procedure of demethylation with compound **18** (100 mg, 0.17 mmol). Purification by flash chromatography (linear gradient petroleum ether/ethyl acetate: 95/5 to 90/10) gave compound **22** as a brown oil (92%, 0.090 g). *R_f* = 0.69 (petroleum ether/ethyl acetate: 7/3). ¹H NMR (300 MHz, CDCl₃) δ 7.37 – 7.27 (m, 4H, ArH); 7.14 – 7.03 (m, 3H, ArH); 7.02 – 6.96 (m, 2H, ArH); 6.93 – 6.88 (m, 2H, ArH); 6.83 – 6.77 (m, 4H, ArH); 3.64 (s, 2H, Ar-CH₂); 3.61 (s, 2H, Ar-CH₂); 2.62 – 2.41 (m, 2H, NCH₂); 1.65 – 1.45 (m, 2H, NCH₂-CH₂ alkyl); 1.29 – 1.16 (m, 10H, CH₂ alkyl); 0.93 – 0.81 (m, 3H, CH₃ alkyl); ¹³C NMR (75 MHz, CDCl₃) δ 156.8; 156.1; 148.6; 147.5; 142.9; 142.2; 133.9; 132.4; 130.8; 129.8; 129.5; 123.5; 121.2; 120.3; 120.1; 118.8; 117.9; 117.4; 117.0; 116.8; 57.1; 57.0; 52.1; 31.8; 29.3; 29.2; 27.1; 25.9; 22.6; 14.1; HRMS (DCI-CH₄, [M+H]⁺) Calculated for C₃₄H₃₉ClNO₄: 560.2568. Found: 560.2574.

5-Chloro-2-(4-((octyl(4-phenoxybenzyl)amino)methyl)phenoxy)phenol (23).

The product **23** was synthesized as described in the general procedure of demethylation with compound **19** (180 mg, 0.322 mmol) solubilized in CH₃COOH/HBr 48% (1.5/1.5 mL). Purification by flash chromatography (linear gradient dichloromethane/methanol: 100/0 to 95/5) gave **23** as a viscous brown oil (quant., 0.210 g). *R_f* = 0.66 (dichloromethane/methanol: 9/1). ¹H NMR (300 MHz, CDCl₃) δ 8.33 (br, 1H, OH), 7.44 – 7.38 (m, 2H, ArH), 7.37 – 7.30 (m, 4H, ArH), 7.15 – 7.08 (m, 2H, ArH), 7.04 – 6.98 (m, 2H, ArH), 6.98 – 6.92 (m, 2H, ArH), 6.89 – 6.84 (m, 2H, ArH), 6.82 (d, *J* = 8.6 Hz, 1H, ArH), 6.76 (dd, *J* = 8.6, 2.3 Hz, 1H, ArH), 3.84 (s, 2H, Ar-CH₂), 3.81 (s, 2H, Ar-CH₂), 2.72 – 2.54 (m, 2H, NCH₂ alkyl), 1.74 – 1.57 (m, 2H, NCH₂-CH₂ alkyl), 1.25 – 1.14 (m, 10H, CH₂ alkyl), 0.87 (t, *J* = 6.7 Hz, 3H, CH₃ alkyl); ¹³C NMR (75 MHz, CDCl₃) δ 157.5; 157.1; 156.7; 149.0; 141.9; 131.5; 129.9; 129.8; 123.7; 120.9; 120.4; 119.3; 118.6; 117.4; 117.2; 56.8; 52.2; 31.8; 29.8; 29.2; 27.1; 25.3; 22.7; 14.2; C_q missing; HRMS (ESI, [M+H]⁺) Calculated for C₃₄H₃₉ClNO₃: 544.2618. Found: 544.2600.

5-((octyl(4-phenoxybenzyl)amino)methyl)-2-phenoxyphenol (24).

The product **24** was synthesized as described in the general procedure of demethylation with compound **20** (91.4 mg, 0.175 mmol) solubilized in CH₃COOH/HBr 48% (1/1 mL). Purification by flash chromatography (linear gradient dichloromethane/methanol: 100/0 to 96/4) gave **24** as a yellow oil (43%, 44.7 mg). *R_f* = 0.26 (dichloromethane/methanol; 97/3). ¹H NMR (300 MHz, CDCl₃) δ 7.37 – 7.27 (m, 6H, ArH); 7.15 – 7.05 (m, 3H, ArH); 7.04 – 6.91 (m, 6H, ArH); 6.87 – 6.78 (m, 2H, ArH); 3.53 (s, 2H, Ar-CH₂-NH); 3.50 (s, 2H, Ar-CH₂-NH); 2.42 (t, *J* = 7.1 Hz, 2H, NHCH₂); 1.58 – 1.44 (m, 2H, NHCH₂-CH₂); 1.36 – 1.16 (m, 10H, CH₂ alkyl); 0.94 – 0.80 (m, 3H, CH₃ alkyl); ¹³C NMR (75 MHz, CDCl₃) δ 157.5; 157.0; 155.9; 147.2; 142.0; 137.1; 134.9; 130.0; 129.8; 129.6; 123.4; 123.0; 120.8; 118.66; 118.65; 118.60; 117.8; 116.3; 57.75; 57.66; 53.34; 31.9; 29.5; 29.3; 27.3; 26.9; 22.6; 14.1; HRMS (DCI-CH₄, [M+H]⁺) Calculated for C₃₄H₄₀NO₃: 510.3008. Found: 510.3008.

5-((Octylamino)methyl)-2-phenoxyphenol (25).

To a solution of compound **13** (104 mg, 0.29 mmol) dissolved in dichloromethane (25 mL), boron tribromide (0.87 mL, 0.87 mmol) was added drop wise at -80 °C under argon. The reaction mixture was stirred at this temperature for 1 h and then was gradually warmed to room temperature and stirred for 4 h. Cold water (10 mL) was added at 4 °C followed by addition of a saturated water solution of NaHCO₃. The aqueous layer was extracted with dichloromethane (2×) and the combined organic layers were dried over MgSO₄, filtered, and concentrated under reduced pressure to give compound **25** as a beige powder (99%, 0.099 g). *R_f* = 0.37 (dichloromethane/methanol: 9/1 with a drop of ammonia solution). ¹H NMR (300 MHz, CDCl₃) δ 7.33 – 7.25 (m, 2H, ArH); 7.10 – 7.01 (m, 1H, ArH); 6.97 – 6.89 (m, 3H, ArH); 6.80 (d, *J* = 8.2 Hz, 1H, ArH); 6.69 (dd, *J* = 8.2, 2.1 Hz, 1H, ArH); 5.14

(br, 1H); 3.67 (br, 1H); 2.66 – 2.55 (m, 2H, Ar-CH₂-NH); 1.54 – 1.41 (m, 2H, -NH-CH₂-alkyl); 1.32 – 1.17 (m, 12H, CH₂ alkyl); 0.94 – 0.80 (m, 3H, CH₃ alkyl); ¹³C NMR (75 MHz, CDCl₃) δ 157.3; 148.3; 142.8; 136.2; 129.7; 123.0; 120.1; 119.5; 117.5; 117.2; 53.2; 49.1; 31.8; 29.5; 29.4; 29.2; 27.3; 22.6; 14.1; HRMS (ESI, [M+H]⁺) Calculated for C₂₁H₃₀NO₂: 328.2271. Found: 328.228545

***N*-(4-(4-Chloro-2-methoxyphenoxy)benzyl)-*N*-octyloctan-1-amine (26).**

Compound **12** (100 mg, 0.27 mmol) and 1-bromooctane (51 mg, 0.27 mmol) were dissolved in acetonitrile (10 mL). Then K₂CO₃ (93 mg, 0.66 mmol) was slowly added. The reaction mixture was stirred at reflux for 22 h. The solvent was removed in vacuo and ethyl acetate was added. The organic layer was washed with water, dried over MgSO₄, filtered, and concentrated *in vacuo*. Purification by flash chromatography (linear gradient dichloromethane/methanol: 100/0 to 95/5) gave **26** as a yellow oil (44%, 0.057 g). *R_f* = 0.29 (dichloromethane/methanol: 97/3). ¹H NMR (300 MHz, CDCl₃) δ 7.28 – 7.22 (m, 2H, ArH); 7.00 – 6.96 (m, 1H, ArH); 6.91 – 6.84 (m, 4H, ArH); 3.84 (s, 3H, OCH₃); 3.51 (s, 2H, Ar-CH₂-N); 2.44 – 2.31 (m, 4H, N-CH₂-alkyl); 1.52 – 1.38 (m, 4H, N-CH₂-CH₂-alkyl); 1.30 – 1.19 (m, 20H, CH₂); 0.95 – 0.81 (m, 6H, CH₃ alkyl); ¹³C NMR (75 MHz, CDCl₃) δ 156.1; 151.7; 144.3; 130.0; 129.2; 121.2; 120.8; 117.0; 113.3; 57.9; 56.1; 53.6; 31.8; 29.5; 29.3; 27.4; 26.9; 22.6; 14.1; C_q missing; HRMS (DCI-CH₄, [M+H]⁺) Calculated for C₃₀H₄₇ClNO₂: 488.3295. Found: 488.3283.

5-Chloro-2-(4-((dioctylamino)methyl)phenoxy)phenol (27).

The product **27** was synthesized as described in the general procedure of demethylation with compound **26** (57 mg, 0.116 mmol). Filtration on silica (dichloromethane/methanol: 9/1) gave **27** as a brown oil (95%, 0.062 g). *R_f* = 0.5 (dichloromethane/methanol: 9/1). ¹H NMR (300 MHz, CDCl₃) δ 10.08 (br, 1H, OH); 7.22 – 7.15 (m, 2H, ArH); 7.09 (d, *J* = 2.4 Hz, 1H, ArH); 6.86 (d, *J* = 8.5 Hz, 1H, ArH); 6.83 – 6.78 (m, 2H, ArH); 6.76 (dd, *J* = 8.6, 2.4 Hz, 1H); 3.95 (s, 2H, Ar-CH₂-N); 2.86 – 2.66 (m, 4H, N-CH₂-alkyl); 1.71 – 1.50 (m, 4H N-CH₂-CH₂-alkyl); 1.32 – 1.13 (m, 20H, CH₂ alkyl); 0.96 – 0.78 (m, 6H, CH₃ alkyl); ¹³C NMR (75 MHz, CDCl₃) δ 156.3; 149.2; 142.4; 130.9; 129.6; 120.3; 119.9; 117.3; 117.2; 57.1; 52.9; 31.8; 29.3; 29.2; 27.2; 22.6; 14.1; C_q missing; HRMS (DCI-CH₄, [M+H]⁺) Calculated for C₂₉H₄₅ClNO₂: 474.3139. Found: 474.3126.

3-Methoxy-4-phenoxybenzotrile (28).

A solution of phenol (0.564 g, 6 mmol), 4-fluoro-3-methoxybenzotrile (0.756 g, 5 mmol) and K₂CO₃ (0.829 g, 6 mmol) in anhydrous *N,N*-dimethylformamide was heated at 120 °C and stirred overnight. The reaction mixture was concentrated and the resulting residue was diluted with ethyl acetate. The organic layer was washed with water and brine, dried over MgSO₄, filtered, and concentrated in

vacuo. Purification by flash chromatography (petroleum ether/ethyl acetate 9/1) gave **28** as a white solid (1.121g, 82%). $R_f = 0.44$ (petroleum ether/ ethyl acetate: 9/1). $^1\text{H NMR}$ (300 MHz, CDCl_3) δ 7.41 – 7.33 (m, 2H, ArH); 7.23 – 7.14 (m, 3H, ArH); 7.05 – 6.98 (m, 2H, ArH); 6.88 – 6.83 (m, 1H, ArH); 3.91 (s, 3H, OCH_3); $^{13}\text{C NMR}$ (75 MHz, CDCl_3) δ 155.6; 150.65; 150.61; 130.0; 125.9; 124.4; 119.1; 118.8; 118.6; 106.7; 115.5; 56.2; HRMS (DCI-CH_4 , $[\text{M}+\text{H}]^+$) Calculated for $\text{C}_{14}\text{H}_{12}\text{NO}_2$: 226.0868. Found: 226.0873.

(3-Methoxy-4-phenoxyphenyl)methanamine (29).

To a solution of compound **28** (207 mg, 0.92 mmol) solubilized in anhydrous tetrahydrofuran (10 mL) under inert gas (argon), LiAlH_4 (2 mL, 4.8 mmol) was added dropwise at $-80\text{ }^\circ\text{C}$. The mixture was stirred 1 h at $-80\text{ }^\circ\text{C}$ then overnight at room temperature. The reaction was neutralized with addition of water, in ice bath. The solvent was then removed in vacuo and ethyl acetate was added. The organic phase was washed with water and brine, dried over MgSO_4 , filtered, and concentrated under reduced pressure to give **29** as a yellowish oil (98 %, 0.206 mg). $R_f = 0.55$ (dichloromethane/methanol: 9/1 with few drops of ammonia solution). $^1\text{H NMR}$ (300 MHz, CDCl_3) δ 7.30 – 7.21 (m, 2H, ArH); 7.04 – 6.97 (m, 2H, ArH); 6.94 – 6.89 (m, 3H, ArH); 6.86 – 6.79 (m, 1H, ArH); 3.84 (s, 2H, Ar- CH_2); 3.81 (s, 3H, OCH_3); 1.97 (b, 2H, NH_2); $^{13}\text{C NMR}$ (75 MHz, CDCl_3) δ 157.9; 151.4; 143.6; 139.6; 129.3; 122.2; 121.0; 119.4; 116.8; 111.7; 55.8; 46.0; HRMS (DCI-CH_4 , $[\text{M}+\text{H}]^+$) Calculated for $\text{C}_{14}\text{H}_{16}\text{NO}_2$: 230.1181. Found: 230.1178.

(4-Phenoxyphenyl)methanamine (30).

The product **30** was synthesized as described for compound **29** [28]. Briefly, to a solution of LiAlH_4 (187 mg, 5.2 mmol) in anhydrous tetrahydrofuran (15 mL), was added 4-phenoxybenzotrile (500 mg, 2.6 mmol) at $4\text{ }^\circ\text{C}$. After 18 h of stirring, water (10 mL) was added and the mixture was stirred for another 45 minutes. The mixture was filtered, concentrated under vacuum, and then ethyl acetate was added. The organic layer was washed with brine, dried over MgSO_4 , filtered, and concentrated under reduced pressure to give compound **32** as a yellowish powder (100%, 0,513 g). ($R_f = 0.17$ dichloromethane/methanol: 90/10 with few drops of ammonia solution). $^1\text{H NMR}$ (300 MHz, CDCl_3) δ 7.37 – 7.28 (m, 3H); 7.28 – 7.25 (m, 1H, ArH); 7.13 – 7.05 (m, 1H, ArH); 7.04 – 6.96 (m, 4H, ArH); 3.84 (s, 2H, Ar- CH_2); $^{13}\text{C NMR}$ (75 MHz, CDCl_3) δ 157.3; 155.8; 138.2; 129.5; 128.3; 122.9; 118.9; 118.5; 45.7. NMR data are in agreement with those already reported in the literature [28].

N-(3-Methoxy-4-phenoxybenzyl)-1-(4-phenoxyphenyl)methanamine (31).

To a solution of compound **29** (150 mg, 0.654 mmol) solubilized in anhydrous dichloromethane (10 mL) with molecular sieves (4 Å) under inert gas (argon), 4-phenoxybenzaldehyde (115 µL, 0.654 mmol) was added. The mixture was stirred overnight at room temperature, filtered, and evaporated under reduced pressure. The resulting dried imine compound was dissolved in methanol/ethanol (1:1, 10 mL) and reduced with sodium borohydride (120 mg, 3.17 mmol) for 5 h. Saturated aqueous solution of NH₄Cl was added to neutralize residual sodium borohydride. The mixture was extracted with ethyl acetate and combined organic layers were washed with brine, dried over MgSO₄, filtered, and concentrated under reduced pressure. Purification by flash chromatography (linear gradient petroleum ether/ethyl acetate: 100/0 to 70-30) gave **31** as a yellowish oil (73 %, 0.197 g). *R_f* = 0.08 (petroleum ether/ethyl acetate: 7/3). ¹H NMR (300 MHz, CDCl₃) δ 7.39 – 7.28 (m, 6H, ArH); 7.16 – 7.09 (m, 1H, ArH); 7.09 – 7.01 (m, 6H, ArH); 7.01 – 6.96 (m, 3H, ArH), 6.92 (dd, *J* = 8.1, 1.9 Hz, 1H, ArH); 3.86 (s, 3H, OCH₃); 3.85 (s, 4H, Ar-CH₂); 2.07 (br, 1H, NH₂); ¹³C NMR (75 MHz, CDCl₃) δ 158.0; 157.3; 156.0; 151.3; 143.7; 137.0; 135.0; 129.6; 129.4; 129.3; 123.0; 122.2; 120.8; 120.5; 118.8; 118.6; 116.9; 112.5; 55.8; 52.8; 52.5; HRMS (DCI-CH₄, [M+H]⁺) Calculated for C₂₇H₂₆NO₃: 412.1913. Found: 412.1903.

***N*-(4-(4-Chloro-2-methoxyphenoxy)benzyl)-1-(4-phenoxyphenyl)methanamine (32).**

Compounds **2** (131 mg, 0.5 mmol) and **30** (100 mg, 0.5 mmol) were dissolved in dry dichloromethane (20 mL) in the presence of molecular sieves (4 Å). The reaction mixture was stirred at room temperature for 20 h. Molecular sieves were filtered and the reaction mixture was concentrated in vacuo. The residue was dissolved in methanol/ethanol (1:1, 20 mL) and NaBH₄ (57 mg, 1.5 mmol) was added. After 2 h, NH₄Cl_{sat} was added and the reaction mixture was extracted with ethyl acetate (3×) and the combined organic layers were washed with brine, dried over MgSO₄, filtered, and concentrated under reduced pressure. Purification by flash chromatography (linear gradient dichloromethane (0.5 % of ammonia solution)/methanol: 100/0 to 92:8) gave compound **32** as a lightly yellow oil (39%, 0.086 g). *R_f* = 0.76 (dichloromethane with few drops of ammonia solution). ¹H NMR (300 MHz, CDCl₃) δ 7.38 – 7.26 (m, 6H, ArH); 7.13 – 7.06 (m, 1H, ArH); 7.03 – 6.95 (m, 5H, ArH); 6.93 – 6.85 (m, 4H, ArH); 3.83 (s, 3H, OCH₃); 3.79 (s, 2H, CH₂); 3.78 (s, 2H, CH₂); ¹³C NMR (75 MHz, CDCl₃) δ 157.4; 156.5; 156.1; 151.8; 144.0; 135.2; 134.7; 129.7; 129.5; 129.4; 123.0; 121.4; 120.8; 118.9; 118.6; 117.2; 113.3; 26.1; 52.6; 52.5; HRMS (ESI, [M+H]⁺) Calculated for C₂₇H₂₅ClNO₃: 446.1523. Found: 446.1522.

2-Phenoxy-5-(((4-phenoxybenzyl)amino)methyl)phenol (33).

To a solution of **31** (157 mg, 0.382 mmol) solubilized in anhydrous CH_2Cl_2 (10 mL), boron tribromide (1.5 mL, 1.5 mmol) was added drop wise at -80°C under inert gas (argon). The mixture was stirred for 5 h followed by the addition of cold methanol (5 mL) to neutralize the reaction. The solvent was removed in vacuo, followed by 3 extractions with ethyl acetate and saturated solution of NaHCO_3 . Combined organic layers were dried over MgSO_4 , filtered, and concentrated at reduced pressure. Purification by flash chromatography (linear gradient dichloromethane/methanol: 100/0 to 90/10) gave **33** as a brown solid (92 %, 0.140 g). $R_f = 0.41$ (dichloromethane/methanol: 9/1). ^1H NMR (300 MHz, CDCl_3) δ 7.37 – 7.26 (m, 6H, ArH); 7.14 – 7.04 (m, 2H, ArH); 7.03 – 7.00 (m, 2H, ArH); 7.00 – 6.96 (m, 3H, ArH); 6.96 – 6.93 (m, 2H, ArH); 6.83 (d, $J = 8.2$ Hz, 1H, ArH); 6.77 (dd, $J = 8.2, 2.0$ Hz, 1H, ArH); 4.65 (br, 2H); 3.79 (s, 2H, Ar- CH_2); 3.74 (s, 2H, Ar- CH_2); ^{13}C NMR (75 MHz, CDCl_3) δ 157.2; 157.1; 156.3; 148.0; 142.7; 135.9; 133.8; 129.8; 129.7; 129.67; 123.1; 120.2; 119.4; 118.8; 118.75; 117.6; 116.8; 52.1; 52.0; HRMS (DCI- CH_4) $[\text{M}+\text{H}]^+$ Calculated for $\text{C}_{26}\text{H}_{24}\text{NO}_3$: 398.1756. Found: 398.1769.

5-Chloro-2-(4-(((4-phenoxybenzyl)amino)methyl)phenoxy)phenol (34).

The product **34** was synthesized as described previously with compound **30** (80 mg, 0.171 mmol) to give **34** as a lightly brown oil (quant., 0.075 g). $R_f = 0.4$ (dichloromethane/methanol with a drop of ammonia solution). ^1H NMR (300 MHz, CDCl_3) δ 7.38 – 7.29 (m, 2H, ArH); 7.29 – 7.23 (m, 2H, ArH); 7.23 – 7.15 (m, 2H, ArH); 7.14 – 7.07 (m, 1H, ArH); 7.02 (p, $J = 1.6$ Hz, 1H, ArH); 7.00 – 6.93 (m, 4H, ArH); 6.82 – 6.73 (m, 4H, ArH); 4.65 (s, 1H, NH); 3.79 (s, 2H, CH_2); 3.73 (s, 2H, CH_2); ^{13}C NMR (75 MHz, CDCl_3) δ 157.2; 156.4; 156.2; 149.3; 142.3; 134.0; 133.9; 129.9; 129.8; 127.7; 129.6; 123.2; 120.6; 120.0; 118.9; 118.8; 117.5; 117.2; 52.5; 52.2; HRMS (ESI, $[\text{M}+\text{H}]^+$) Calculated for $\text{C}_{26}\text{H}_{23}\text{ClNO}_3$: 432.1366. Found: 442.1369.

4-(4-Formylphenoxy)-3-methoxybenzaldehyde (35).

The product **35** was synthesized as described previously. Briefly, to a solution of vanilline (5.93 g, 39 mmol) dissolved in anhydrous *N,N*-dimethylformamide (70 mL), were added K_2CO_3 (10.78 g, 78 mmol) and 4-fluorobenzaldehyde (6.28 mL, 58.5 mmol). The solution was heated to 120°C overnight and then the solvent was removed in vacuo. The mixture was dissolved with EtOAc and washed with H_2O and brine, dried over MgSO_4 , filtered, and concentrated at reduced pressure to give **35** as a beige solid compound (92%, 9.27 g). $R_f = 0.48$ (petroleum ether/EtOAc; 7/3). ^1H NMR (300 MHz, CDCl_3): δ 9.96 (d, $J = 7.4$ Hz, 2H), 7.90 – 7.84 (m, 2H), 7.57 (d, $J = 1.8$ Hz, 1H), 7.50 (dd, $J = 8.1, 1.8$ Hz, 1H), 7.19 (d, $J = 8.1$ Hz, 1H), 7.11 – 7.00 (m, 2H), 3.89 (s, 3H); ^{13}C NMR (75 MHz, CDCl_3) δ 190.7; 190.6; 162.0; 151.9; 148.9; 134.1; 131.9; 131.8; 125.3; 121.4; 117.3; 111.2; 56.0; HRMS (DCI- CH_4 , $[\text{M}+\text{H}]^+$) Calculated for $\text{C}_{15}\text{H}_{13}\text{O}_4$: 257.0814. Found: 257.0821.

N-Benzyl-1-(4-(4-((benzylamino)methyl)-2-methoxyphenoxy)phenyl)methanamine (36).

The product **36** was synthesized as described previously. Briefly, to a solution of compound **35** (100 mg, 0.39 mmol) dissolved in dichloromethane (30 mL), benzylamine (85 μ L, 0.78 mmol) was added. This mixture was stirred at room temperature for 24 h. The solvent was evaporated and ethanol/methanol (1:1, 20 mL) was added followed by sodium borohydride (44.3 mg, 1.17 mmol) at 4 °C. The reaction was stirred 24 h at room temperature. The solvent was then removed in vacuo and the mixture was dissolved with dichloromethane. The organic layer was washed with saturated NaHCO₃ solution and brine, dried over MgSO₄, filtered, and concentrated in vacuo. Purification by flash chromatography (linear gradient dichloromethane/methanol: 100/0 to 91/10) gave **36** as a yellow oil (46%, 78.6 mg). R_f = 0.39 (Petroleum ether/ethyl acetate: 6/4 with few drops of ammonia solution). ¹H NMR (300 MHz, CDCl₃): δ 7.41 – 7.35 (m, 8H, ArH); 7.32 – 7.27 (m, 4H, ArH); 7.08 (d, J = 1.8 Hz, 1H, ArH); 6.99 – 6.94 (m, 3H, ArH); 6.91 (dd, J = 8.1, 1.9 Hz, 1H, ArH); 3.87 (s, 2H, Ar-CH₂-NH); 3.86 (s, 3H, OCH₃); 3.84 (s, 4H, NH-CH₂); 3.79 (s, 2H, Ar-CH₂-NH); ¹³C NMR (75 MHz, CDCl₃) δ 156.9; 151.2; 143.8; 140.08; 140.02; 136.9; 134.1; 129.2; 128.3; 128.2; 128.01; 127.98; 126.85; 126.77; 120.6; 120.4; 116.9; 112.5; 55.8; 53.1; 52.9; 52.8; 52.4; HRMS (DCI-CH₄, [M+H]⁺) Calculated for C₂₉H₃₁N₂O₂: 439.2386. Found: 439.2357

N-(4-(2-Methoxy-4-((octylamino)methyl)phenoxy)octan-1-amine (37)

Compound **35** (100 mg, 0.39 mmol), octylamine (130 μ L, 0.78 mmol) and sodium borohydride (44.3 mg, 1.17 mmol) were used to give **37** as an orange oil (100%, 188.2 mg). R_f = 0.45 (petroleum ether/ethyl acetate: 6/4 with few drops of ammonia solution). ¹H NMR (300 MHz, CDCl₃): δ 7.23 – 7.16 (m, 2H, ArH); 6.98 (d, J = 1.8 Hz, 1H, ArH); 6.89 – 6.83 (m, 3H, ArH); 6.80 (dd, J = 8.1, 1.9 Hz, 1H, ArH); 3.79 (s, 3H, OCH₃); 3.74 (s, 2H, ArCH₂); 3.69 (s, 2H, ArCH₂); 2.60 (dt, J = 10.6, 7.2 Hz, 4H, NCH₂); 1.54 – 1.40 (m, 4H, NCH₂-CH₂); 1.34 – 1.19 (m, 20H, CH₂ alkyl); 0.90 – 0.80 (m, 6H, CH₃ alkyl); ¹³C NMR (75 MHz, CDCl₃) δ 156.8; 151.1; 143.8; 137.1; 134.2; 129.1; 120.5; 120.3; 116.8; 112.4; 55.7; 53.7; 53.3; 49.4; 49.3; 31.7; 29.9; 29.8; 29.4; 29.1; 27.2; 22.5; 13.4; HRMS (DCI-CH₄, [M+H]⁺) Calculated for C₃₁H₅₁N₂O₂: 483.3951. Found: 483.3930.

5-((benzylamino)methyl)-2-(4-((benzylamino)methyl)phenoxy)phenol (38).

The product **38** was synthesized as described previously. Briefly, to a solution of compound **35** (78.6 mg, 0.18 mmol) dissolved in anhydrous dichloromethane (25 mL), boron tribromide (0.54 mL, 0.54 mmol) was added dropwise at -80 °C under argon. The mixture was stirred at the same temperature for 1 h, then warmed to room temperature for 4 h. Cold water (10 mL) was added and the solution was extracted with dichloromethane. The organic layer was washed with saturated NaHCO₃, dried

over MgSO_4 , filtered, and concentrated under reduced pressure to give **38** as a beige oil (78%, 62 mg). $R_f = 0.31$ (dichloromethane/methanol with a drop of ammonia solution; 90/10). ^1H NMR (300 MHz, DMSO): δ 7.37 – 7.23 (m, 12H, ArH); 6.96 (s, 1H, ArH); 6.94 – 6.88 (m, 2H, ArH); 6.82 (d, $J = 8.2$ Hz, 1H, ArH); 6.77 (dd, $J = 8.2, 1.8$ Hz, 1H, ArH); 3.81 (d, $J = 1.3$ Hz, 4H, NH-CH_2 alkyl); 3.76 (s, 2H, $\text{Ar-CH}_2\text{-NH}$); 3.73 (s, 2H, $\text{Ar-CH}_2\text{-NH}$); 2.66 (br, 1H); ^{13}C NMR (75 MHz, DMSO) δ 156.2; 147.9; 142.5; 139.9; 139.8; 136.9; 134.8; 129.7; 128.44; 128.41; 128.2; 127.1; 127.0; 120.1; 119.3; 117.5; 116.3; 53.1; 53.0; 52.5; 52.3; HRMS (ESI, $[\text{M}+\text{H}]^+$) Calculated for $\text{C}_{28}\text{H}_{29}\text{N}_2\text{O}_2$: 425.2229. Found: 425.2226.

5-((octylamino)methyl)-2-(4-((octylamino)methyl)phenoxy)phenol (39).

The product **39** was synthesized as described previously for compound **38**. Compound **37** (188.2 mg, 0.39 mmol) and boron tribromide (1.17 mL, 1.17 mmol) were used to give **39** as a yellow oil (90%, 182.8 mg). $R_f = 0.11$ (petroleum ether/ethyl acetate: 6/4 with few drops of ammonia solution). ^1H NMR (300 MHz, CDCl_3): δ 7.20 – 7.13 (m, 2H); 6.82 – 6.75 (m, 3H); 6.73 (d, $J = 2.0$ Hz, 1H); 6.66 (dd, $J = 8.1, 2.0$ Hz, 1H); 4.42 – 4.16 (m, 3H); 3.68 (s, 2H); 3.62 (s, 2H); 2.59 (td, $J = 7.3, 3.2$ Hz, 4H); 1.56 – 1.40 (m, 4H); 1.35 – 1.18 (m, 20H); 0.94 – 0.76 (m, 6H); ^{13}C NMR (75 MHz, CDCl_3) δ 156.9; 149.3; 142.7; 136.6; 133.5; 129.7; 120.3; 119.5; 117.6; 116.9; 74.5; 53.18; 53.12; 49.3; 49.0; 31.76; 31.75; 29.5; 29.46; 29.43; 29.40; 29.20; 29.18; 27.28; 27.26; 22.6; 14.0; HRMS (DCI- CH_4 , $[\text{M}+\text{H}]^+$) Calculated for $\text{C}_{30}\text{H}_{49}\text{N}_2\text{O}_2$: 469.3794. Found: 469.3782.

4.2. Molecular docking simulations

Molecular graphics were performed with the UCSF Chimera package [29]. The protein structures were downloaded from the RCSB Protein Database and aligned with MatchMaker [30] on the reference structure 1BVR (1BVR:A) [6]. The protein structures were prepared (structure checks, rotamers, hydrogenation, splitting of chains) using Biovia (www.3dsbiovia.com) Discovery Studio Visualizer 2021 (DSV), UCSF Chimera and in-house Python codes. Molecular modeling studies were carried out with Molegro Virtual Docker 6 (www.molexus.com) software using PDB entry 2X22:A [12], characterized by an opened minor portal, as docking target. Three molecular docking protocols (MSE, OPT and OPT-S) and two internal scoring schemes (Moldock and Rerank) [31] were combined in a multimodal (docking) and consensus (scoring) approach. The OPT-S calculation set is similar to OPT protocol but it is extended to a higher number of runs.

The protocols share the same set of flexible residues: Ala154, Ala157, Ala164, Ala198, Ala201, Ala206, Arg195, Asn231, Asp148, Asp150, Gln214, Glu219, Ile202, Ile215, Leu217, Leu218, Lys165, Met98, Met103, Met155, Met161, Met199, Met232, Phe149, Phe97, Pro193, Thr162, Thr195, Trp160, Trp22, Tyr158. Softened potentials were used with a tolerance of 1 and a strength 0.9.

According to structural studies, these residues cover different cases of minor and major portal fluctuations in known InhA structures. No displaceable water molecules were considered in the binding site (known as mainly hydrophobic). The corresponding NAD molecule (from 2X22:A) was treated as cofactor and was set as NAD⁺ with partial negative charges on phosphates and positive charge on nicotinamide group. Clustering of poses (tabu clustering) was set with an RMS threshold of 1.9 Å in order to be a little more discriminant on the best poses. Templates (pharmacophoric profile) were used with a strength of -500 and a grid resolution of 0.4 Å using conserved atom positions along InhA ligands: ether group (oxygen, hydrogen donor); alcohol group (oxygen, hydrogen donor/acceptor) and ring (carbons) of ligand TCU (PT70, taken from 2X22:A), similarity measure parameters were let at their default values. In the case of OPT (Differential evolution algorithm) protocol, the docking process used 10,000 iteration steps, and a grid resolution of 0.3 Å, along 40 independent runs. The convergence was reached for all ligands, internal parameters (population size, crossover rate, scaling factor...) of the algorithm were let as default. A final minimization (per run) was parameterized using 4,000 steps for side chains and 2,000 steps for protein backbone followed by a minimization and optimization (hydrogen bonds) of ligands. The same parameters were applied to the MSE (Simplex evolution algorithm) protocol, internal parameters (population size, number of iterations, energy threshold...) of the algorithm were let as default. These protocols were validated with ligands such as TCU of 2X22:A. Typical RMSD (Root Mean Square Deviation) values between the docking poses and X-ray structures were in the range 0.5-1.0 Å for the best poses. The most realistic complexes (best poses) were selected on the basis of best combination of MolDock, Rerank scores and similarities (or compliance) with X-ray crystal structure complexes of InhA with known inhibitors.

4.3. Preparation and evaluation of inhibition of InhA

All experiments were carried out as recently described [22].

4.4. Crystallization and structure determination

To obtain crystals of the InhA/NAD⁺/**21** complex, cleaved InhA (in 30 mM PIPES, 150 mM NaCl, pH 6.8) was incubated at 8 mg mL⁻¹ with 5.6 mM NAD⁺ for 1 h at 4 °C (corresponding to a protein/NAD⁺ ratio of 1:20) followed by 4 h incubation with compound **21** at a final concentration of 28 mM (corresponding to a protein/ligand ratio of 1:100) and 5.6% DMSO. Crystallization assays were performed using the vapor diffusion method by mixing, with the help of a Mosquito crystallization robot (SPT Labtech, Melbourn, UK), 200 nL of InhA previously incubated with NAD⁺ and compound **21** with 200 nL of reservoir containing 14% (w/v) PEG 4000, 100 mM ADA (*N*-2(acetamido)iminodiacetic acid), 100 mM ammonium acetate, 5% (v/v) DMSO, pH 6.8. Crystals were obtained within a few days at 22 °C. These crystals were cryoprotected with glycerol before being flash frozen in liquid nitrogen.

Diffraction data were collected at the ESRF beamline ID30B [32] and processed with autoProc [33] and XDS [34] (**Table 3**). The structure was solved by molecular replacement with MOLREP [35] using the A chain of PDB 4TRO as template. Refinement was performed using Buster/TNT [36]. The dictionary for compound **21** (5-(((4-(2-hydroxyphenoxy)benzyl)(octyl)amino)methyl)-2-phenoxyphenol) was generated using Grade2 [37] and used in Coot (0.9.8.1) for model building [38].

Hydrogen bonds and non-bonded contacts between InhA and ligands were analysed using the LigPlot⁺ program [25].

Table 3. Crystallographic data for the InhA/NAD⁺/21 structure.

PDB code		8OTL	
Data Collection and processing			
Beamline		ESRF, ID30B	
Space group		C222 ₁	
Cell parameters			
<i>a, b, c</i> (Å)		80.85, 100.88, 376.07	
α, β, γ (°)		90.00, 90.00, 90.00	
Resolution range (Å)	62.22 – 2.11	62.22 – 5.72	2.14 – 2.11
No. observations	752,360	38,030	38,601
No. reflections	84,677	4,652	4,438
Multiplicity	8.9	8.2	8.7
Completeness (%)	95.0	98.3	99.2
<I/σ>	9.7	22.1	2.4
R _{merge}	0.165	0.063	0.877
R _{pim}	0.058	0.031	0.310
CC(1/2)	0.996	0.998	0.673
Structure refinement			
Resolution range (Å)		30.65 – 2.11	
No. reflections (work/test)		80,266 / 4,373	
Rwork/Rfree		0.1998 / 0.2373	
No. non-H atoms			
Protein		11,603	
Cofactor		264	
Ligand		47	
Solvent		496	
Average B factors (Å²)			
Overall		31.57	
Protein		31.42	
Cofactor		27.63	
Ligand		33.60	
Solvent		36.83	
Model quality			
Rms deviation			
Bond lengths (Å)		0.0075	
Bond angles (°)		0.94	
Ramachandran plot			
Most favoured (%)		96.36	
Allowed/outliers (%)		3.26 0.38	

4.5. Inhibition of *Mtb* growth

Mycobacterium tuberculosis H37Rv reference strain was used. It was cultivated at 37 °C in Middlebrook 7H9 (liquid medium, Difco - Becton Dickinson), supplemented with 0.05% v/v Tween-80 (Sigma-Aldrich) or on Middlebrook 7H10, both supplemented with 0.2% v/v glycerol (Sigma-Aldrich) and 10% Middlebrook OADC enrichment (Difco - Becton Dickinson). All the tested compounds were dissolved in DMSO (Sigma Aldrich), instead Streptomycin (Duchefa Biochemie), used as control, was

dissolved in water. Experiments performed with Mtb strain were conducted in the BLS3 safety laboratory by authorized researchers.

The minimum inhibitory concentration (MIC₉₀) of the compounds against Mtb H37Rv strain was established using the REMA method [39]. Mtb H37Rv cultures in exponential phase of growth were diluted to concentrations of about 10⁵ bacteria/mL. 100 µL of bacterial suspensions were added to each 96-well black plate (Fluoronunc, Thermo Fisher, Waltham, MA, USA) containing 100 µL of Middlebrook 7H9 in the absence of Tween 80 and in the presence of a serial two-fold dilution of the tested compounds. A positive growth control and a negative control without inoculum were also included. After 7 days of incubation at 37°C, 10 µL of resazurin (0.025% w/v) was added to each well. Then, after an additional night of incubation, bacterial viability was assessed using a FluoroskanTM Microplate Fluorometer (Thermo Fisher Scientific, Waltham, MA, USA; excitation = 544 nm, emission = 590 nm). Finally, bacterial viability was measured as the percentage of resazurin turnover in the absence of the compound. Experiments were performed in duplicate at least twice.

Acknowledgments

We thank the staff of the mass spectrometry service, Institut de Chimie de Toulouse ICT-UAR 2599 (Université de Toulouse, CNRS, Toulouse, France, <https://ict.cnrs.fr>) for his help with chemical analyses. We thank the scientific staff of the European Synchrotron Radiation Facility (Grenoble, France), SOLEIL (Gif sur Yvette, France) and ALBA (Barcelona, Spain). We particularly thank the staff of beamline ID30B at the European Synchrotron Radiation Facility, where the crystallographic experiments were conducted. We thank Valérie Guillet for managing synchrotron radiation trips. The crystallization and macromolecular crystallography equipment used in this study are part of the Integrated Screening Platform of Toulouse (PICT, IBISA, <http://www.pict.ipbs.fr>).

Funding

We thank the Université de Toulouse, Université Toulouse III – Paul Sabatier (UT3), and CNRS for financial support. Rasoul Tamhaev thanks the Région Occitanie and the Université Fédérale de Toulouse Midi-Pyrénées (UFTMiP) for a PhD grant. This project has received funding from the Agence Nationale de la Recherche (ANR-23-CE44-0002) to C.L. and L.Mo. This research was partially supported by EU funding within the NextGenerationEU-MUR PNRR Extended Partnership initiative on Emerging Infectious Diseases (Project no. PE00000007, INF-ACT) to M.R.P.

References

- [1] WHO, Global Tuberculosis Report 2022, World Health Organization, Geneva, 2022.
- [2] D.T. Hoagland, J. Liu, R.B. Lee, R.E. Lee, New agents for the treatment of drug-resistant Mycobacterium tuberculosis, *Adv. Drug Deliv. Rev.* 102 (2016) 55-72. <http://dx.doi.org/10.1016/j.addr.2016.04.026>.
- [3] C. Vilcheze, H.R. Morbidoni, T.R. Weisbrod, H. Iwamoto, M. Kuo, J.C. Sacchettini, W.R. Jacobs, Jr., Inactivation of the inhA-encoded fatty acid synthase II (FASII) enoyl-acyl carrier protein reductase

- induces accumulation of the FASII end products and cell lysis of *Mycobacterium smegmatis*, J. Bacteriol. 182 (2000) 4059-67. <http://dx.doi.org/10.1128/JB.182.14.4059-4067.2000>.
- [4] A. Bhatt, V. Molle, G.S. Besra, W.R. Jacobs, Jr., L. Kremer, The *Mycobacterium tuberculosis* FAS-II condensing enzymes: their role in mycolic acid biosynthesis, acid-fastness, pathogenesis and in future drug development, Mol. Microbiol. 64 (2007) 1442-54. <http://dx.doi.org/10.1111/j.1365-2958.2007.05761.x>.
- [5] A. Chollet, L. Mourey, C. Lherbet, A. Delbot, S. Julien, M. Baltas, J. Bernadou, G. Pratviel, L. Maveyraud, V. Bernardes-Genisson, Crystal structure of the enoyl-ACP reductase of *Mycobacterium tuberculosis* (InhA) in the apo-form and in complex with the active metabolite of isoniazid pre-formed by a biomimetic approach, J. Struct. Biol. 190 (2015) 328-37. <http://dx.doi.org/10.1016/j.jsb.2015.04.008>.
- [6] D.A. Rozwarski, C. Vilchèze, M. Sugantino, R. Bittman, J.C. Sacchettini, Crystal structure of the *Mycobacterium tuberculosis* enoyl-ACP reductase, InhA, in complex with NAD⁺ and a C16 fatty acyl substrate, J. Biol. Chem. 274 (1999) 15582-9. <http://dx.doi.org/10.1074/jbc.274.22.15582>.
- [7] J.N. Torres, L.V. Paul, T.C. Rodwell, T.C. Victor, A.M. Amallraja, A. Elghraoui, A.P. Goodmanson, S.M. Ramirez-Busby, A. Chawla, V. Zadorozhny, E.M. Streicher, F.A. Sirgel, D. Catanzaro, C. Rodrigues, M.T. Gler, V. Crudu, A. Catanzaro, F. Valafar, Novel katG mutations causing isoniazid resistance in clinical *M. tuberculosis* isolates, Emerg. Microbes Infect. 4 (2015) e42. <http://dx.doi.org/10.1038/emi.2015.42>.
- [8] A. Chollet, L. Maveyraud, C. Lherbet, V. Bernardes-Genisson, An overview on crystal structures of InhA protein: Apo-form, in complex with its natural ligands and inhibitors, Eur. J. Med. Chem. 146 (2018) 318-343. <http://dx.doi.org/10.1016/j.ejmech.2018.01.047>.
- [9] C.W. am Ende, S.E. Knudson, N. Liu, J. Childs, T.J. Sullivan, M. Boyne, H. Xu, Y. Gegina, D.L. Knudson, F. Johnson, C.A. Peloquin, R.A. Slayden, P.J. Tonge, Synthesis and *in vitro* antimycobacterial activity of B-ring modified diaryl ether InhA inhibitors, Bioorg. Med. Chem. Lett. 18 (2008) 3029-33. <http://dx.doi.org/10.1016/j.bmcl.2008.04.038>.
- [10] M.E. Boyne, T.J. Sullivan, C.W. amEnde, H. Lu, V. Gruppo, D. Heaslip, A.G. Amin, D. Chatterjee, A. Lenaerts, P.J. Tonge, R.A. Slayden, Targeting fatty acid biosynthesis for the development of novel chemotherapeutics against *Mycobacterium tuberculosis*: evaluation of A-ring-modified diphenyl ethers as high-affinity InhA inhibitors, Antimicrob. Agents Chemother. 51 (2007) 3562-7. <http://dx.doi.org/10.1128/AAC.00383-07>.
- [11] J.S. Freundlich, F. Wang, C. Vilchèze, G. Gulten, R. Langley, G.A. Schiehser, D.P. Jacobus, W.R. Jacobs Jr., J.C. Sacchettini, Triclosan derivatives: towards potent inhibitors of drug-sensitive and drug-resistant *Mycobacterium tuberculosis*, ChemMedChem 4 (2009) 241-248. <http://dx.doi.org/https://doi.org/10.1002/cmdc.200800261>.
- [12] S.R. Luckner, N. Liu, C.W. am Ende, P.J. Tonge, C. Kisker, A slow, tight binding inhibitor of InhA, the enoyl-acyl carrier protein reductase from *Mycobacterium tuberculosis*, J. Biol. Chem. 285 (2010) 14330-7. <http://dx.doi.org/10.1074/jbc.M109.090373>.
- [13] P. Pan, S.E. Knudson, G.R. Bommineni, H.J. Li, C.T. Lai, N. Liu, M. Garcia-Diaz, C. Simmerling, S.S. Patil, R.A. Slayden, P.J. Tonge, Time-dependent diaryl ether inhibitors of InhA: structure-activity relationship studies of enzyme inhibition, antibacterial activity, and *in vivo* efficacy, ChemMedChem 9 (2014) 776-91. <http://dx.doi.org/10.1002/cmdc.201300429>.
- [14] T.J. Sullivan, J.J. Truglio, M.E. Boyne, P. Novichenok, X. Zhang, C.F. Stratton, H.J. Li, T. Kaur, A. Amin, F. Johnson, R.A. Slayden, C. Kisker, P.J. Tonge, High affinity InhA inhibitors with activity against drug-resistant strains of *Mycobacterium tuberculosis*, ACS Chem. Biol. 1 (2006) 43-53. <http://dx.doi.org/10.1021/cb0500042>.
- [15] M. Sabbah, V. Mendes, R.G. Vistal, D.M.G. Dias, M. Zahorszka, K. Mikusova, J. Kordulakova, A.G. Coyne, T.L. Blundell, C. Abell, Fragment-Based Design of *Mycobacterium tuberculosis* InhA Inhibitors, J. Med. Chem. 63 (2020) 4749-4761. <http://dx.doi.org/10.1021/acs.jmedchem.0c00007>.
- [16] P.S. Shirude, P. Madhavapeddi, M. Naik, K. Murugan, V. Shinde, R. Nandishaiah, J. Bhat, A. Kumar, S. Hameed, G. Holdgate, G. Davies, H. McMiken, N. Hegde, A. Ambady, J. Venkatraman, M. Panda, B. Bandodkar, V.K. Sambandamurthy, J.A. Read, Methyl-thiazoles: a novel mode of inhibition

with the potential to develop novel inhibitors targeting InhA in *Mycobacterium tuberculosis*, J. Med. Chem. 56 (2013) 8533-42. <http://dx.doi.org/10.1021/jm4012033>.

[17] M.R. Kuo, H.R. Morbidoni, D. Alland, S.F. Sneddon, B.B. Gourlie, M.M. Staveski, M. Leonard, J.S. Gregory, A.D. Janjigian, C. Yee, J.M. Musser, B. Kreiswirth, H. Iwamoto, R. Perozzo, W.R. Jacobs, Jr., J.C. Sacchettini, D.A. Fidock, Targeting tuberculosis and malaria through inhibition of Enoyl reductase: compound activity and structural data, J. Biol. Chem. 278 (2003) 20851-9. <http://dx.doi.org/10.1074/jbc.M211968200>.

[18] F. Rodriguez, N. Saffon, J.C. Sammartino, G. Degiacomi, M.R. Pasca, C. Lherbet, First triclosan-based macrocyclic inhibitors of InhA enzyme, Bioorg. Chem. 95 (2020). <http://dx.doi.org/10.1016/j.bioorg.2019.103498>.

[19] T. Armstrong, M. Lamont, A. Lanne, L.J. Alderwick, N.R. Thomas, Inhibition of *Mycobacterium tuberculosis* InhA: Design, synthesis and evaluation of new di-triclosan derivatives, Bioorganic & medicinal chemistry 28 (2020) 115744. <http://dx.doi.org/10.1016/j.bmc.2020.115744>.

[20] S. Chetty, T. Armstrong, S. Sharma Kharkwal, W.C. Drewe, C.I. De Matteis, D. Evangelopoulos, S. Bhakta, N.R. Thomas, New InhA inhibitors based on expanded triclosan and di-triclosan analogues to develop a new treatment for tuberculosis, Pharmaceuticals (Basel) 14 (2021). <http://dx.doi.org/10.3390/ph14040361>.

[21] T.S. Ibrahim, E.S. Tahe, E. Samir, A.M. Malebar, A.N. Khayya, M.F.A. Mohamed, R.M. Bokhti, M.A. AlAwad, I.A. Seliem, H.Z. Asfou, N.A. Alhakamy, S.S. Panda, A.M.M. Al-Mahmoudy, In vitro antimycobacterial activity and physicochemical characterization of diaryl ether triclosan analogues as potential inhA reductase inhibitors, Molecules 25 (2020). <http://dx.doi.org/10.3390/molecules25143125>.

[22] M. Chebaiki, E. Delfourne, R. Tamhaev, S. Danoun, F. Rodriguez, P. Hoffmann, E. Grosjean, F. Goncalves, J. Azema-Despeyroux, A. Pal, J. Kordulakova, N. Preuilh, S. Britton, P. Constant, H. Marrakchi, L. Maveyraud, L. Mourey, C. Lherbet, Discovery of new diaryl ether inhibitors against *Mycobacterium tuberculosis* targeting the minor portal of InhA, Eur. J. Med. Chem. 259 (2023) 115646. <http://dx.doi.org/10.1016/j.ejmech.2023.115646>.

[23] H.J. Li, C.T. Lai, P. Pan, W. Yu, N. Liu, G.R. Bommineni, M. Garcia-Diaz, C. Simmerling, P.J. Tonge, A structural and energetic model for the slow-onset inhibition of the *Mycobacterium tuberculosis* enoyl-ACP reductase InhA, ACS Chem. Biol. 9 (2014) 986-93. <http://dx.doi.org/10.1021/cb400896g>.

[24] H. Doğan, Ş.D. Doğan, M.G. Gündüz, V.S. Krishna, C. Lherbet, D. Sriram, O. Şahin, E. Sarıpinar, Discovery of hydrazone containing thiadiazoles as *Mycobacterium tuberculosis* growth and enoyl acyl carrier protein reductase (InhA) inhibitors, Eur. J. Med. Chem. 188 (2020). <http://dx.doi.org/10.1016/j.ejmech.2020.112035>.

[25] R.A. Laskowski, M.B. Swindells, LigPlot+: multiple ligand-protein interaction diagrams for drug discovery, J. Chem. Inf. Model. 51 (2011) 2778-86. <http://dx.doi.org/10.1021/ci200227u>.

[26] S.L. Kostiuik, T. Woodcock, L.F. Dudin, P.D. Howes, D.C. Harrowven, Unified syntheses of cavicularin and riccardin C: addressing the synthesis of an arene adopting a boat configuration, Chem. Eur. J. 17 (2011) 10906-15. <http://dx.doi.org/10.1002/chem.201101550>.

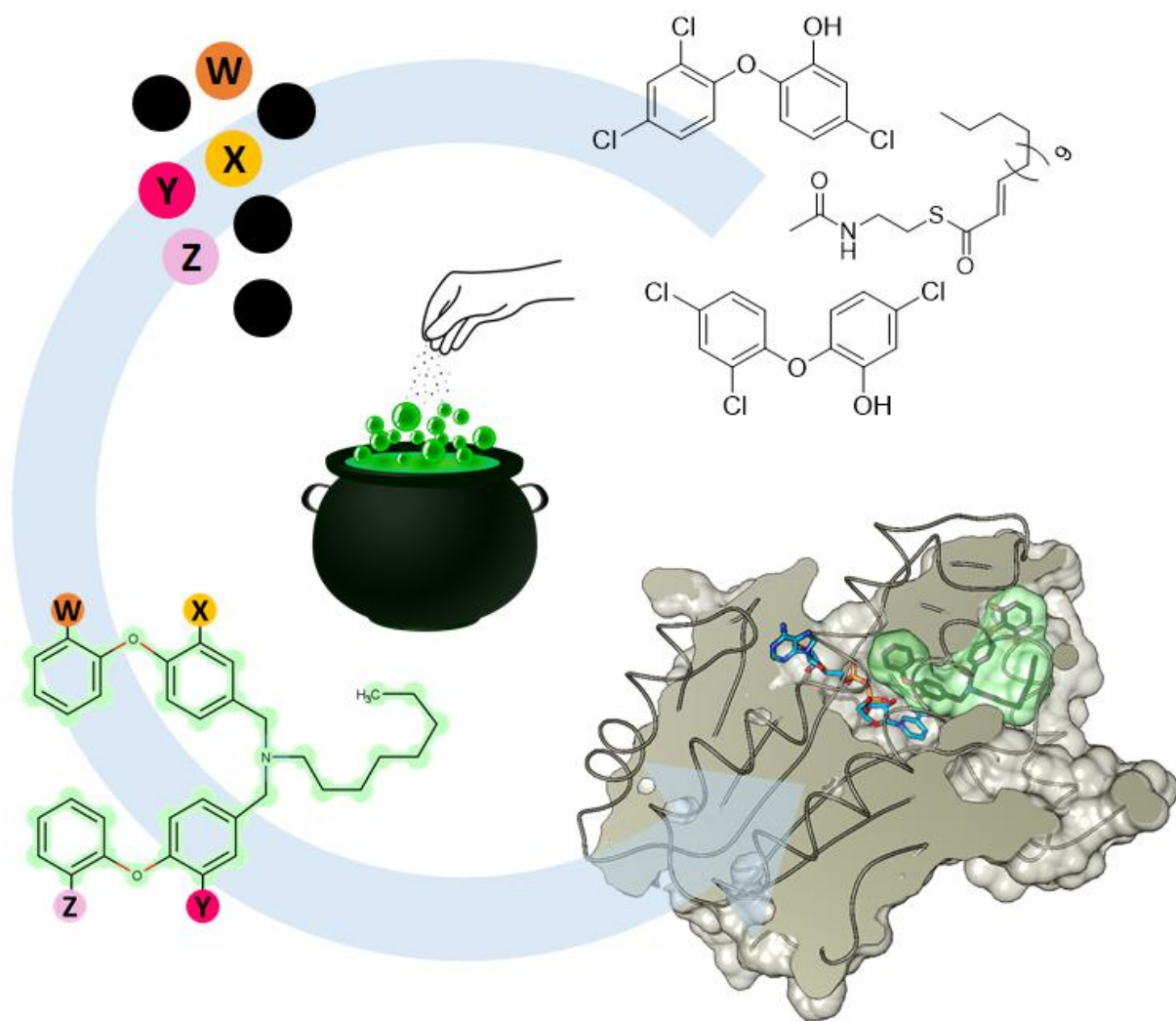
[27] J. Stec, A. Fomovska, G.A. Afanador, S.P. Muench, Y. Zhou, B.-S. Lai, K. El Bissati, M.R. Hickman, P.J. Lee, S.E. Leed, J.M. Auschwitz, C. Sommerville, S. Woods, C.W. Roberts, D. Rice, S.T. Prigge, R. McLeod, A.P. Kozikowski, Modification of triclosan scaffold in search of improved inhibitors for enoyl-acyl carrier protein (ACP) reductase in *Toxoplasma gondii*, ChemMedChem 8 (2013) 1138-1160. <http://dx.doi.org/https://doi.org/10.1002/cmdc.201300050>.

[28] C. Fotsch, J.D. Sonnenberg, N. Chen, C. Hale, W. Karbon, M.H. Norman, Synthesis and structure-activity relationships of trisubstituted phenyl urea derivatives as neuropeptide Y5 receptor antagonists, J. Med. Chem. 44 (2001) 2344-2356. <http://dx.doi.org/10.1021/jm0004547>.

[29] E.F. Pettersen, T.D. Goddard, C.C. Huang, G.S. Couch, D.M. Greenblatt, E.C. Meng, T.E. Ferrin, UCSF Chimera--a visualization system for exploratory research and analysis, J. Comput. Chem. 25 (2004) 1605-12. <http://dx.doi.org/10.1002/jcc.20084>.

- [30] E.C. Meng, E.F. Pettersen, G.S. Couch, C.C. Huang, T.E. Ferrin, Tools for integrated sequence-structure analysis with UCSF Chimera, *BMC Bioinform.* 7 (2006). <http://dx.doi.org/10.1186/1471-2105-7-339>.
- [31] R. Thomsen, M.H. Christensen, MolDock: a new technique for high-accuracy molecular docking, *J. Med. Chem.* 49 (2006) 3315-21. <http://dx.doi.org/10.1021/jm051197e>.
- [32] A.A. McCarthy, R. Barrett, A. Beteva, H. Caserotto, F. Dobias, F. Felisaz, T. Giraud, M. Guijarro, R. Janocha, A. Khadrouche, M. Lentini, G.A. Leonard, M. Lopez Marrero, S. Malbet-Monaco, S. McSweeney, D. Nurizzo, G. Papp, C. Rossi, J. Sinoir, C. Sorez, J. Surr, O. Svensson, U. Zander, F. Cipriani, P. Theveneau, C. Mueller-Dieckmann, ID30B - a versatile beamline for macromolecular crystallography experiments at the ESRF, *J. Synchrotron Radiat.* 25 (2018) 1249-1260. <http://dx.doi.org/doi:10.1107/S1600577518007166>.
- [33] C. Vonrhein, C. Flensburg, P. Keller, A. Sharff, O. Smart, W. Paciorek, T. Womack, G. Bricogne, Data processing and analysis with the autoPROC toolbox, *Acta Crystallogr. D Biol. Crystallogr.* 67 (2011) 293-302. <http://dx.doi.org/10.1107/s0907444911007773>.
- [34] W. Kabsch, XDS, *Acta crystallographica. Section D, Biological crystallography* 66 (2010) 125-32. <http://dx.doi.org/10.1107/s0907444909047337>.
- [35] A. Vagin, A. Teplyakov, Molecular replacement with MOLREP, *Acta Crystallogr. D Biol. Crystallogr.* 66 (2010) 22-5. <http://dx.doi.org/10.1107/s0907444909042589>.
- [36] G. Bricogne, E. Blanc, M. Brandl, C. Flensburg, P. Keller, W. Paciorek, P. Roversi, A. Sharff, O.S. Smart, C. Vonrhein, T.O. Womack, BUSTER version 2.10.4. Cambridge, United Kingdom: Global Phasing Ltd, 2017
- [37] O.S. Smart, A. Sharff, J. Holstein, T.O. Womack, C. Flensburg, P. Keller, W. Paciorek, C. Vonrhein, G. Bricogne, Grade2 version 1.3, 2021.
- [38] P. Emsley, K. Cowtan, Coot: model-building tools for molecular graphics, *Acta Crystallogr. D Biol. Crystallogr.* 60 (2004) 2126-32. <http://dx.doi.org/10.1107/s0907444904019158>.
- [39] J.-C. Palomino, A. Martin, M. Camacho, H. Guerra, J. Swings, F. Portaels, Resazurin microtiter assay plate: simple and inexpensive method for detection of drug resistance in *Mycobacterium tuberculosis*, *Antimicrob. Agents Chemother.* 46 (2002) 2720-2722. <http://dx.doi.org/doi:10.1128/aac.46.8.2720-2722.2002>.

Graphical Abstract



SUPPLEMENTARY MATERIAL

Exploring the plasticity of the InhA substrate-binding site using new diaryl ether inhibitors

Rasoul Tamhaev,^{a,b} Emeline Grosjean,^a Hikmat Ahamed,^a Mélina Chebaiki,^{a,b} Frédéric Rodriguez,^a Deborah Recchia,^c Giulia Degiacomi,^c Maria Rosalia Pasca,^c Laurent Maveyraud,^{b,*} Lionel Mourey,^{b,**} Christian Lherbet^{a,***}

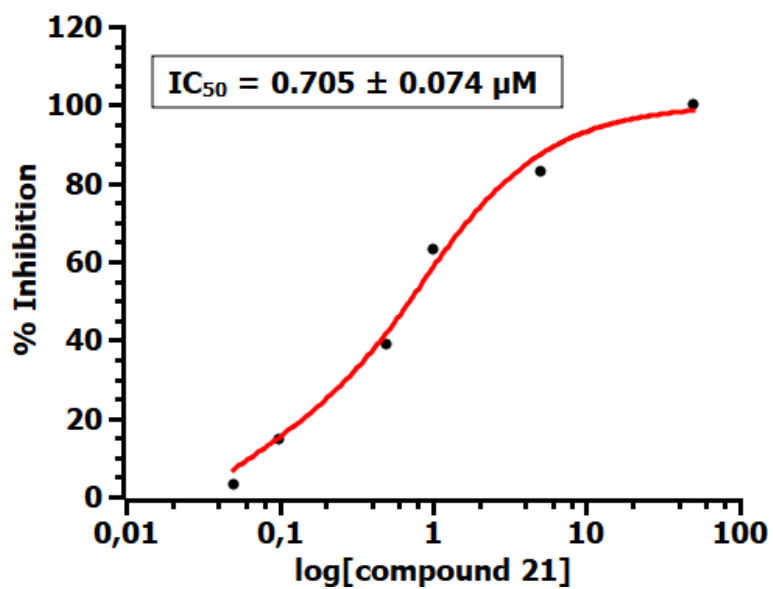
^a Synthèse et Physico-Chimie de Molécules d'Intérêt Biologique (LSPCMIB), UMR 5068, CNRS, Université Toulouse III – Paul Sabatier (UT3), Toulouse, France

^b Institut de Pharmacologie et de Biologie Structurale (IPBS), Université de Toulouse, CNRS, Université Toulouse III – Paul Sabatier (UT3), Toulouse, France.

^c Department of Biology and Biotechnology “Lazzaro Spallanzani”, University of Pavia, 27100 Pavia, Italy.

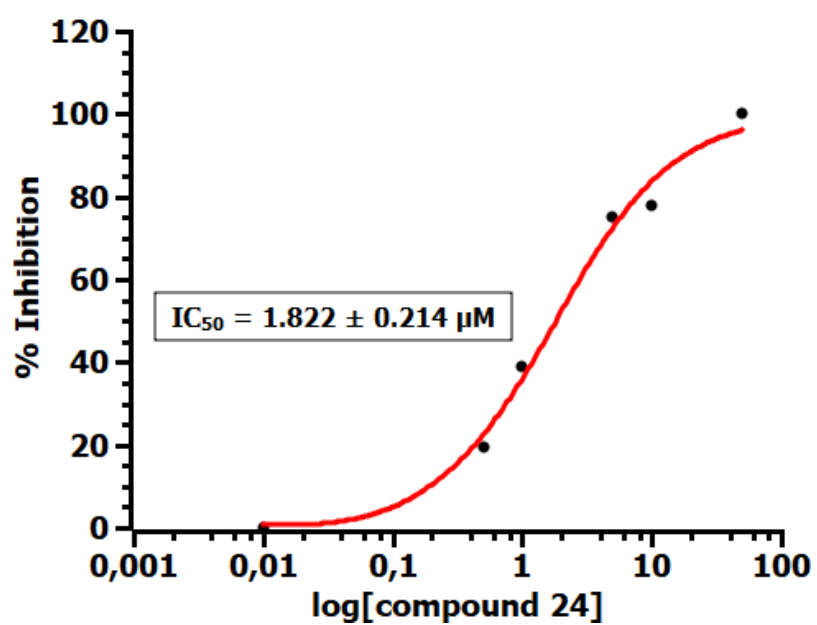
Determination of IC₅₀ for compound 21

[Inhibitor 24] (μM)	% Inhibition
50	100
5	83.2
1	63.0
0.5	39.0
0.1	14.6
0.05	3.3



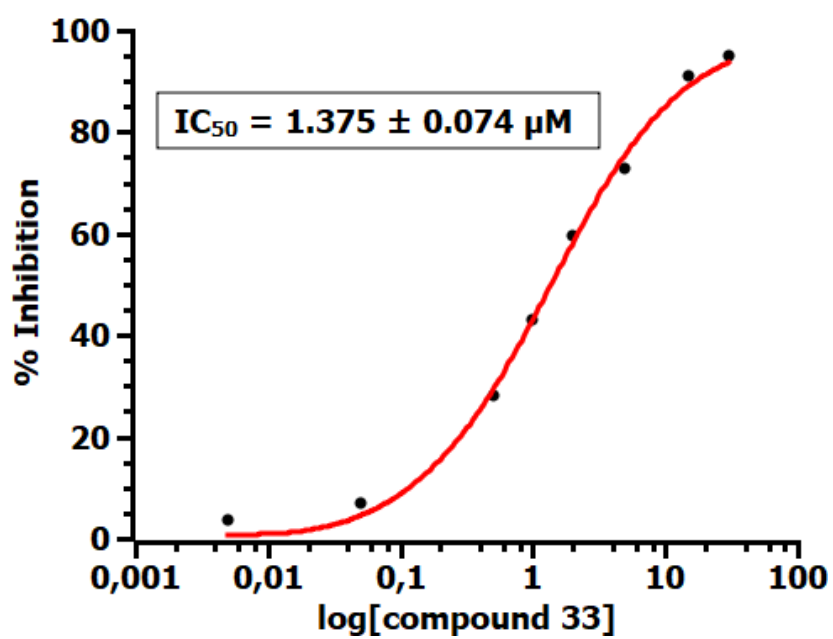
Determination of IC₅₀ for compound 24

[Inhibitor 24] (μM)	% Inhibition
50	100
10	78.0
5	75.0
1	38,9
0,5	19,3
0,01	0

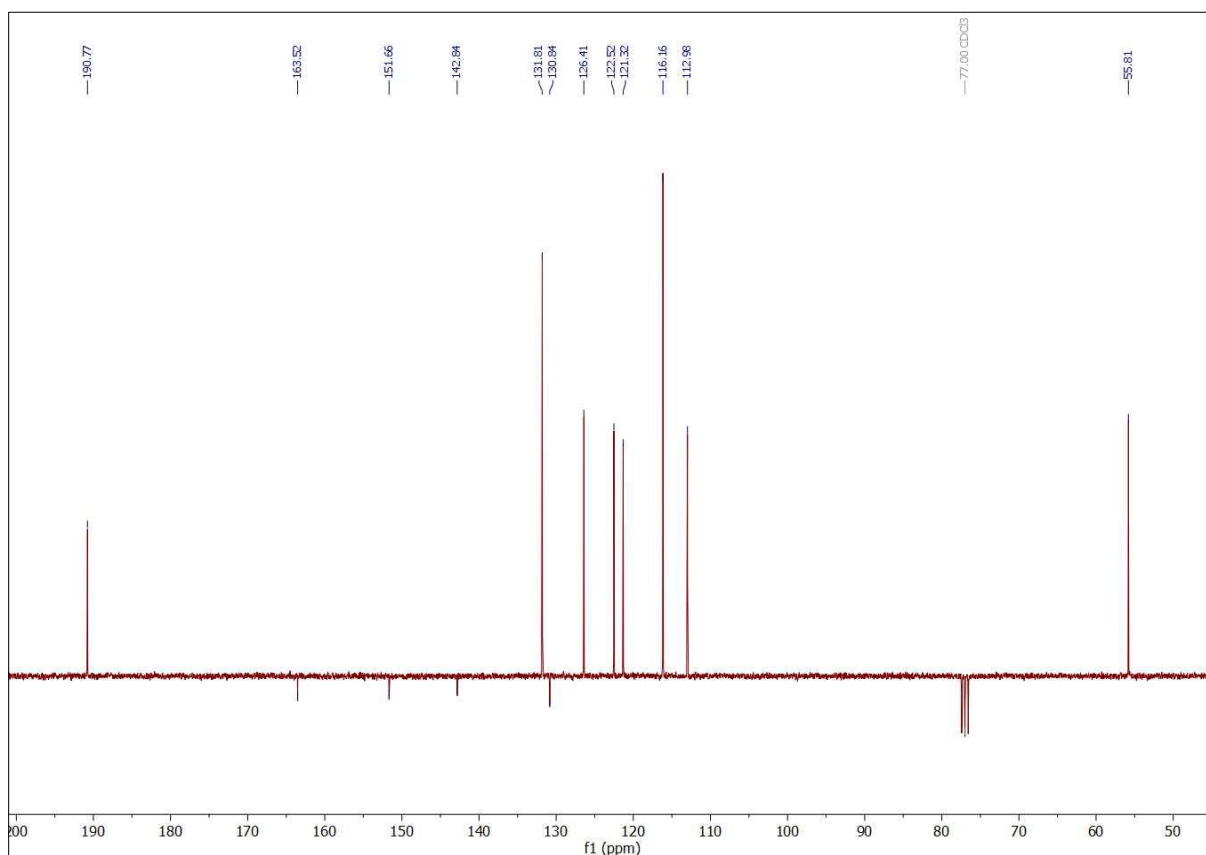
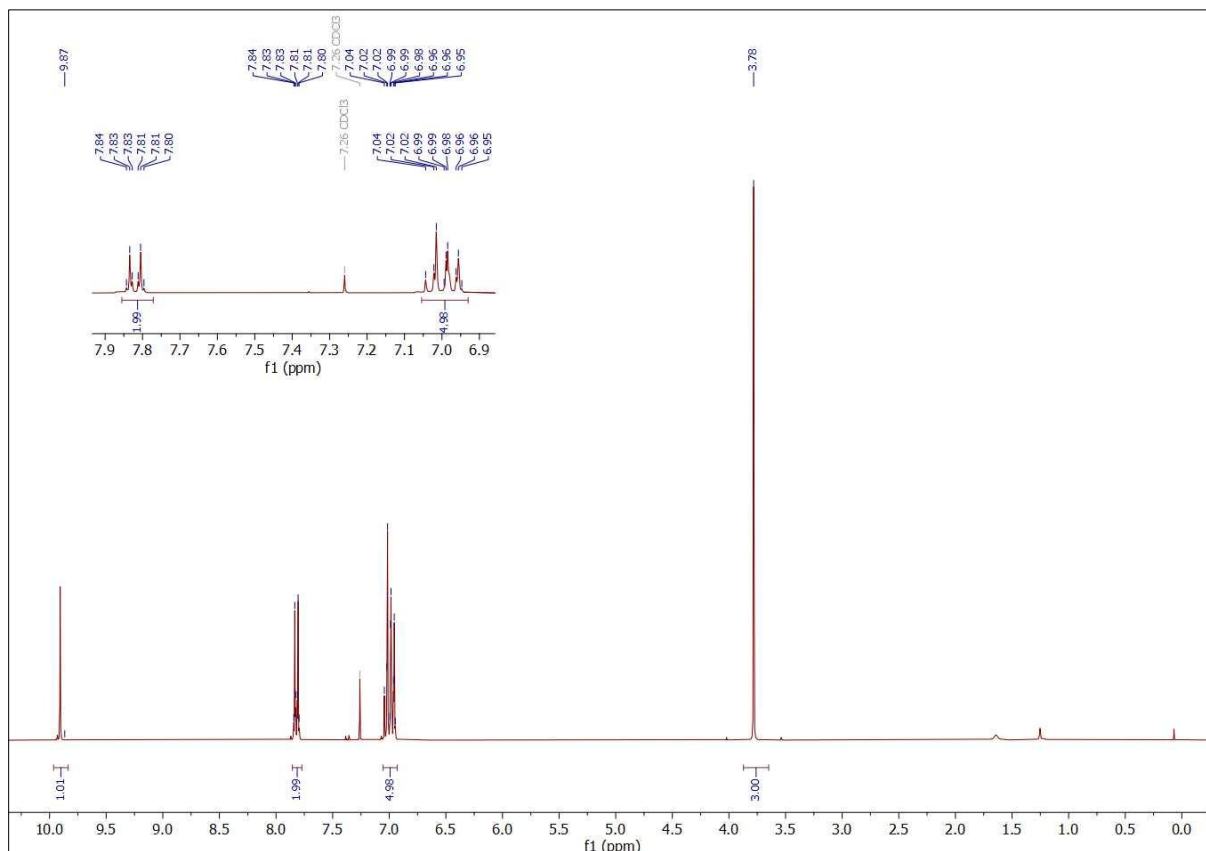


Determination of IC₅₀ for compound 33

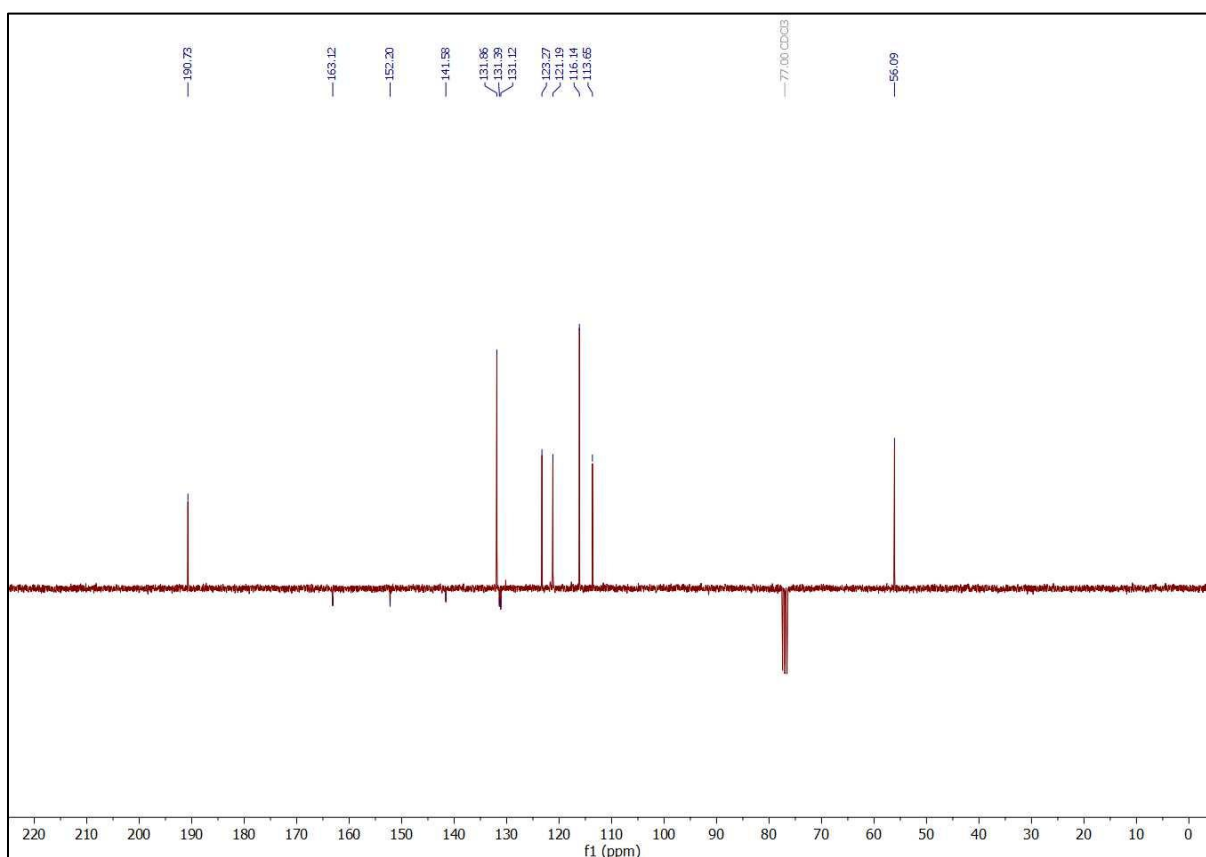
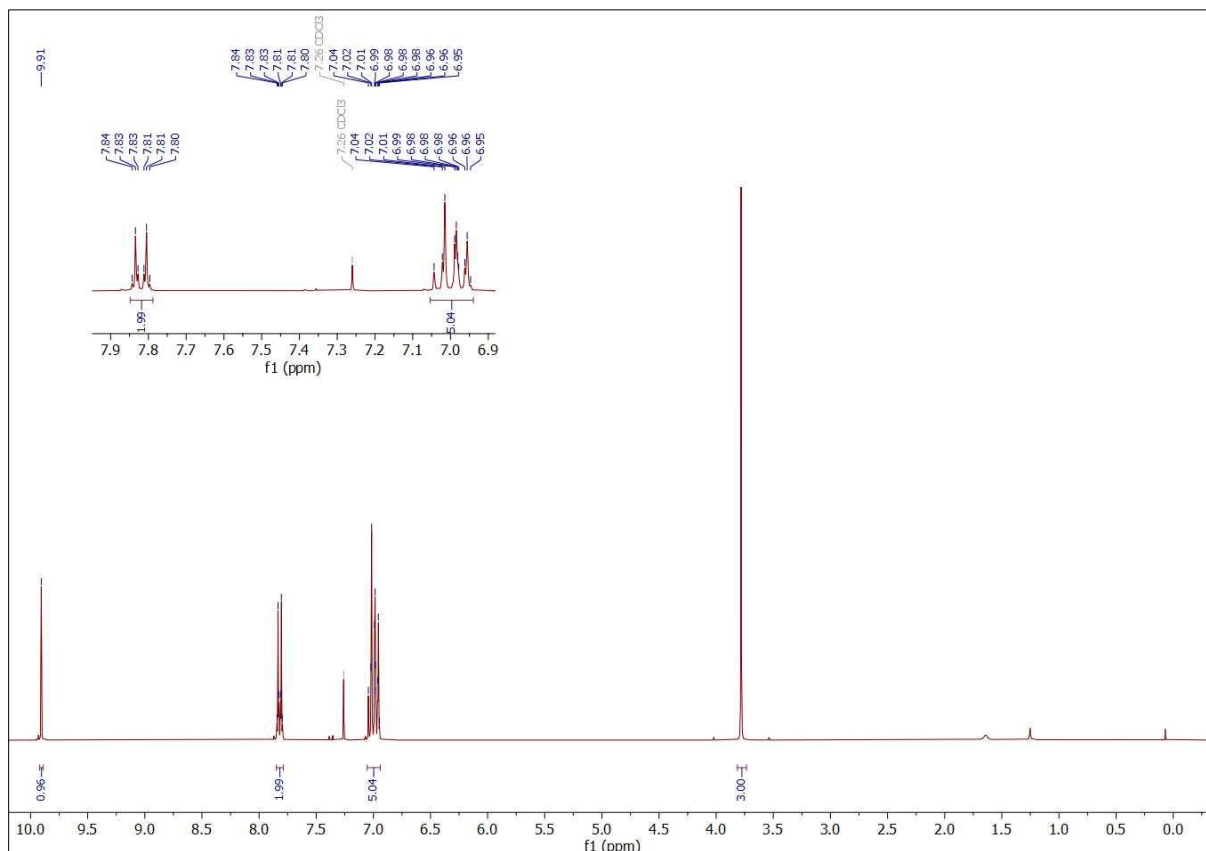
[Inhibitor 33] (μM)	% Inhibition
30	95.0
15	91.0
5	73.0
2	59.5
1	42.9
0.5	28.3
0.05	7.0
0.005	3.8



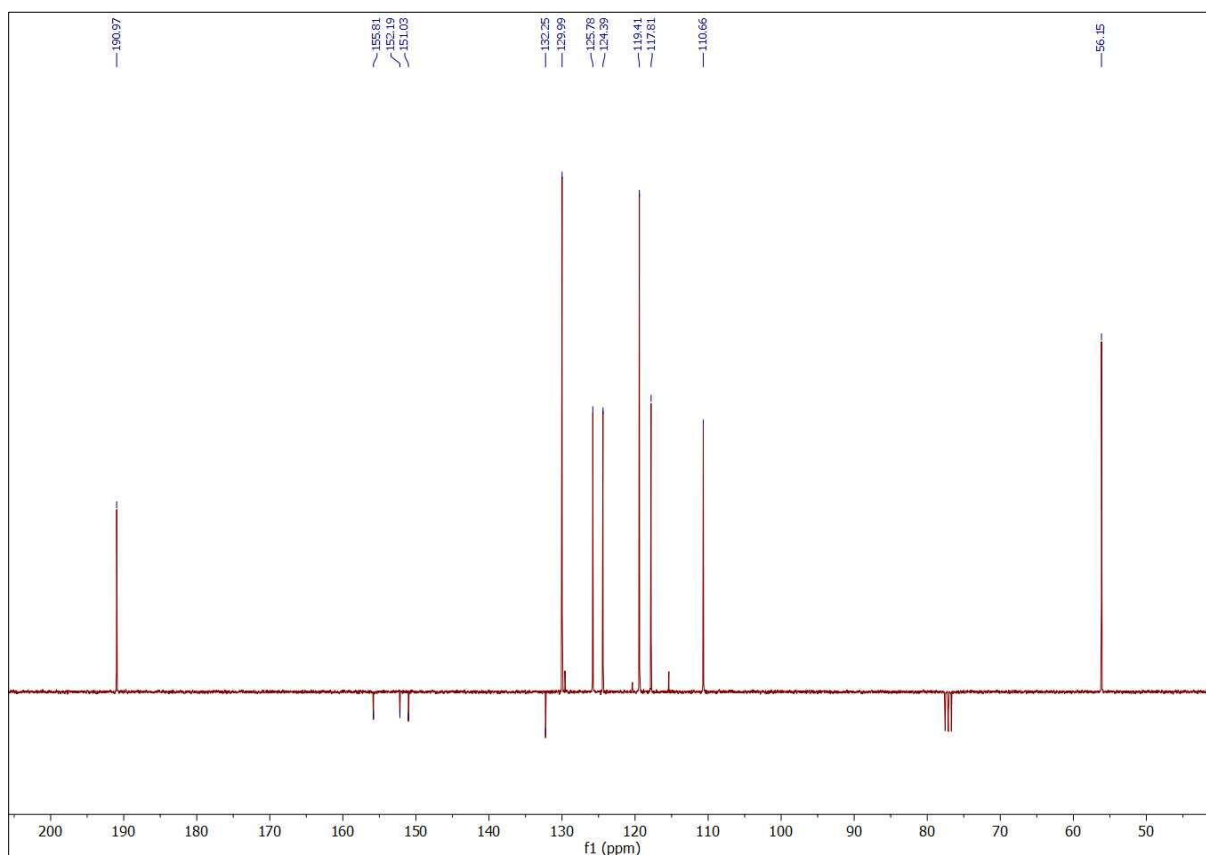
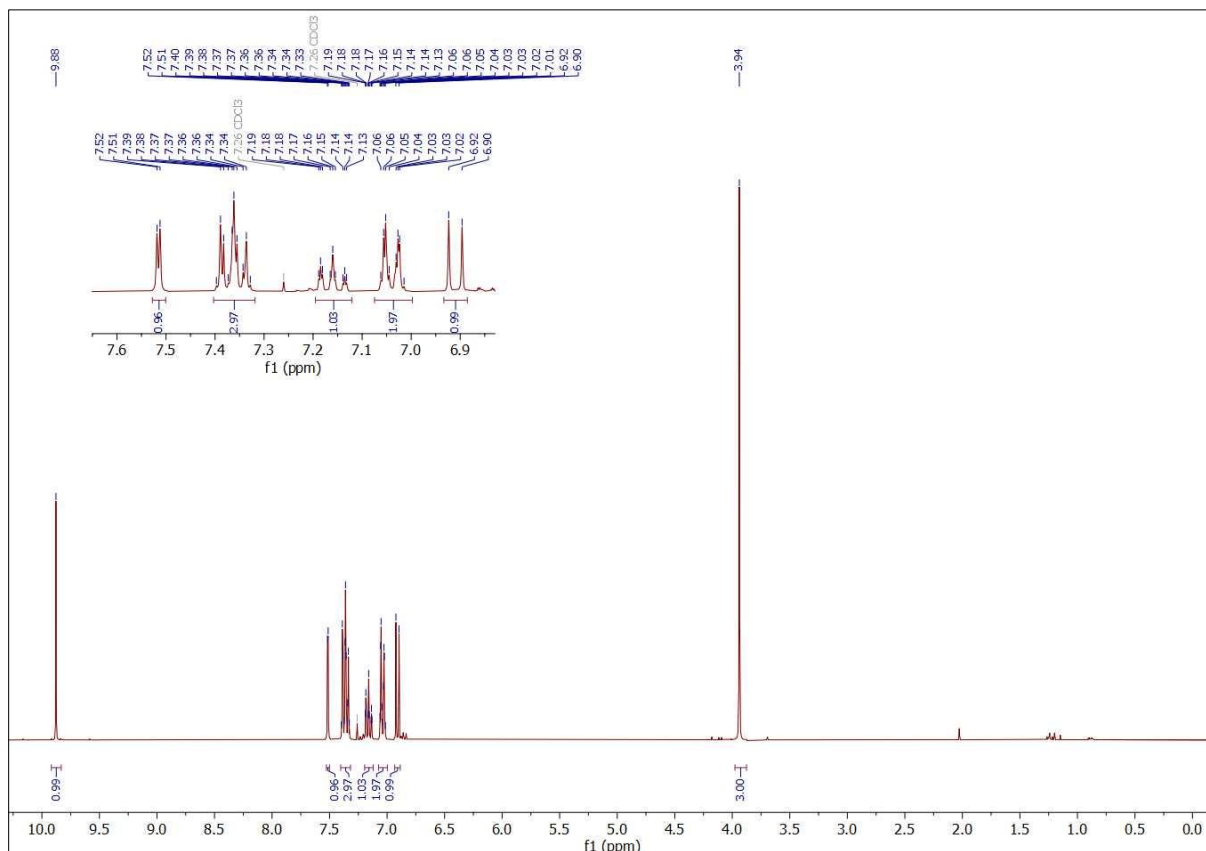
4-(2-Methoxyphenoxy)benzaldehyde (1).



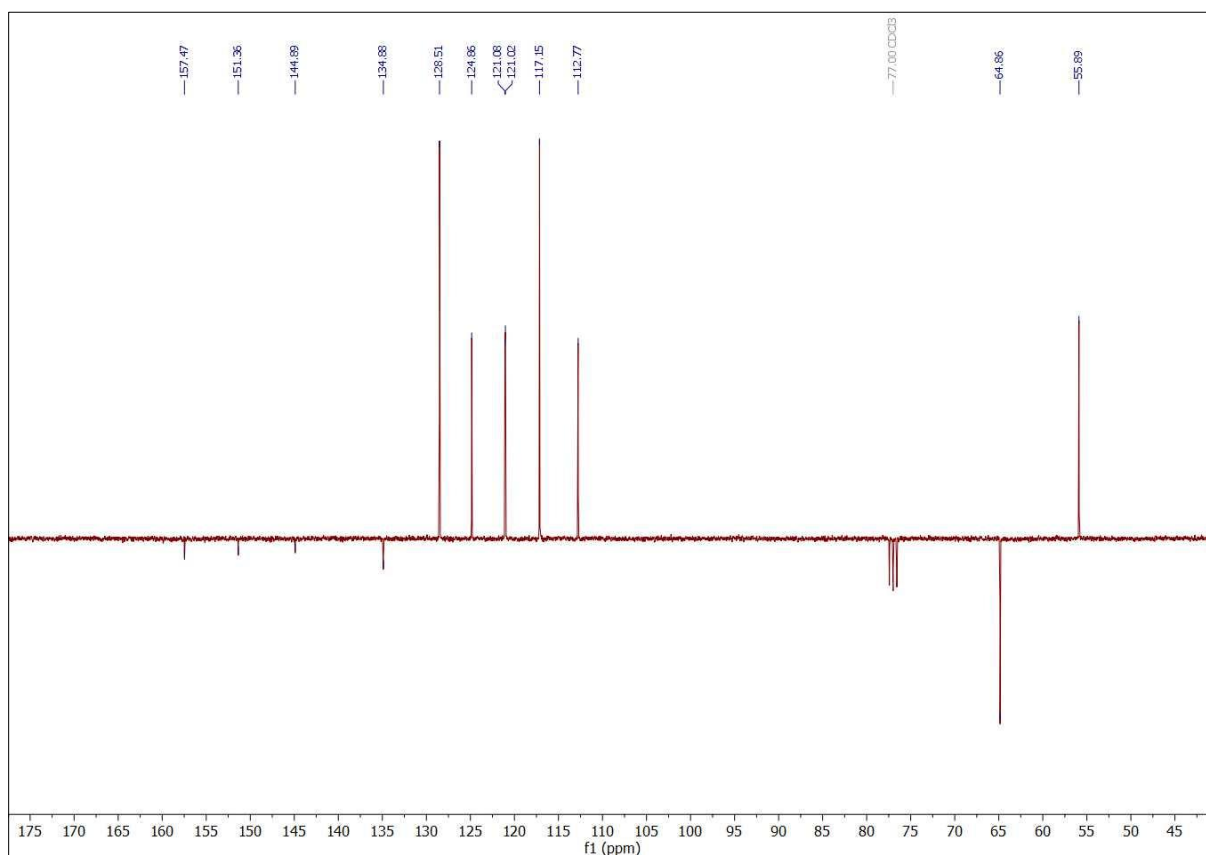
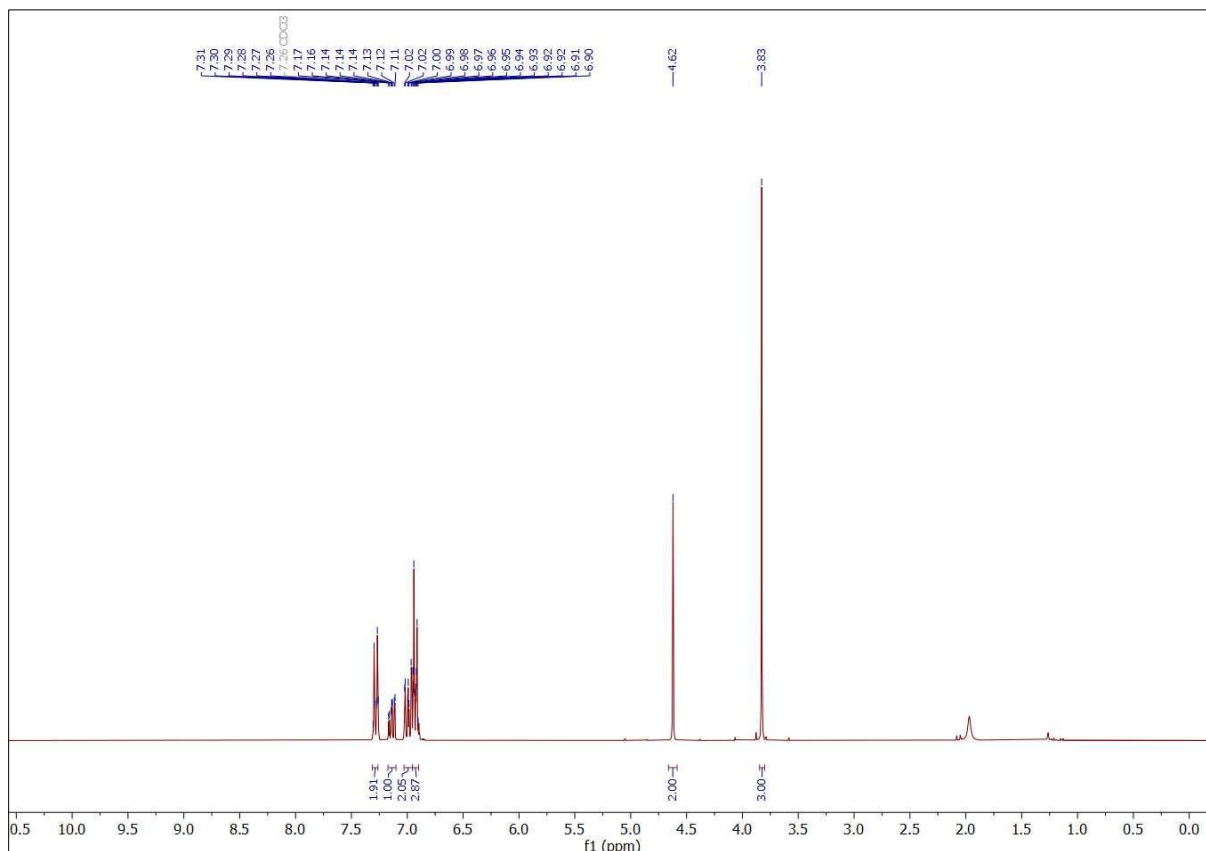
4-(4-Chloro-2-methoxyphenoxy)benzaldehyde (2).



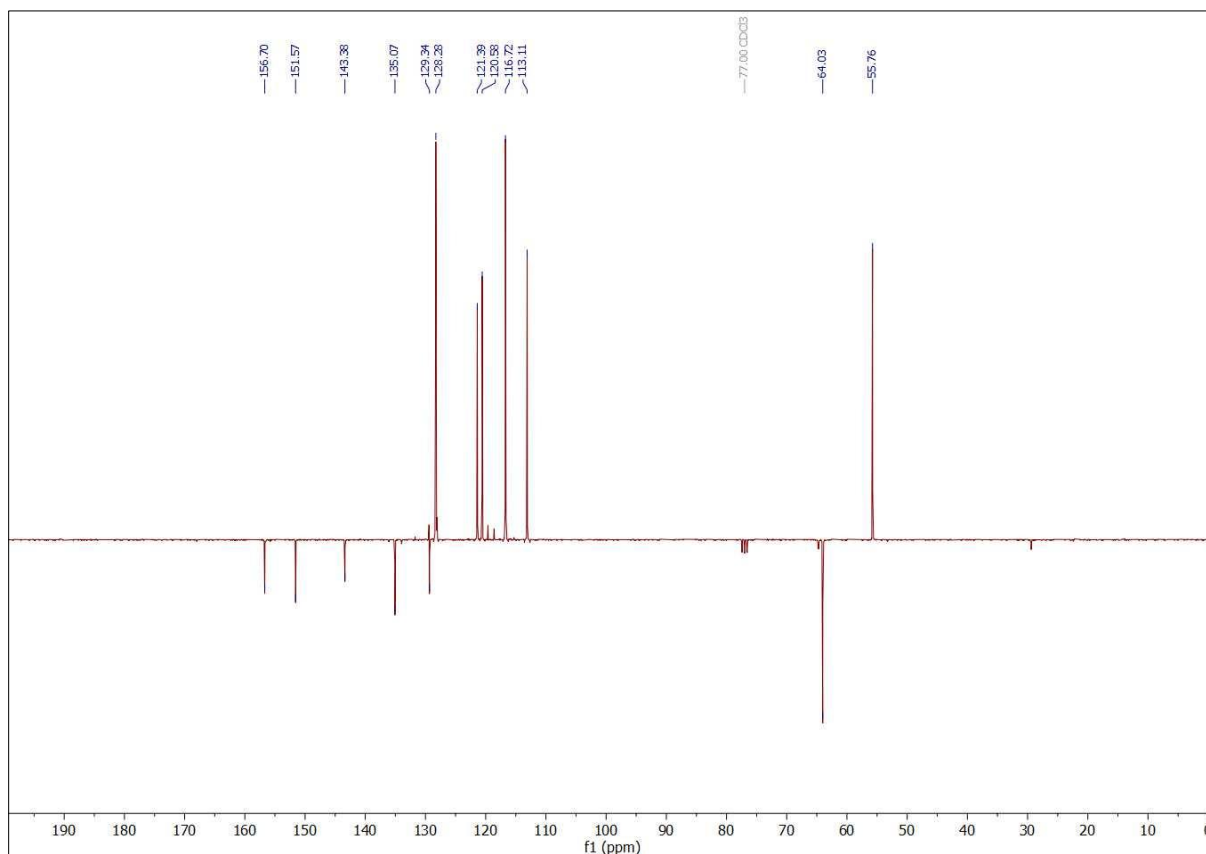
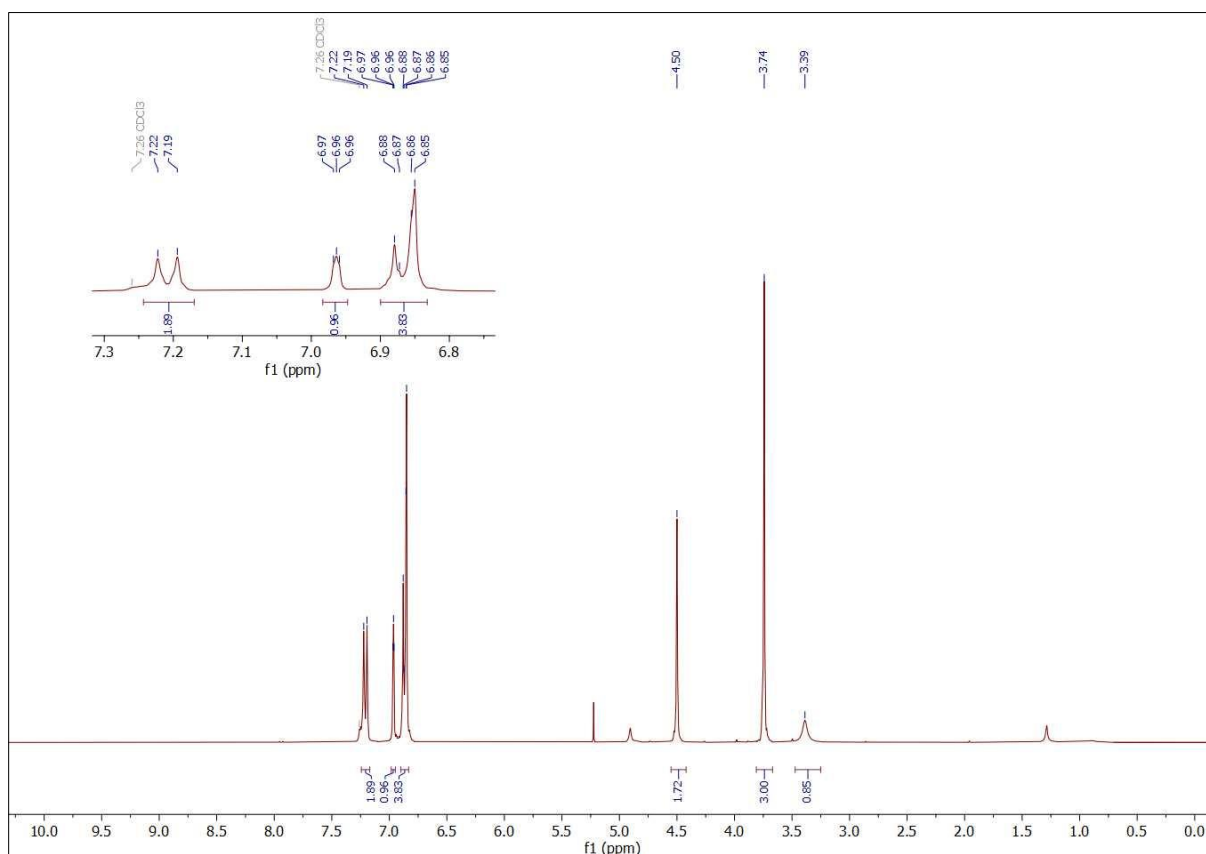
3-Methoxy-4-phenoxybenzaldehyde (3).



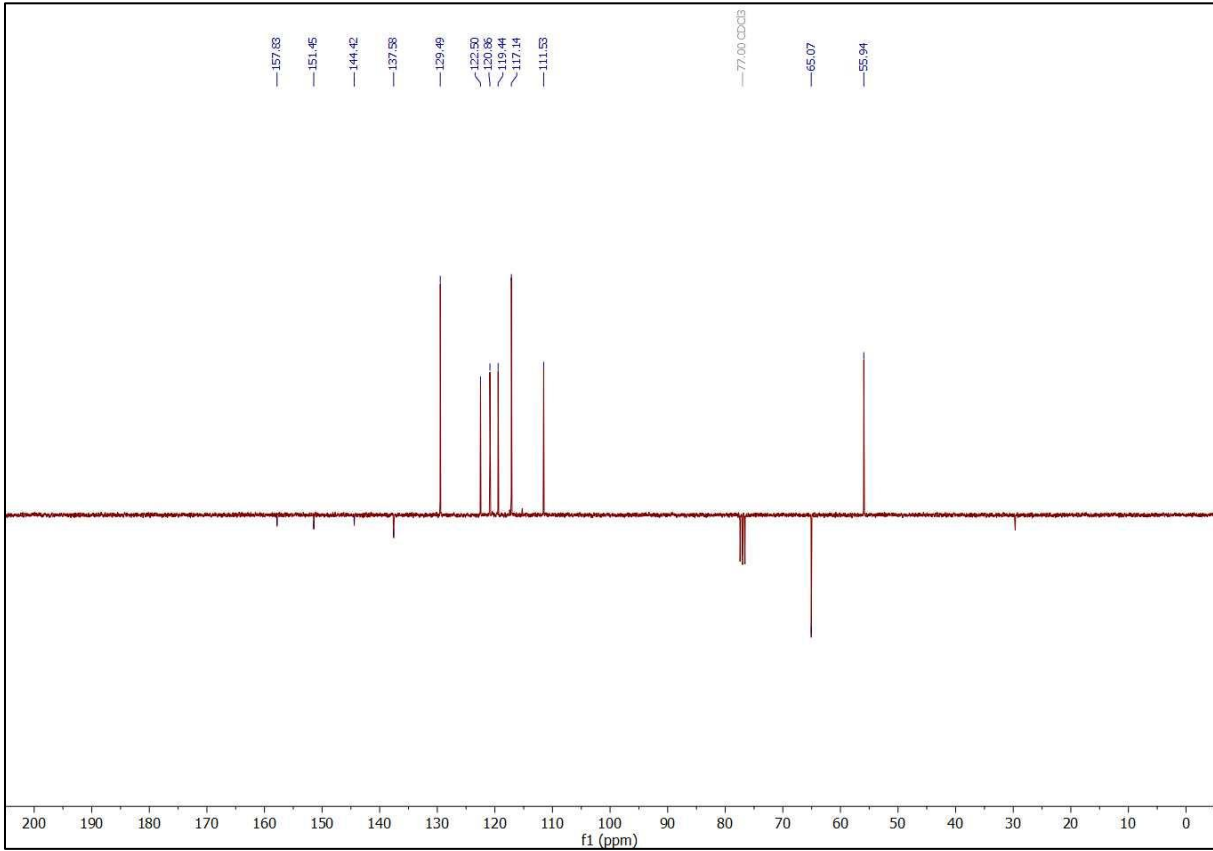
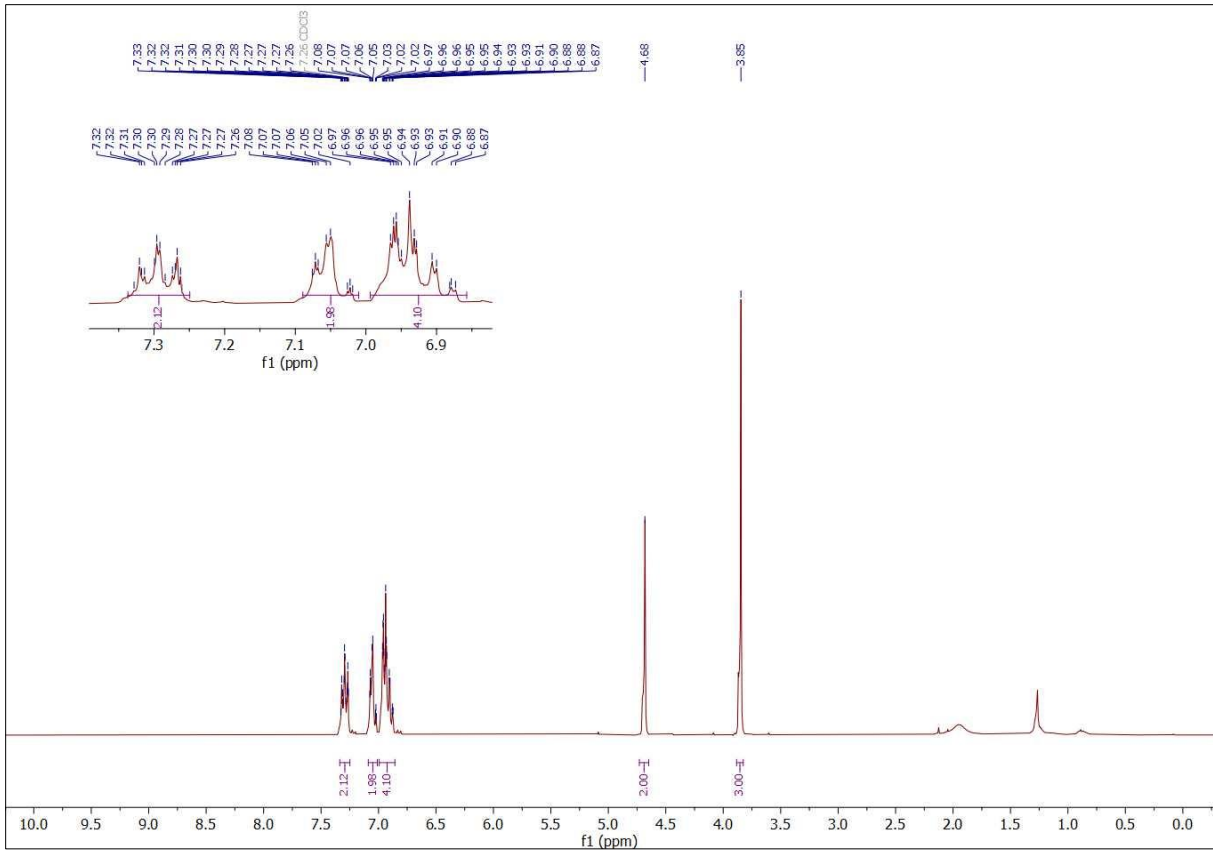
(4-(2-Methoxyphenoxy)phenyl)methanol (4).



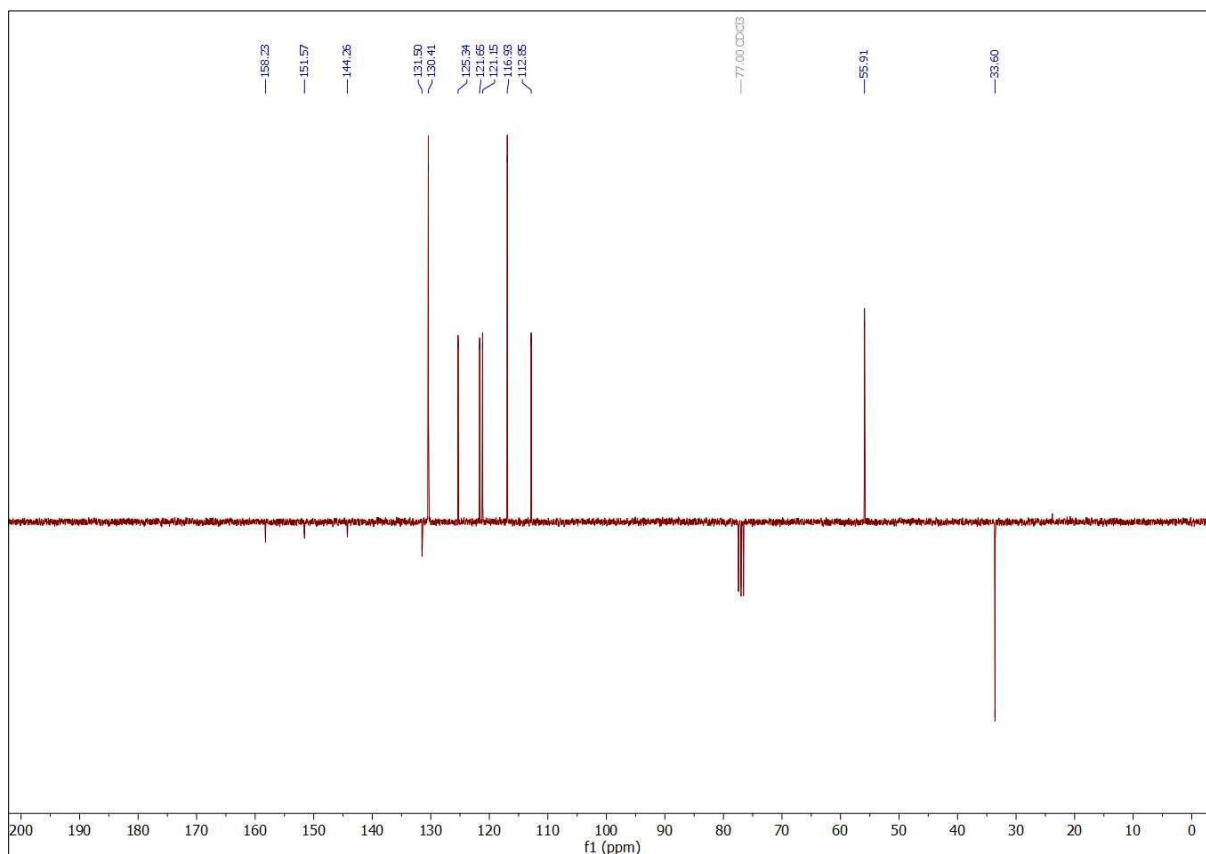
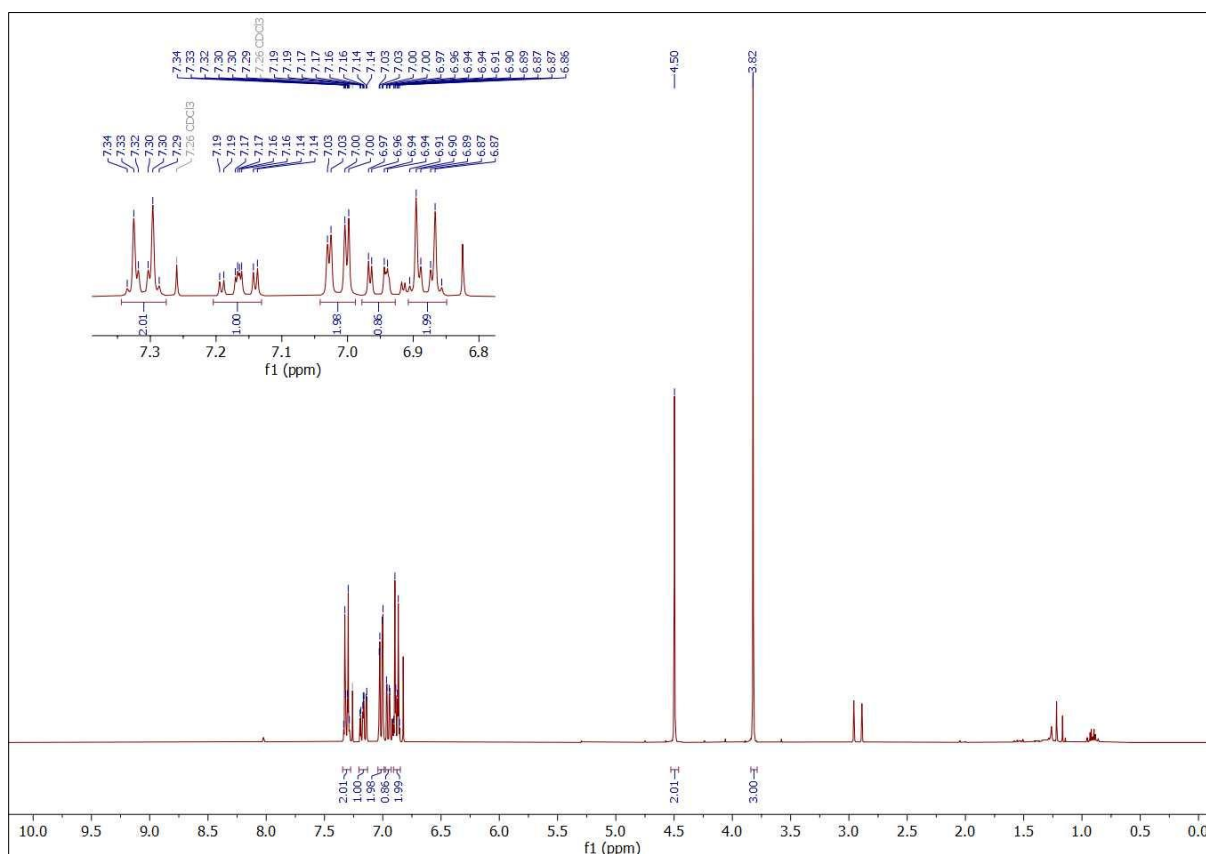
(4-(4-Chloro-2-methoxyphenoxy)phenyl)methanol (5).



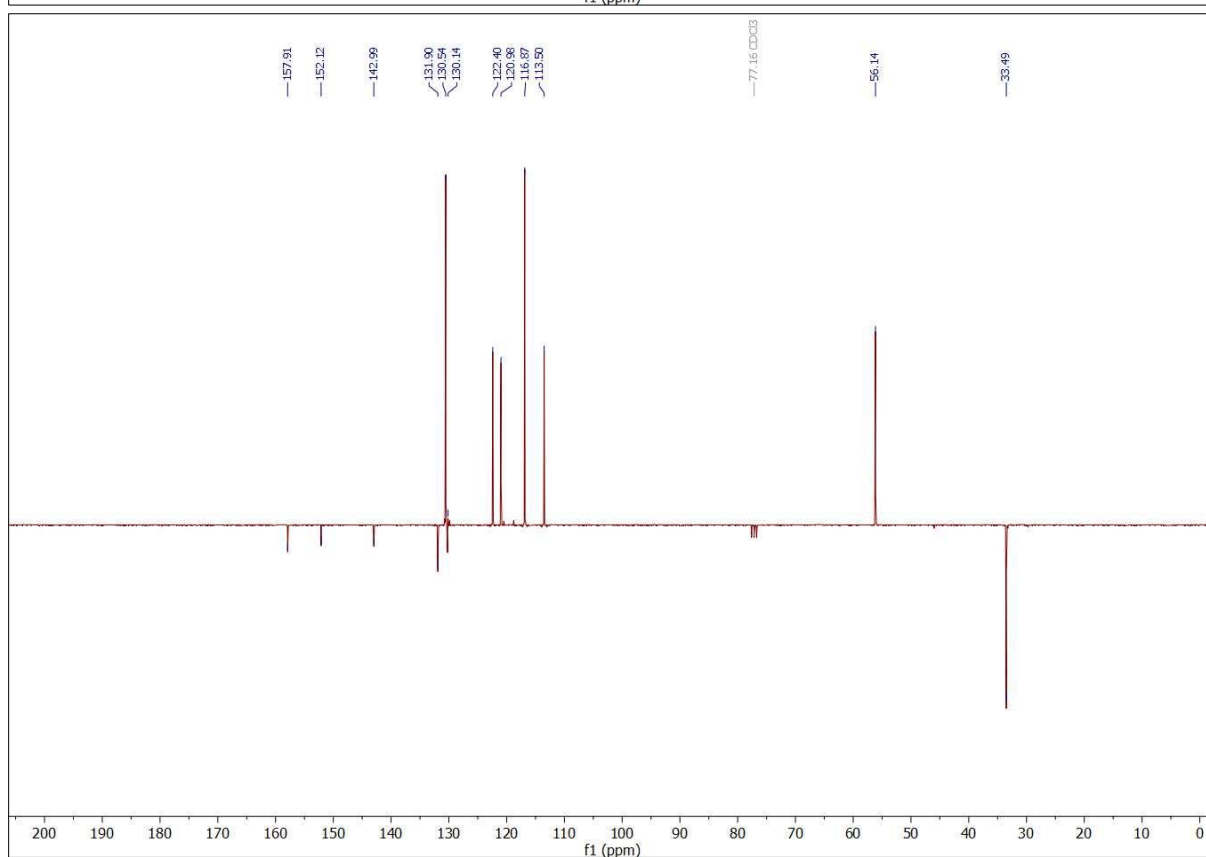
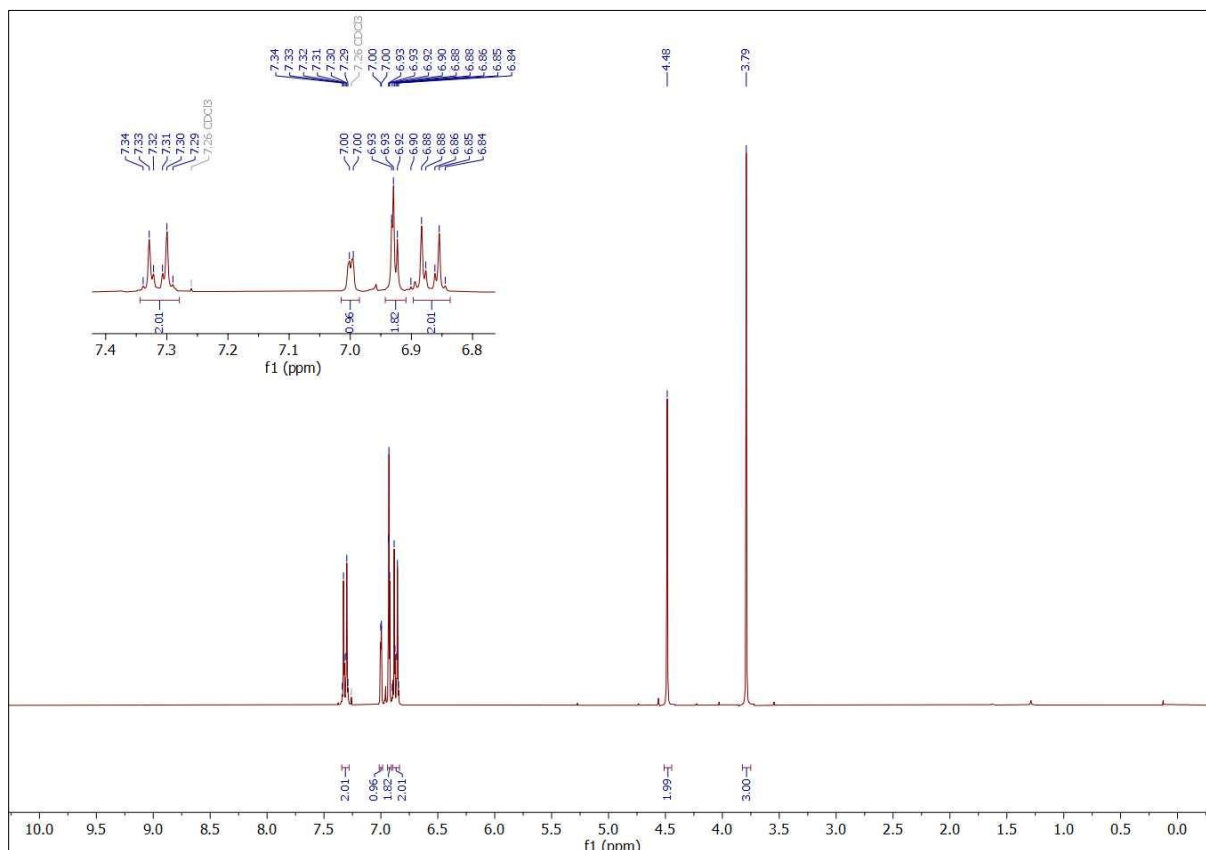
(3-Methoxy-4-phenoxyphenyl)methanol (6).



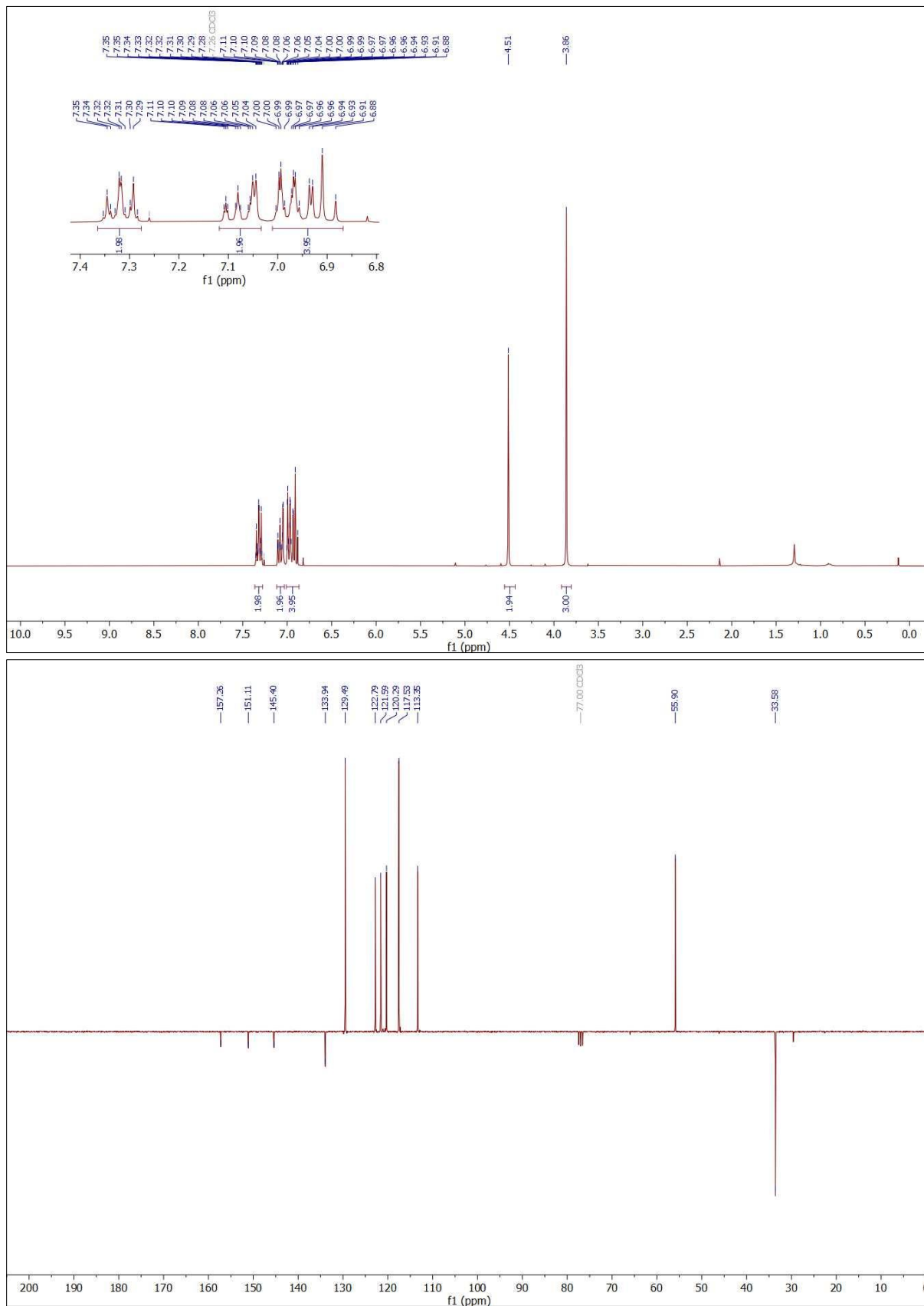
1-(4-(Bromomethyl)phenoxy)-2-methoxybenzene (7).



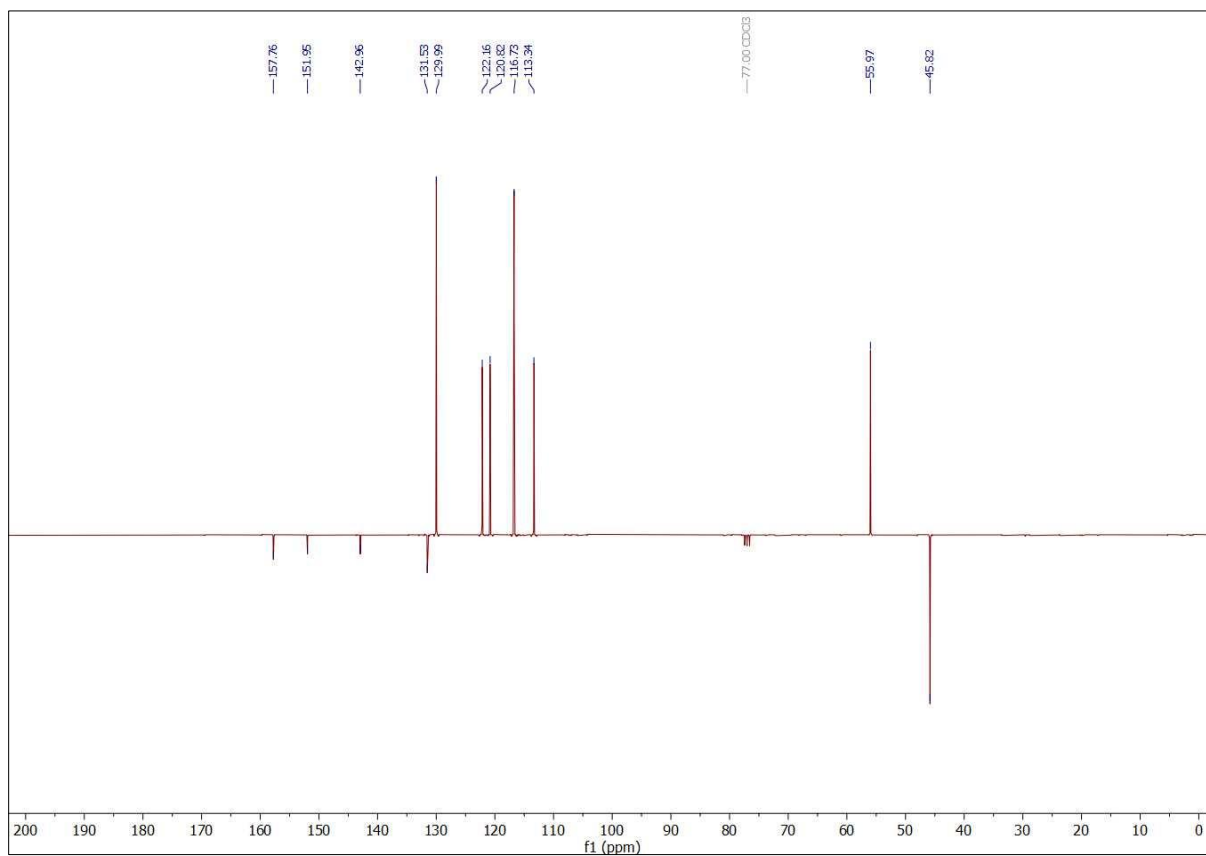
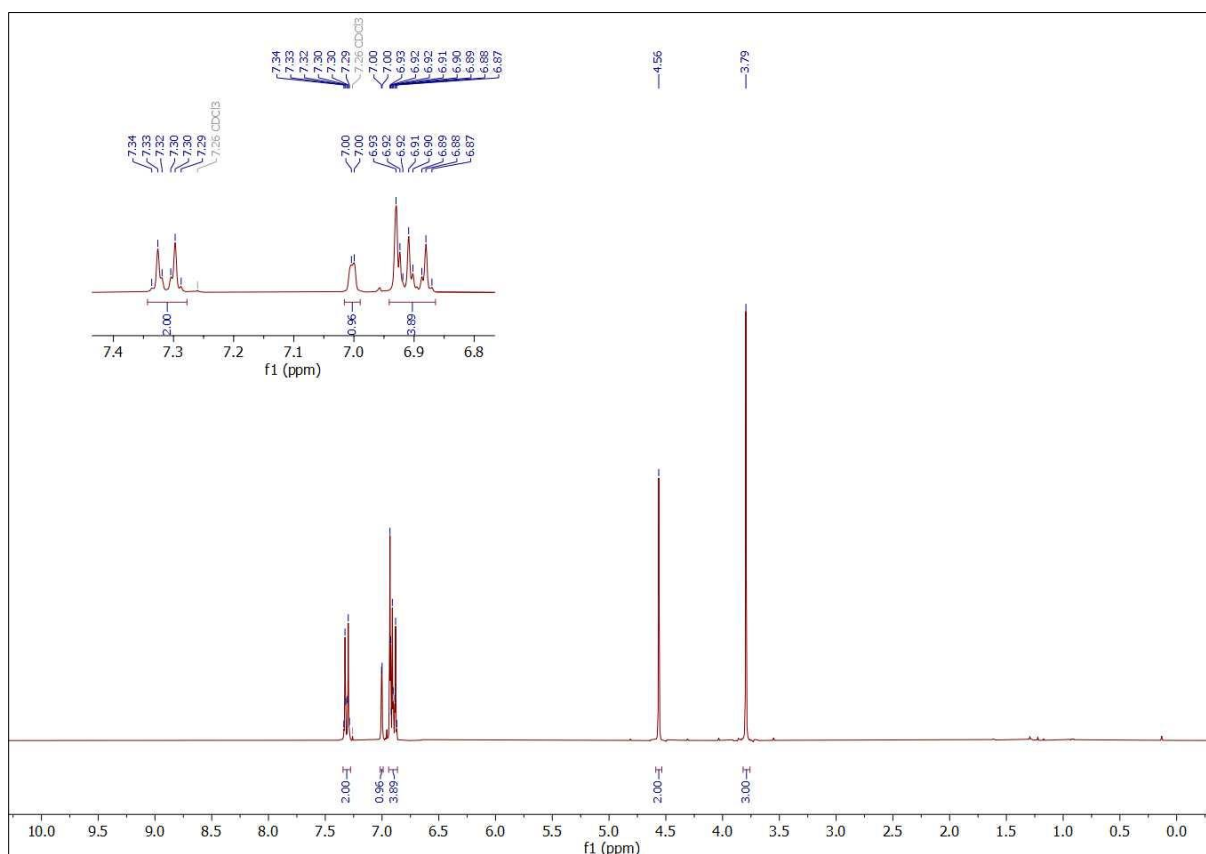
1-(4-(Bromomethyl)phenoxy)-4-chloro-2-methoxybenzene (8).



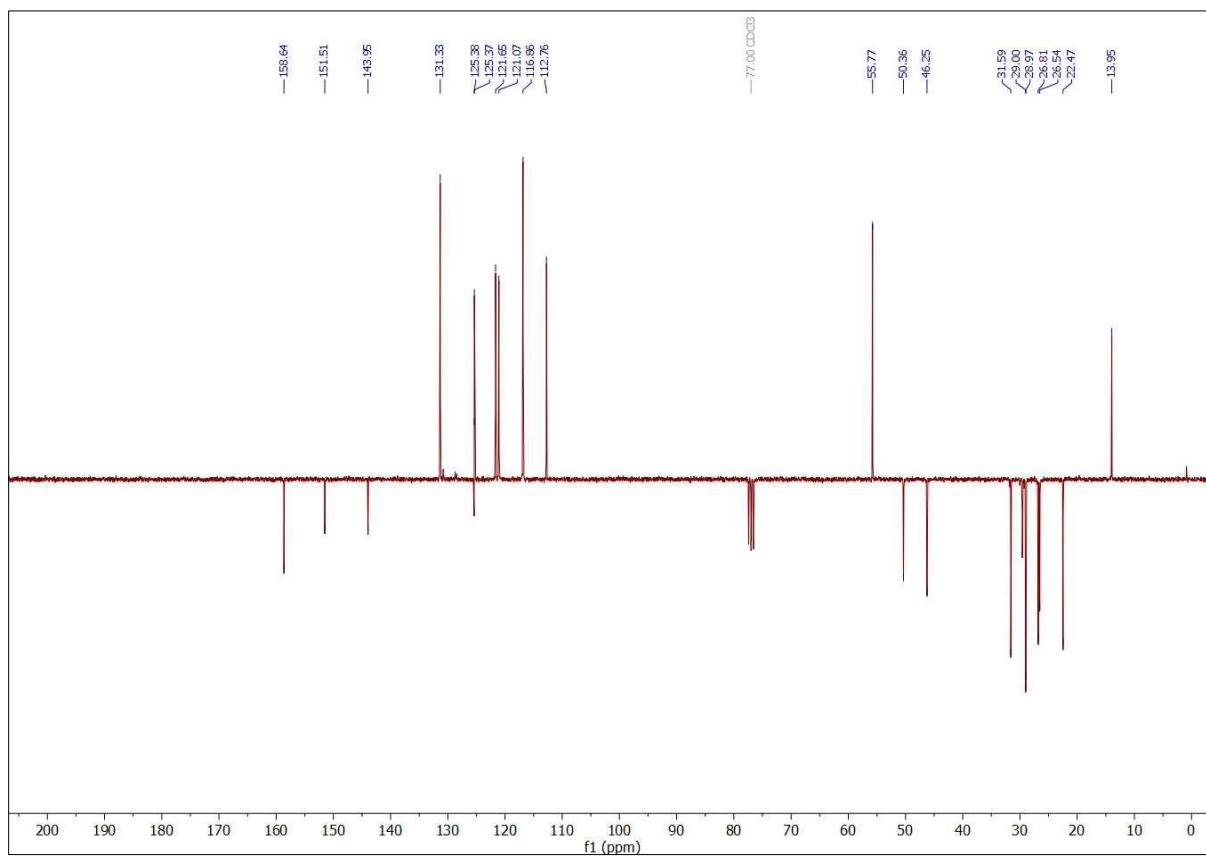
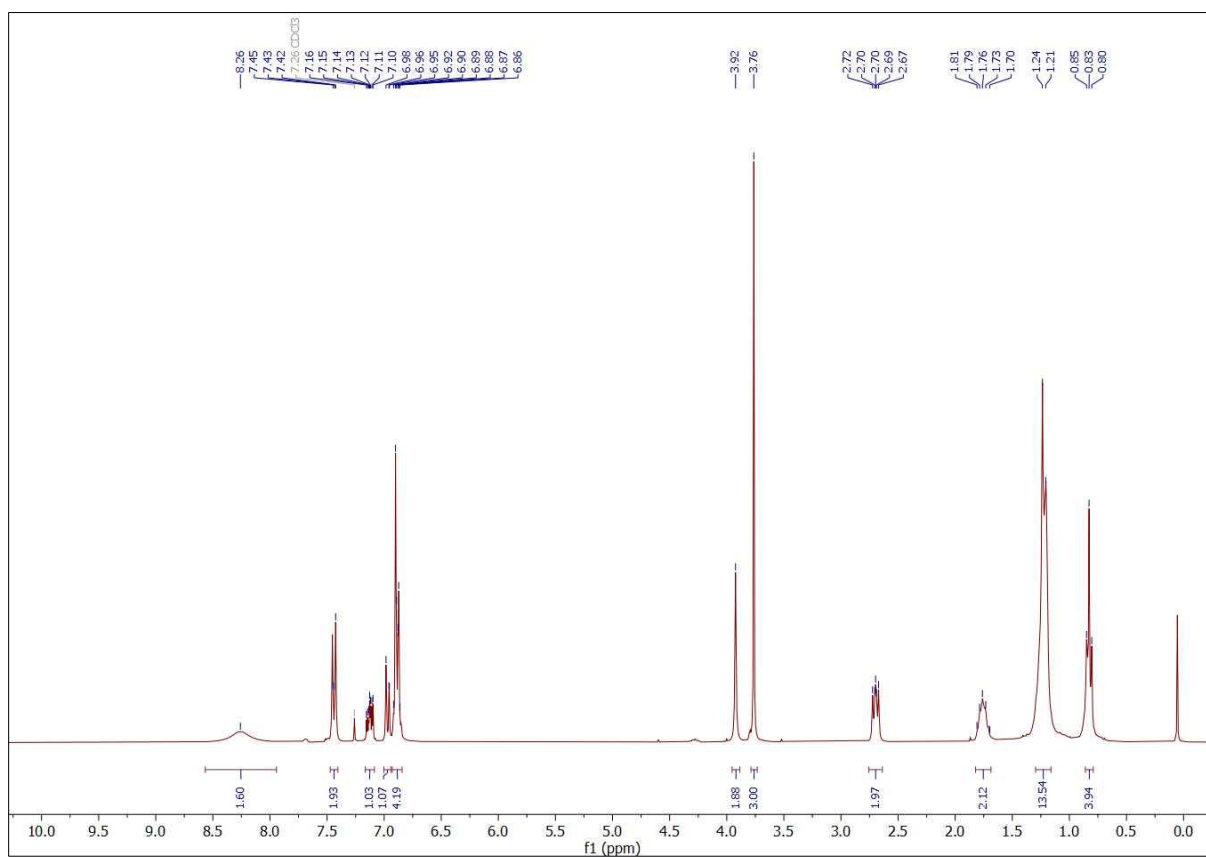
4-(Bromomethyl)-2-methoxy-1-phenoxybenzene (9).



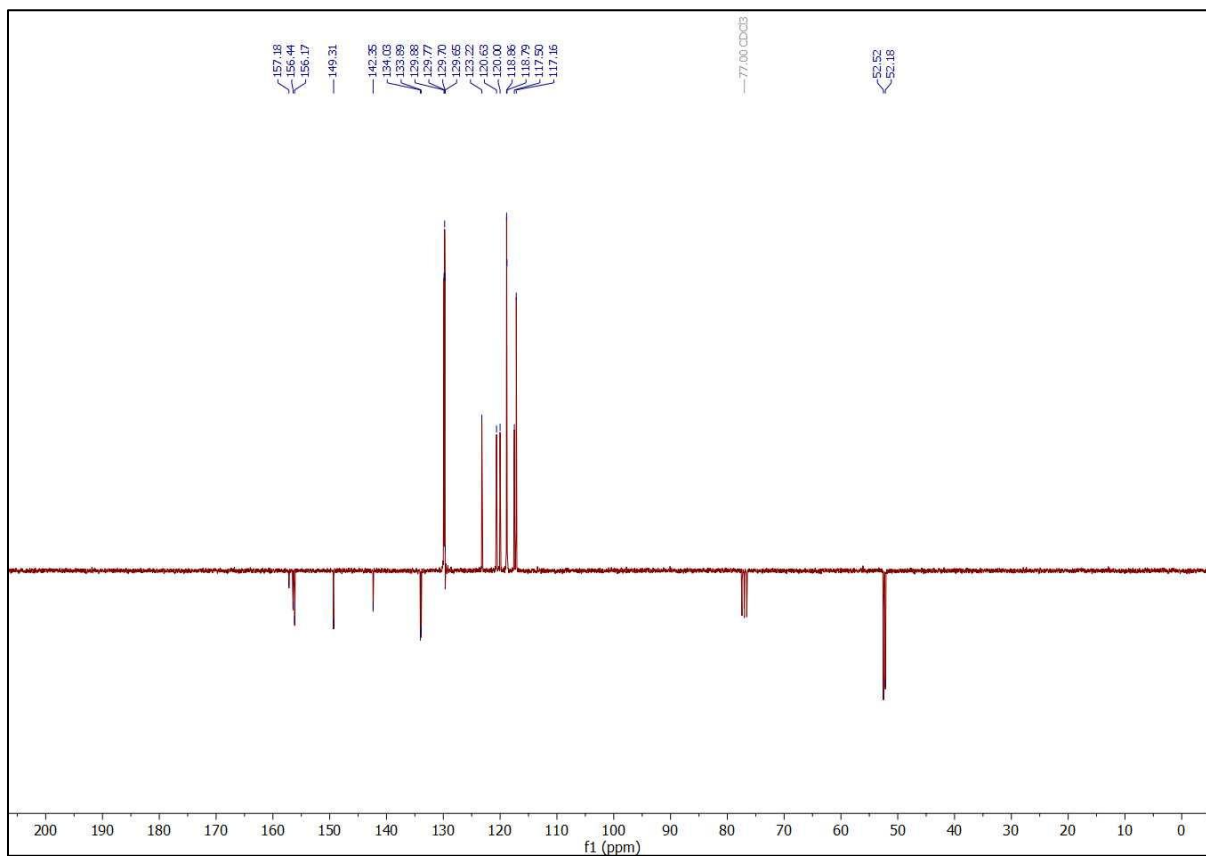
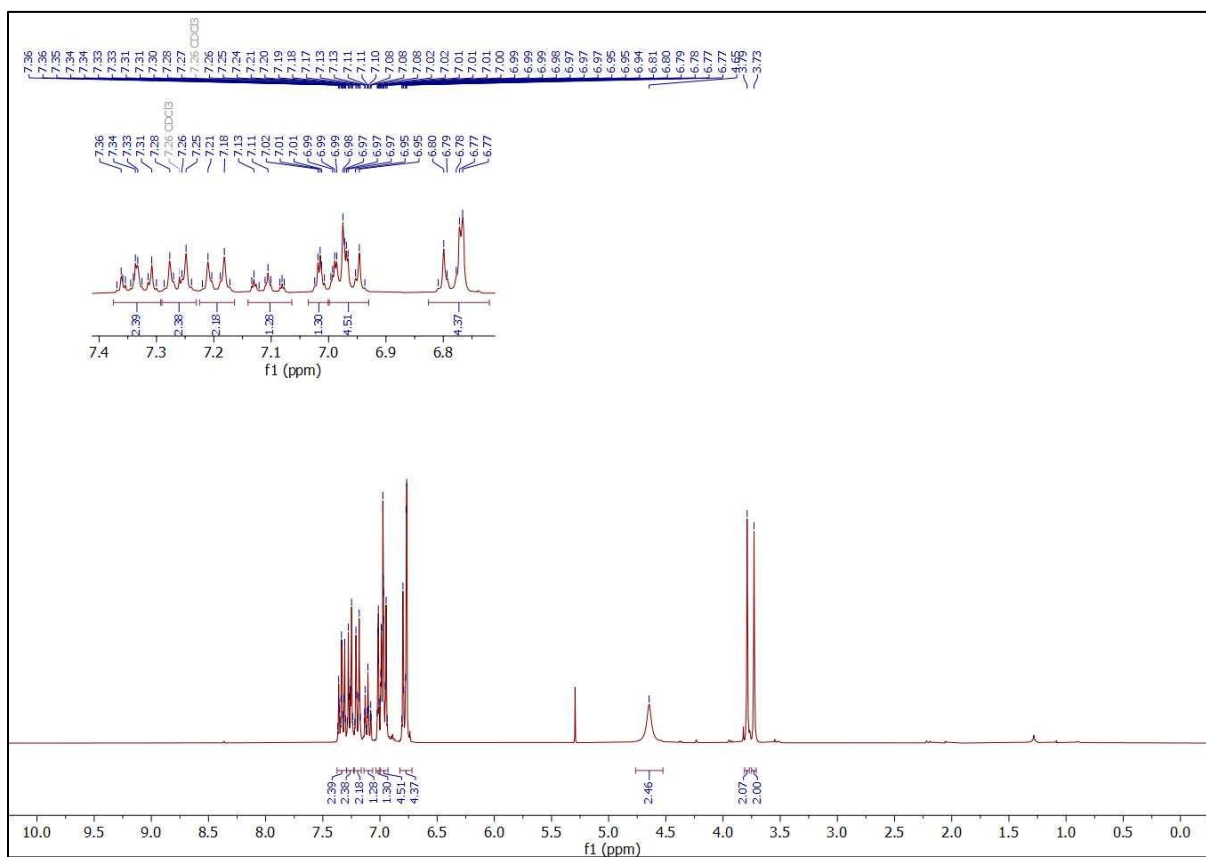
4-Chloro-1-(4-chloromethyl)phenoxy)-2-methoxybenzene (10).



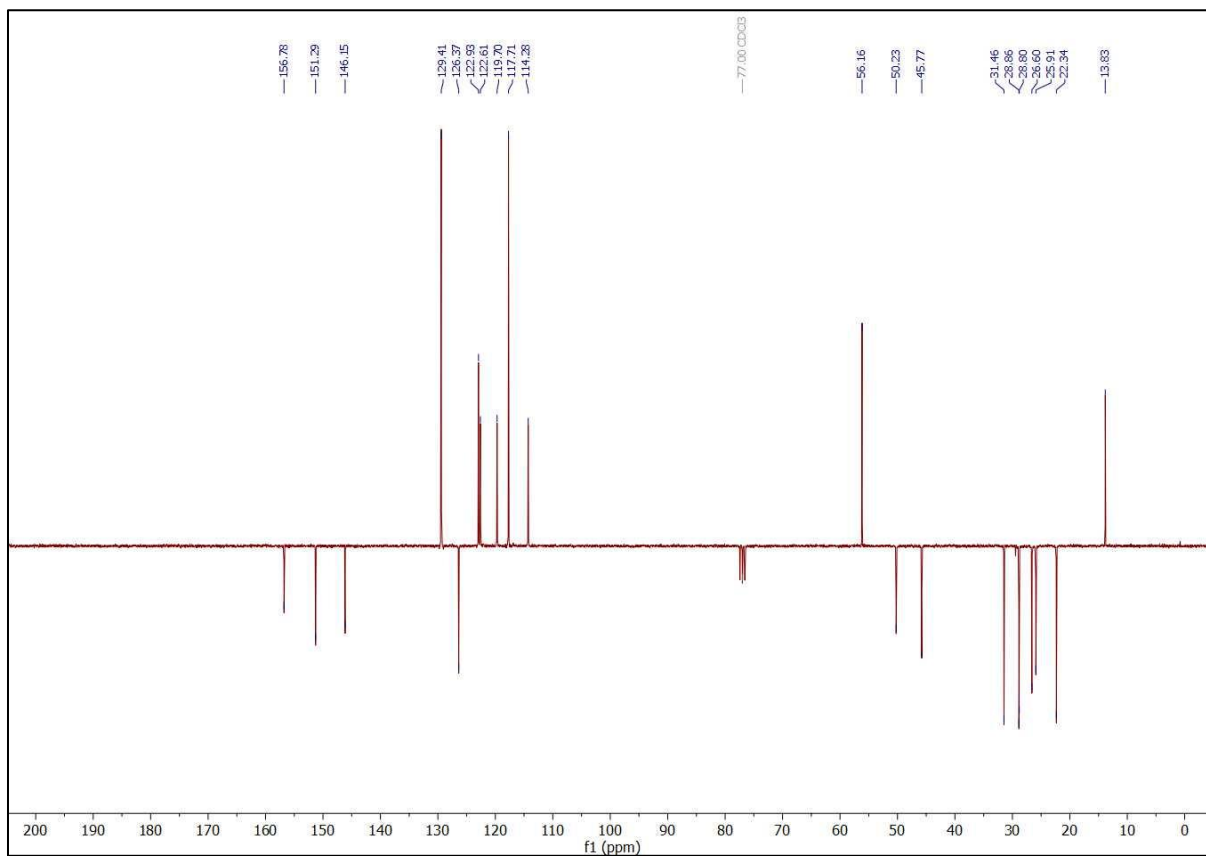
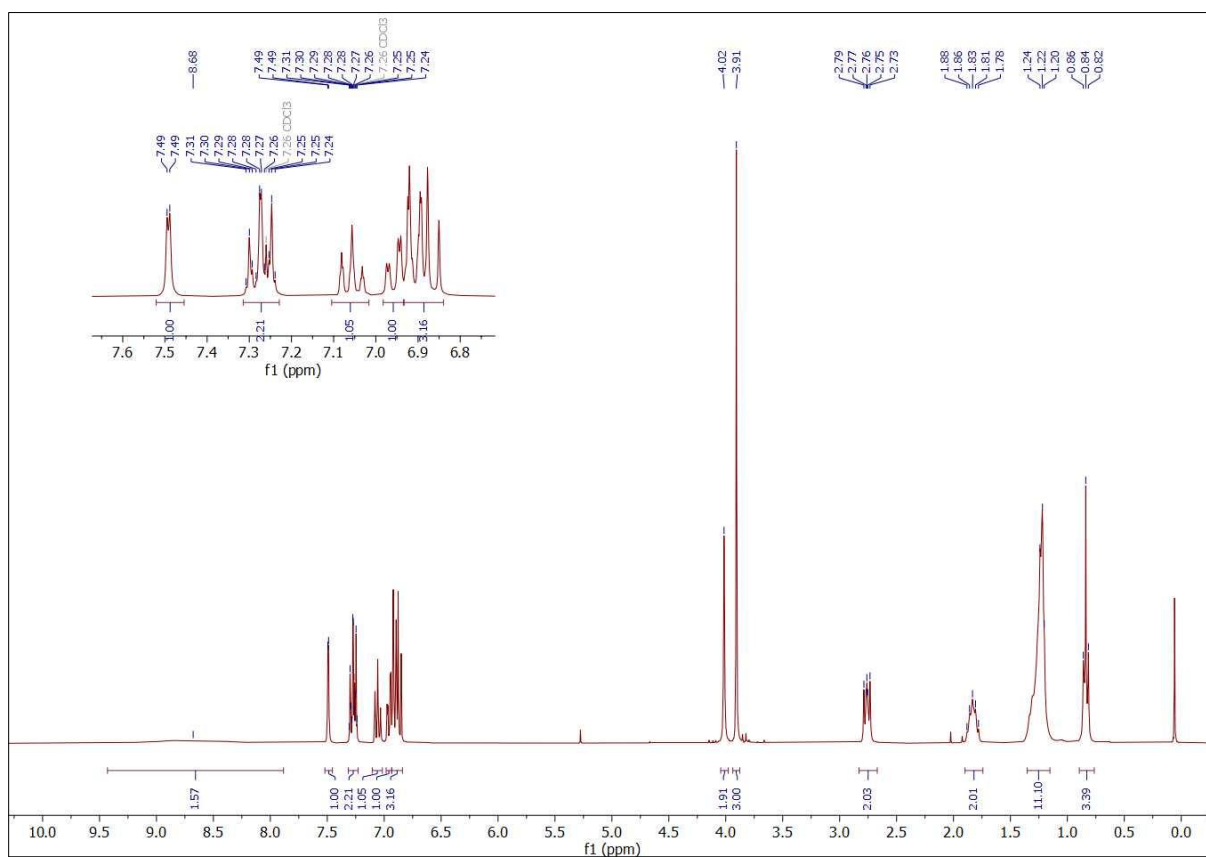
N-(4-(2-Methoxyphenoxy)benzyl)octan-1-amine (11).



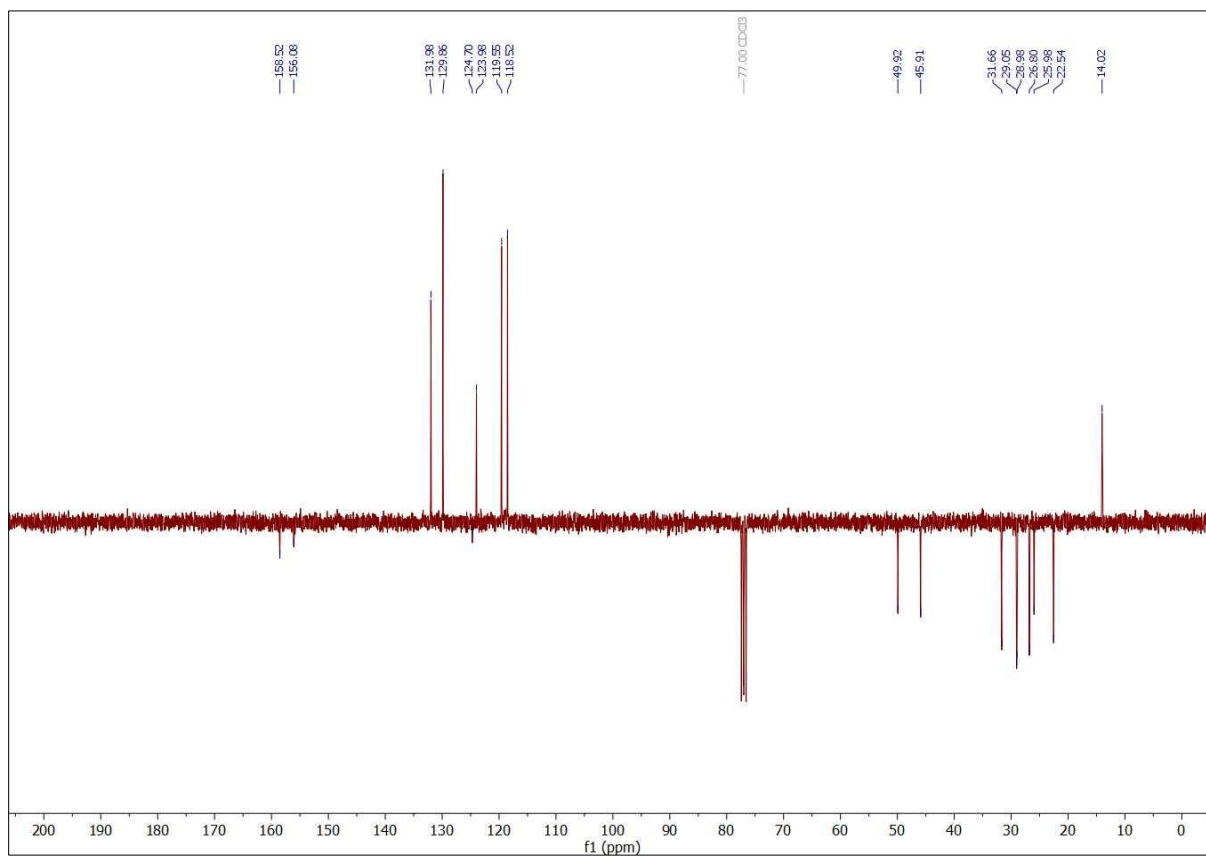
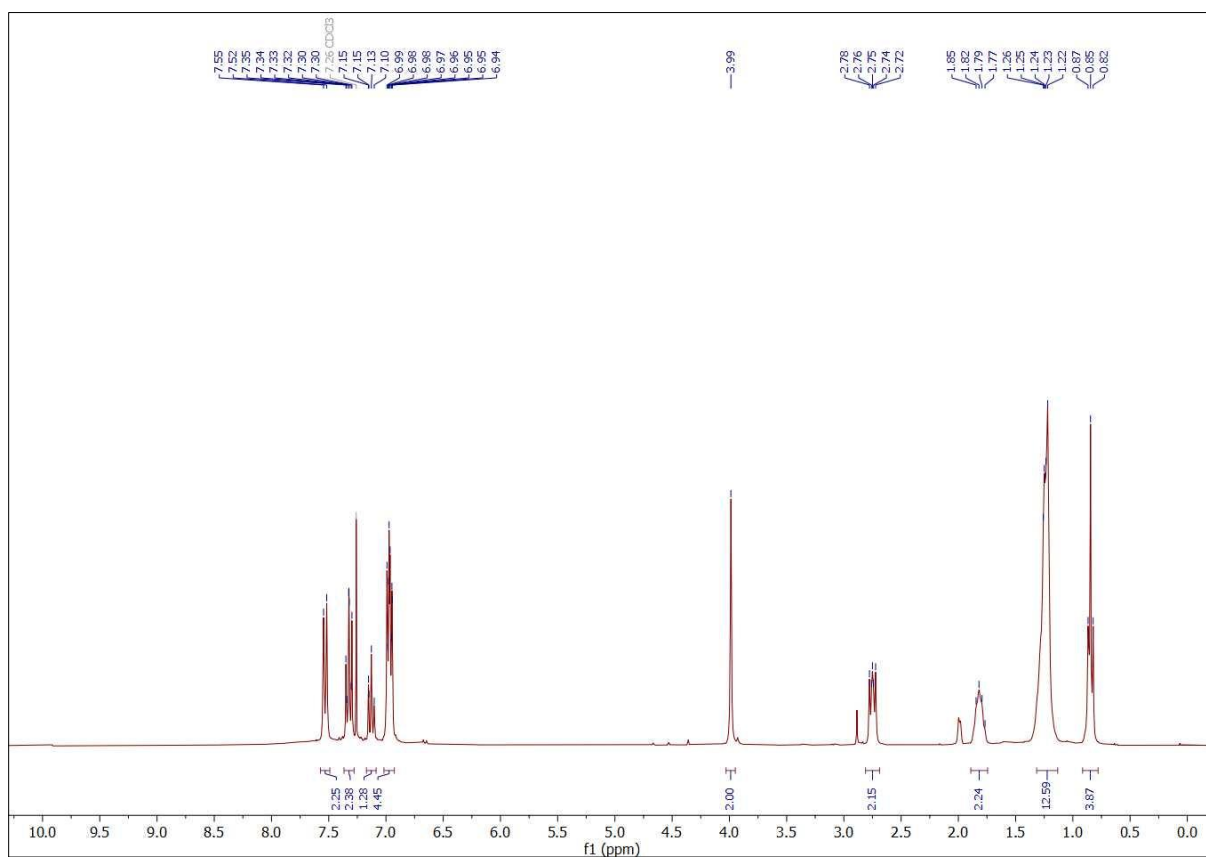
N-(4-(4-Chloro-2-methoxyphenoxy)benzyl)octan-1-amine (12).



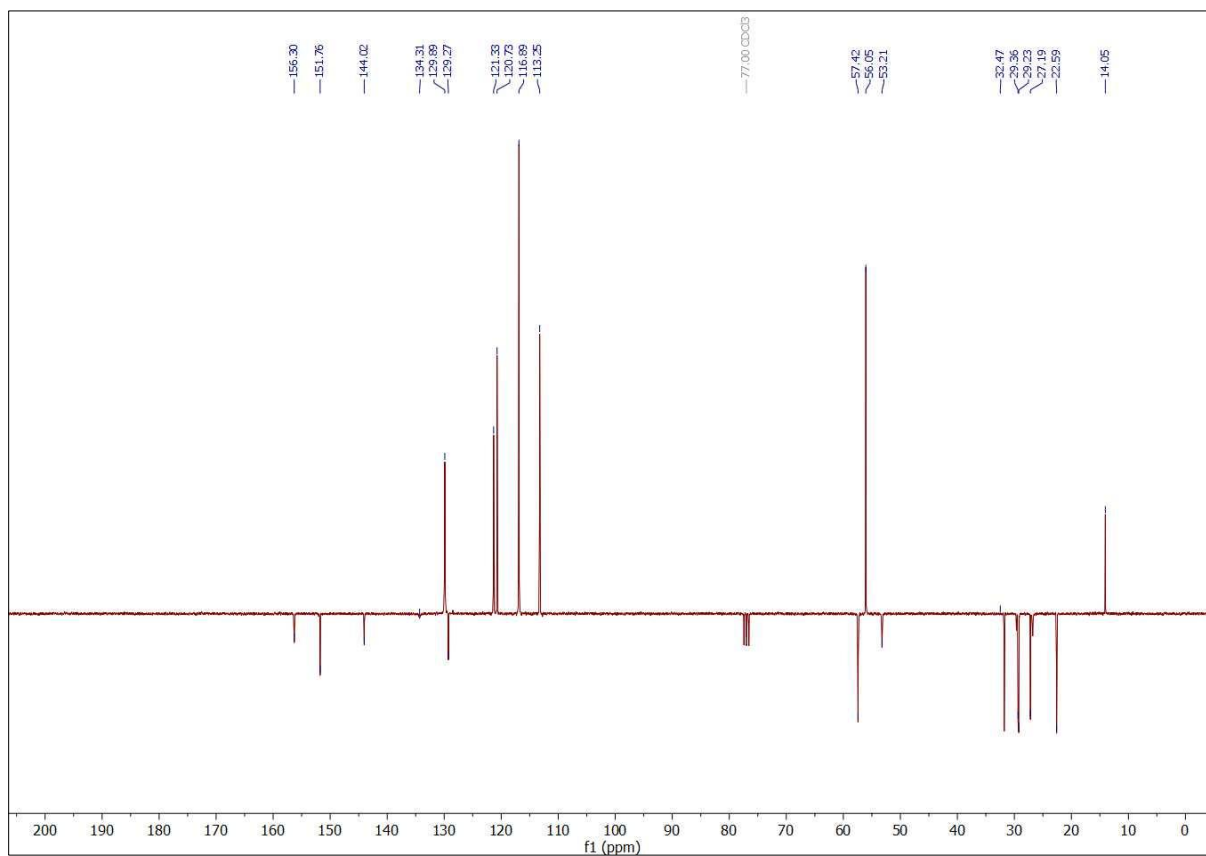
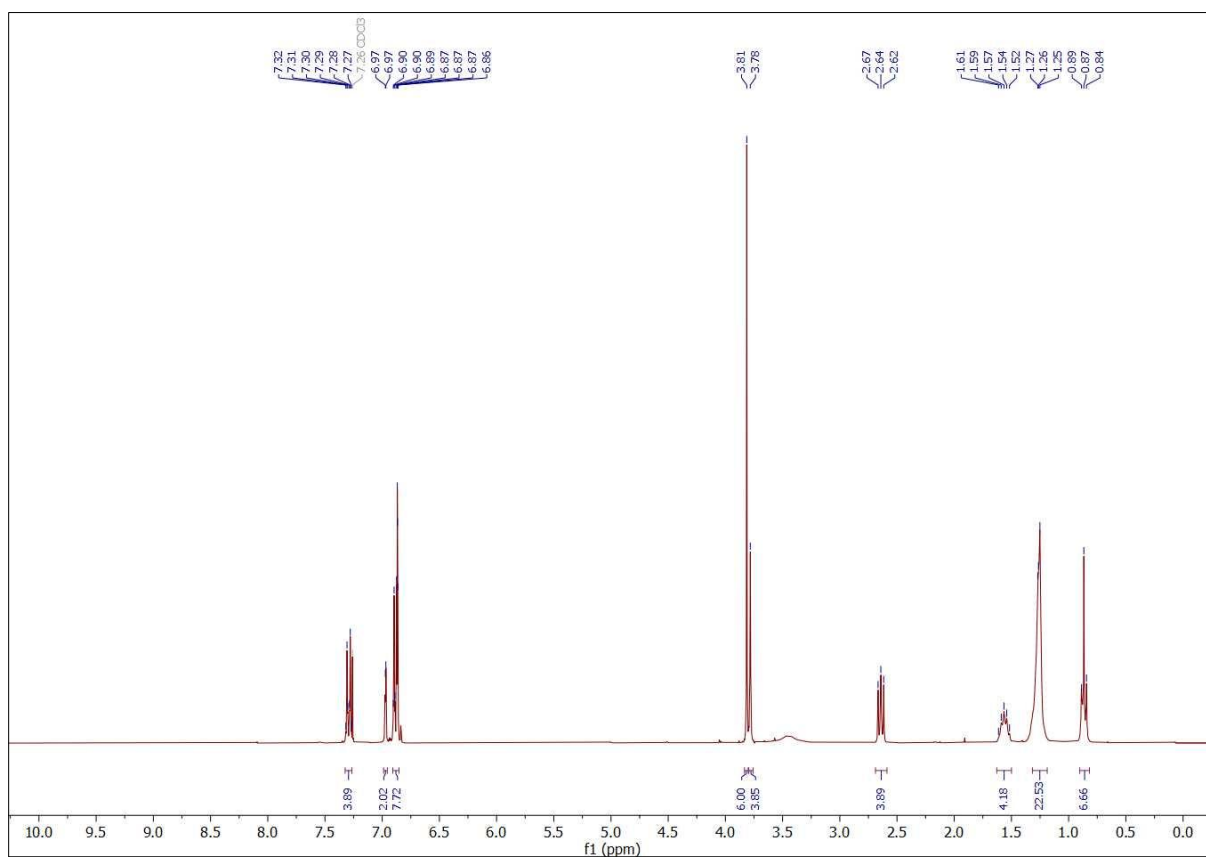
N-(3-Methoxy-4-phenoxybenzyl)octan-1-amine (13).



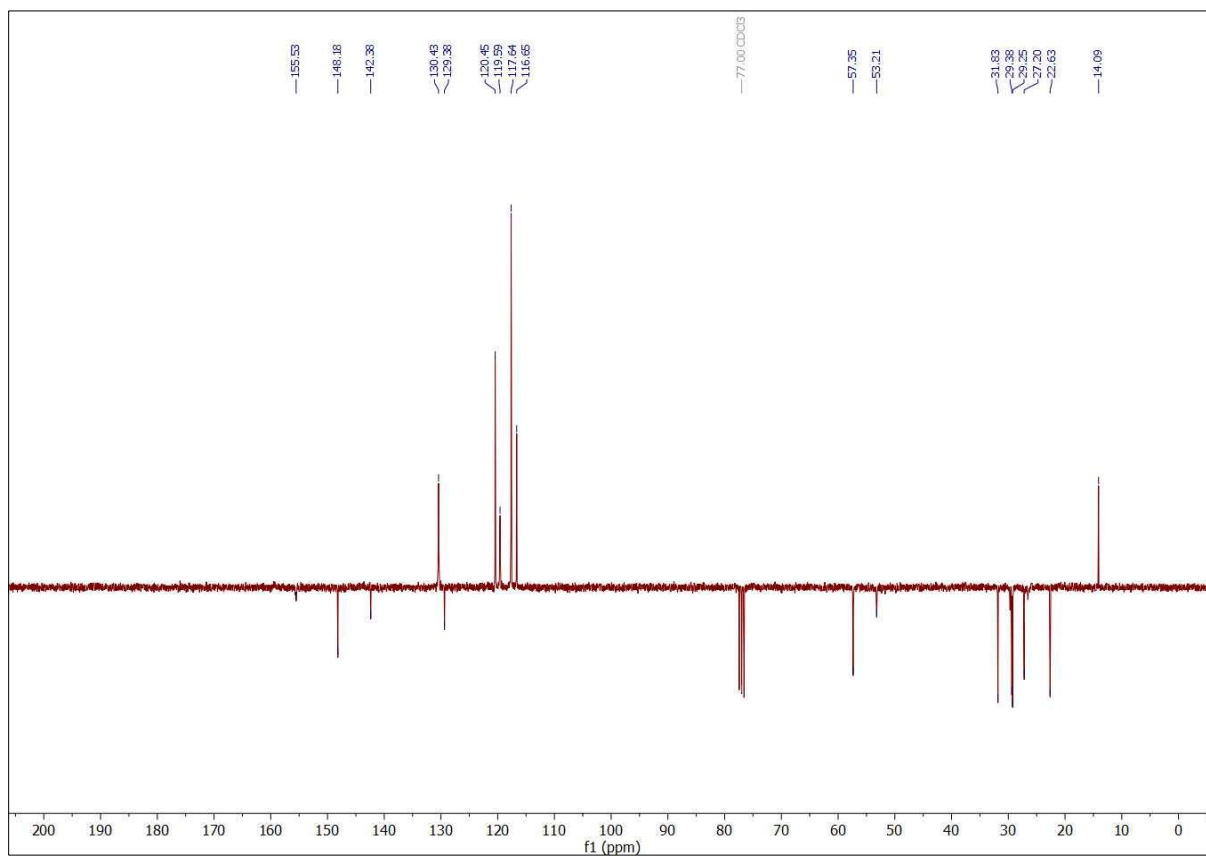
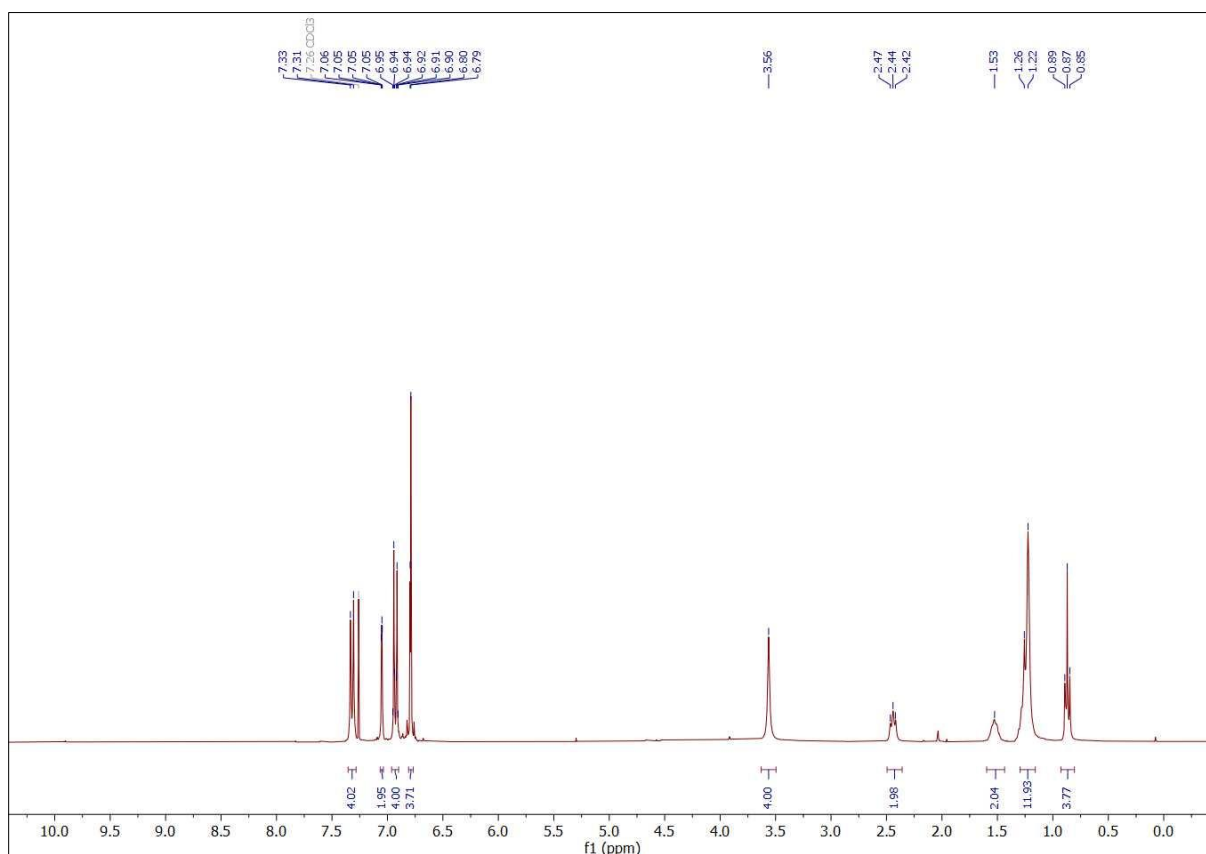
N-(4-Phenoxybenzyl)octan-1-amine (14).



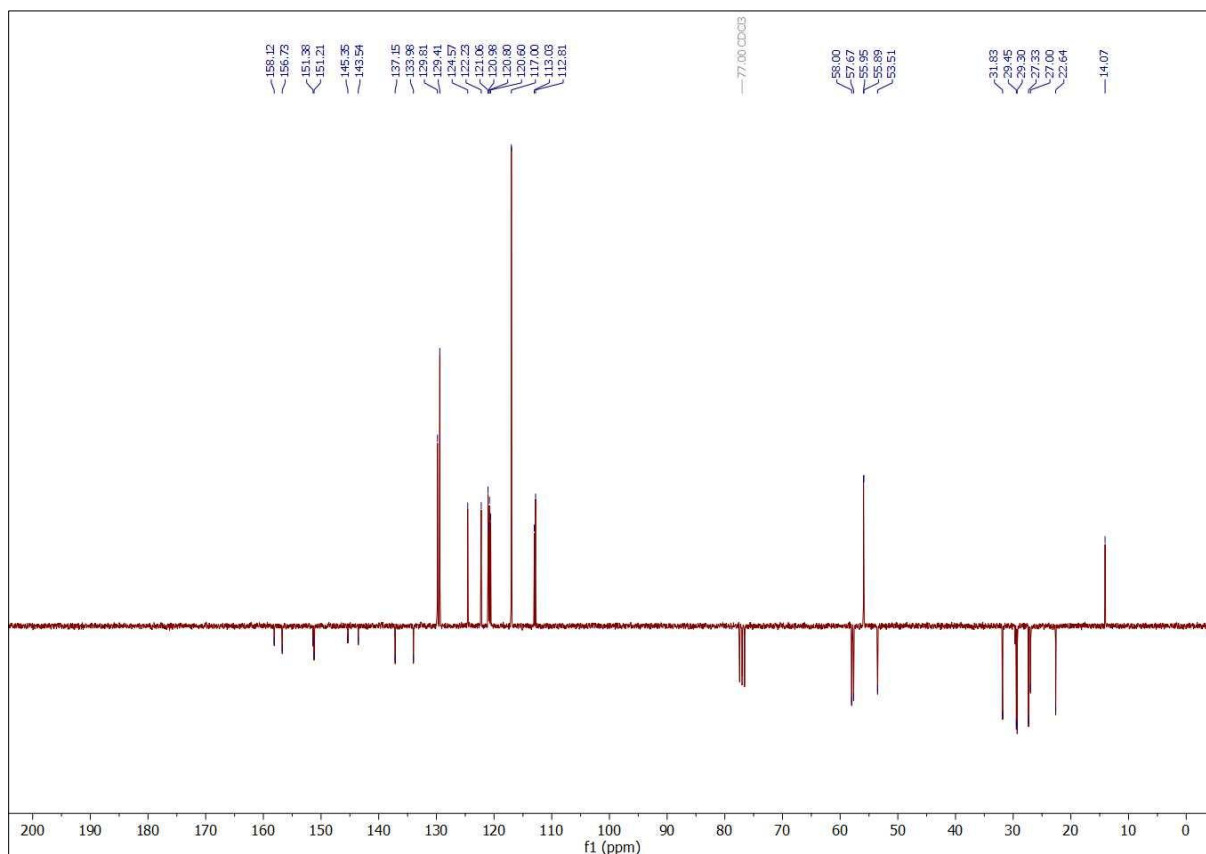
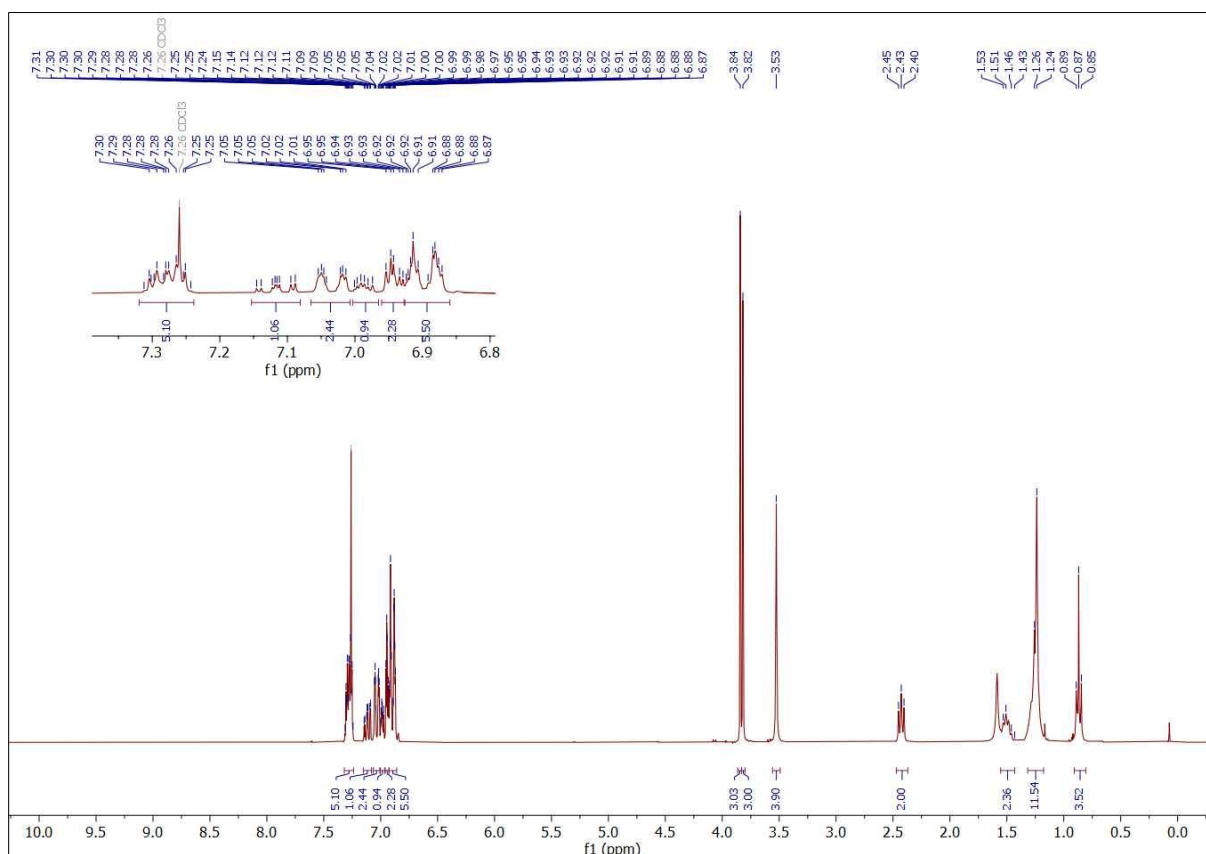
***N,N*-Bis(4-(4-chloro-2-methoxyphenoxy)benzyl)octan-1-amine (15).**



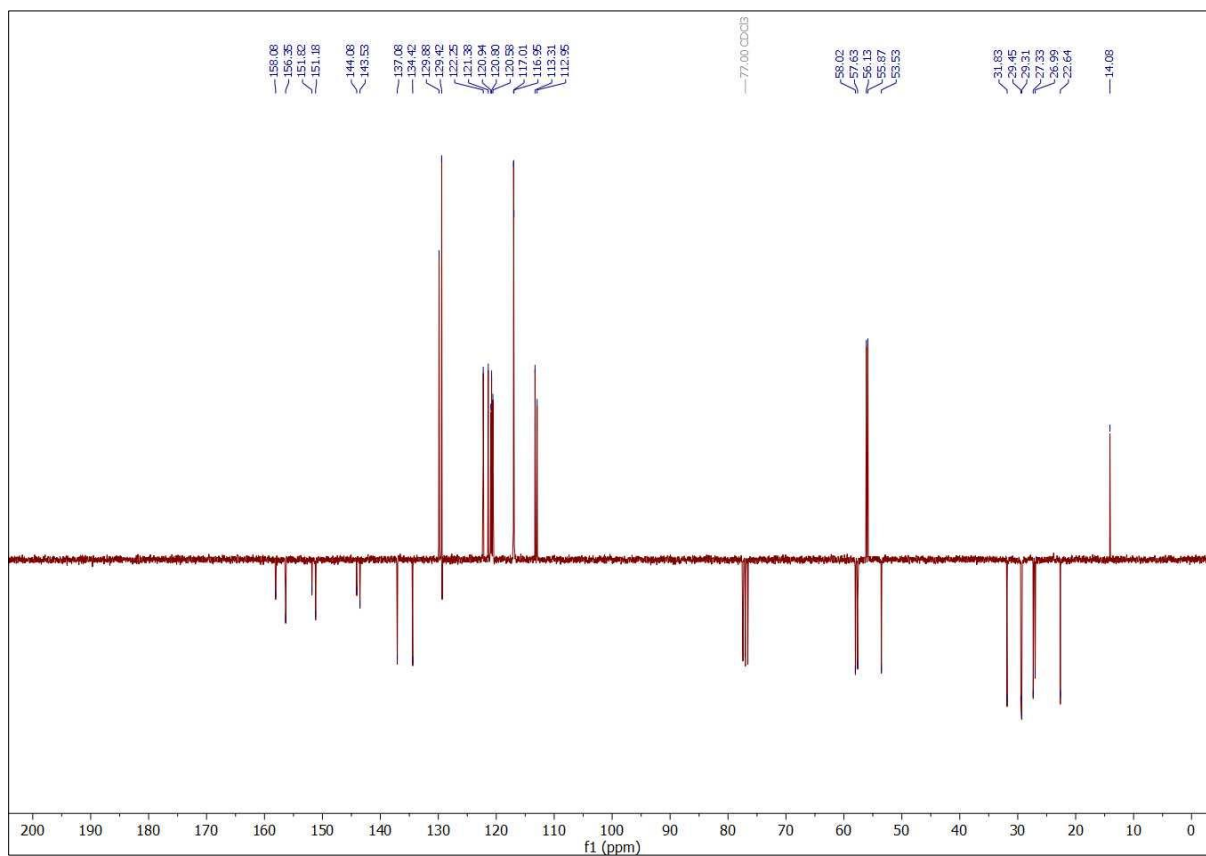
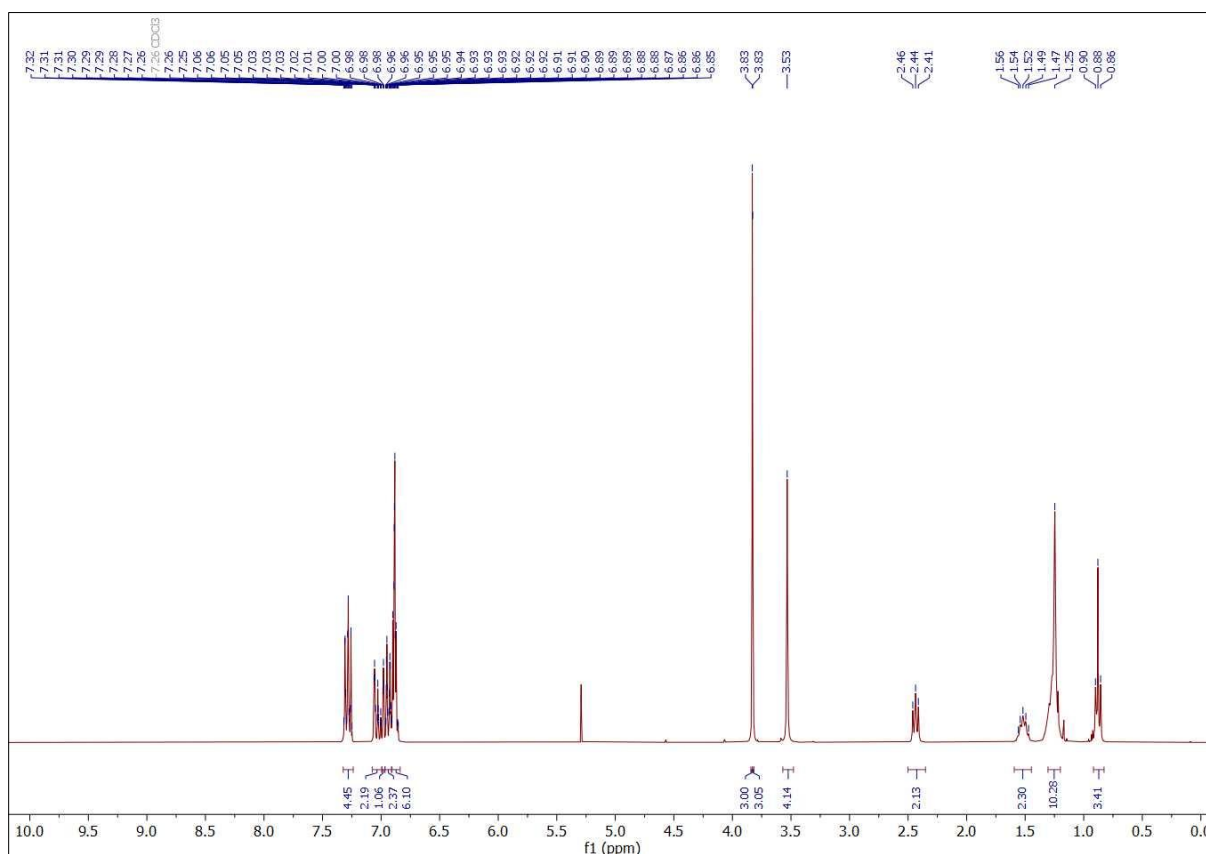
***N,N*-Bis(4-(4-chloro-2-hydroxyphenoxy)benzyl)octan-1-amine (16).**



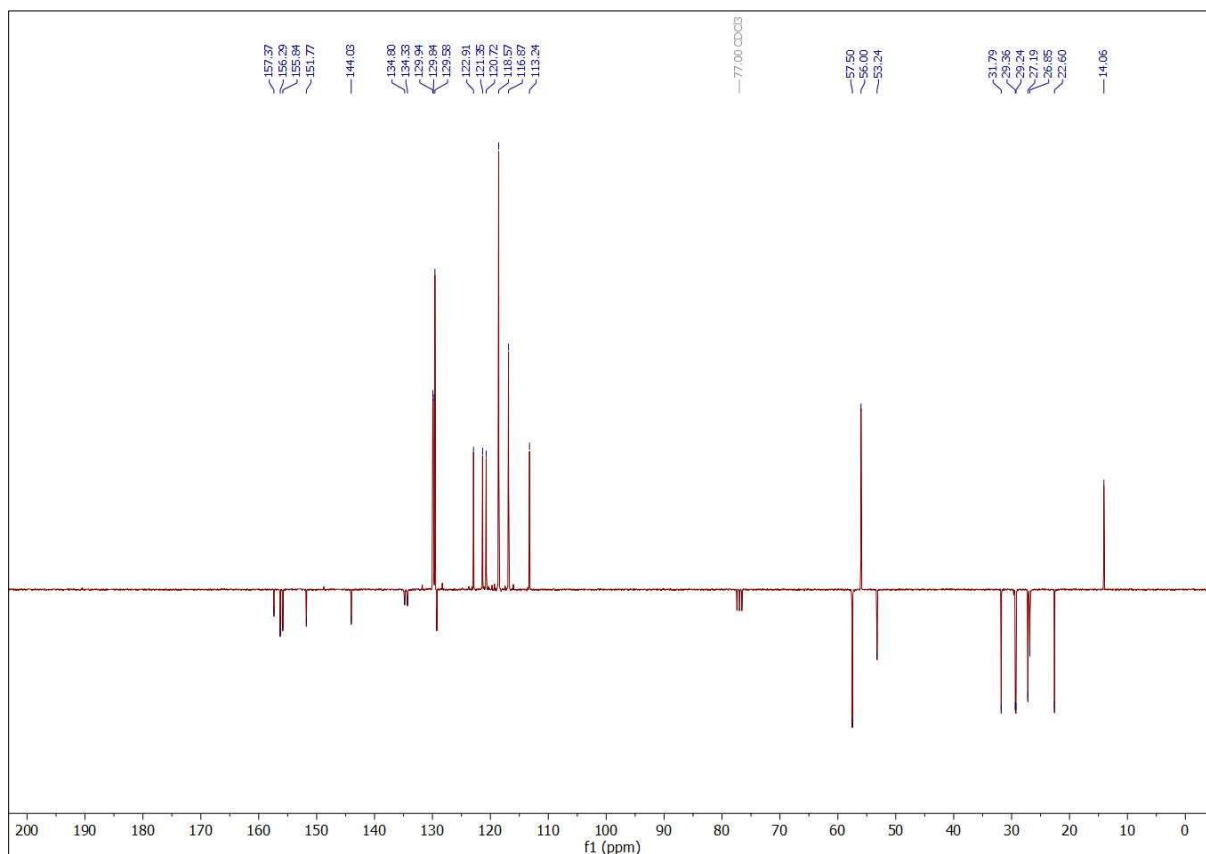
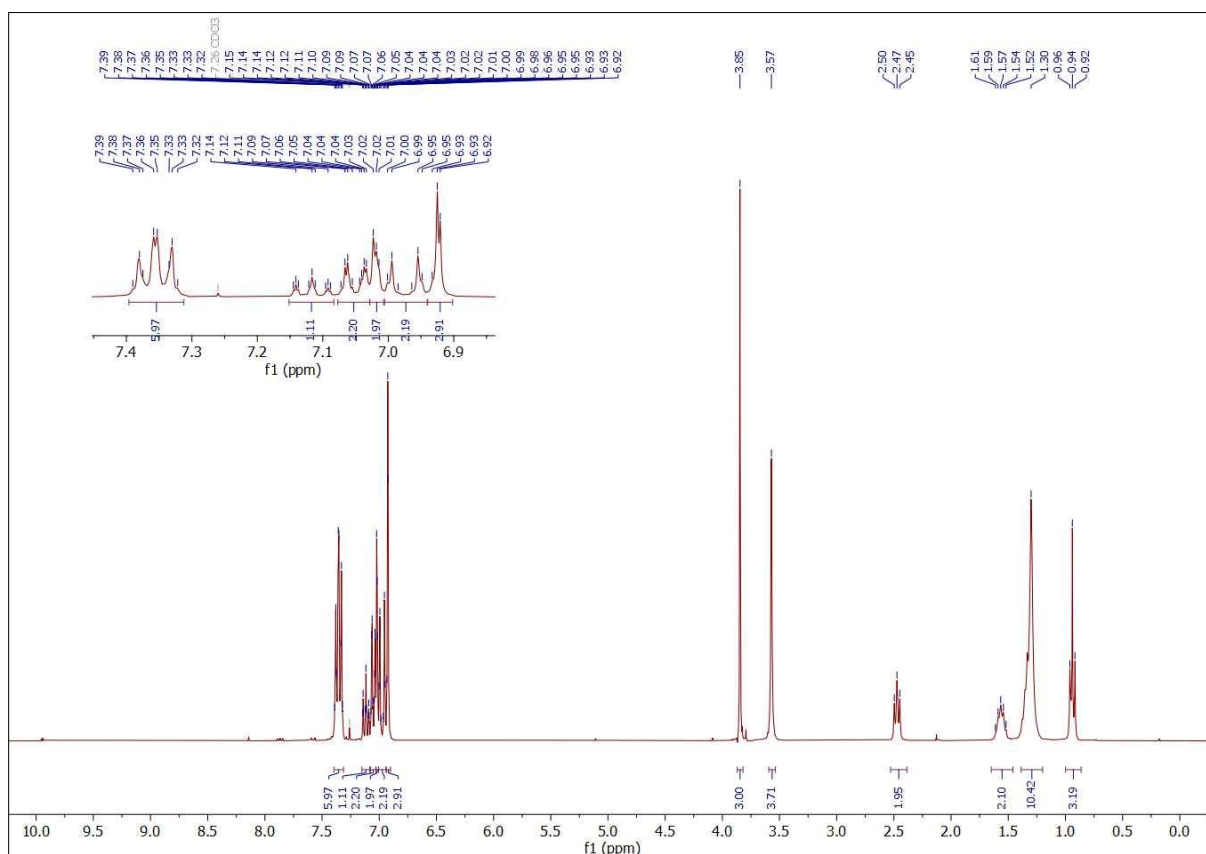
***N*-(3-Methoxy-4-phenoxybenzyl)-*N*-(4-(2-methoxyphenoxy)benzyl)octan-1-amine (17).**



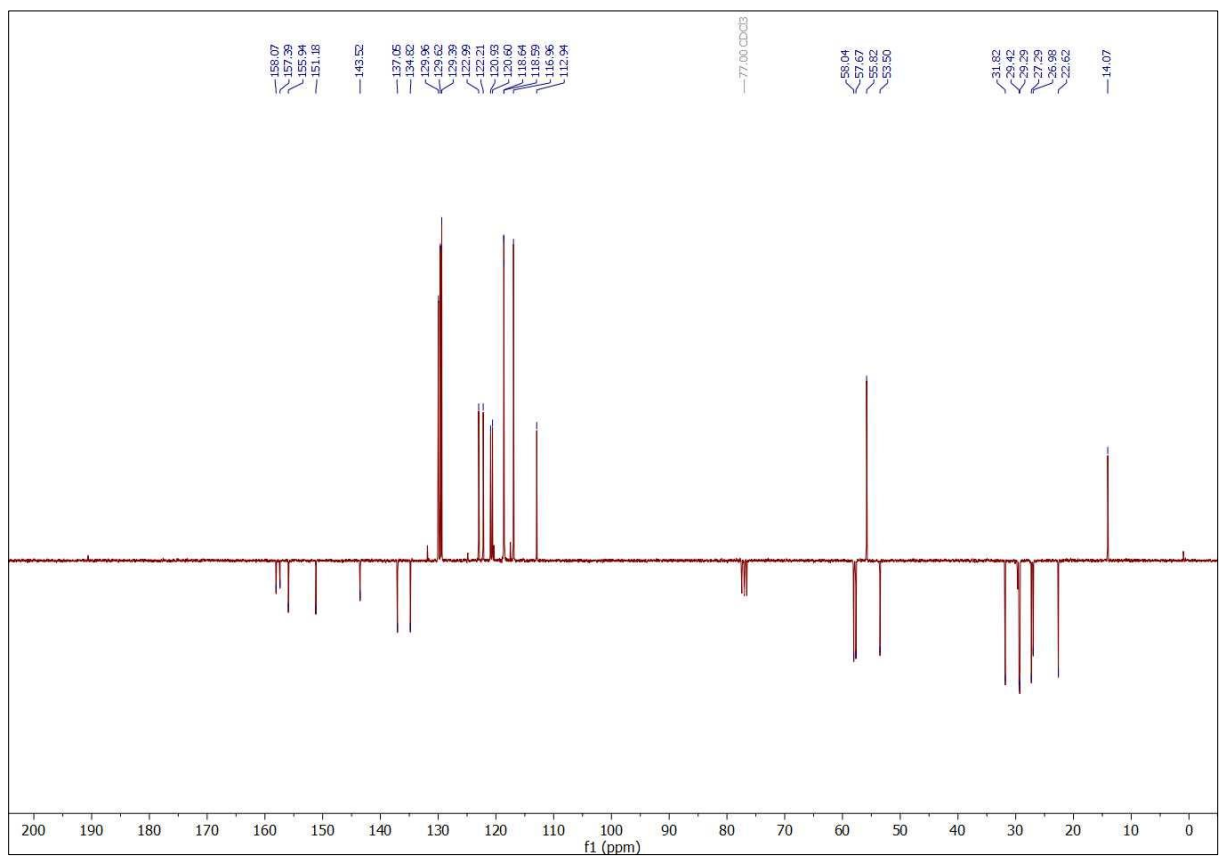
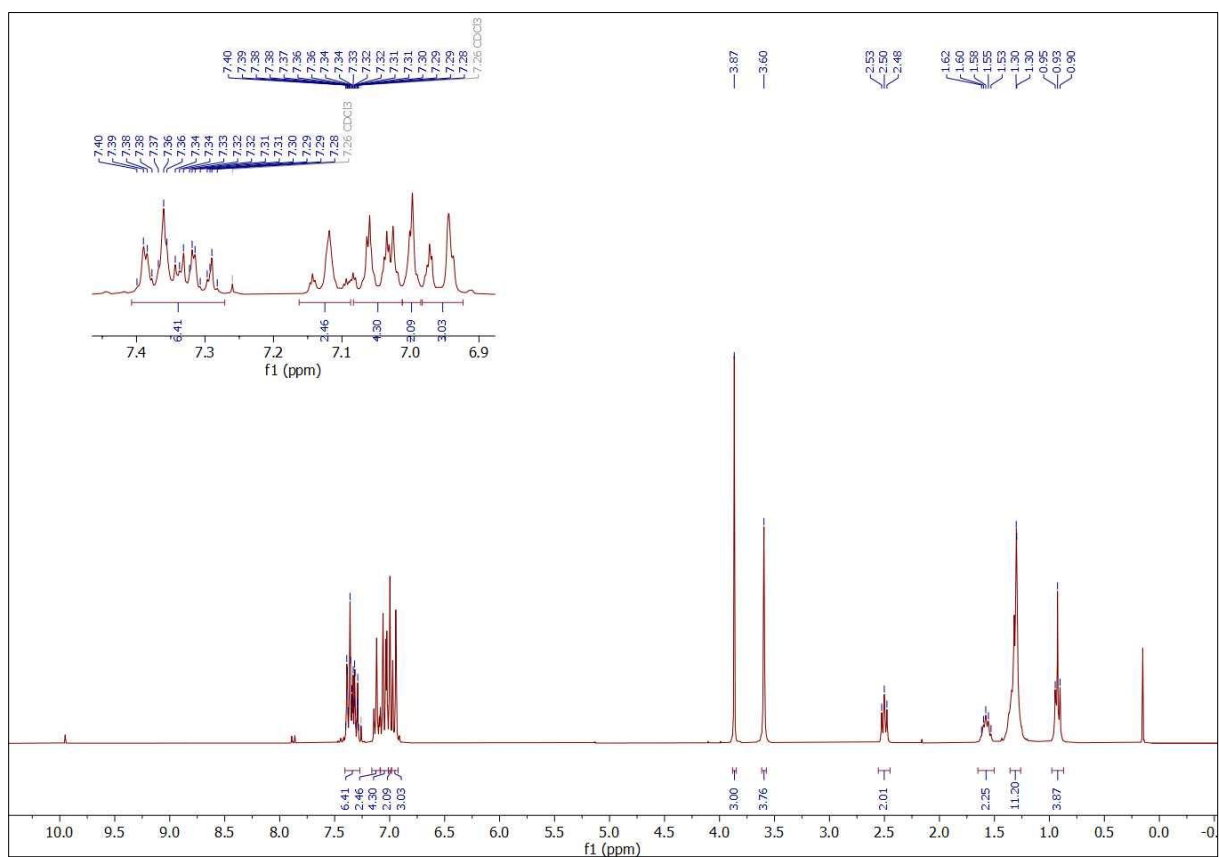
***N*-(4-(4-Chloro-2-methoxyphenoxy)benzyl)-*N*-(3-methoxy-4-phenoxybenzyl)octan-1-amine (18).**



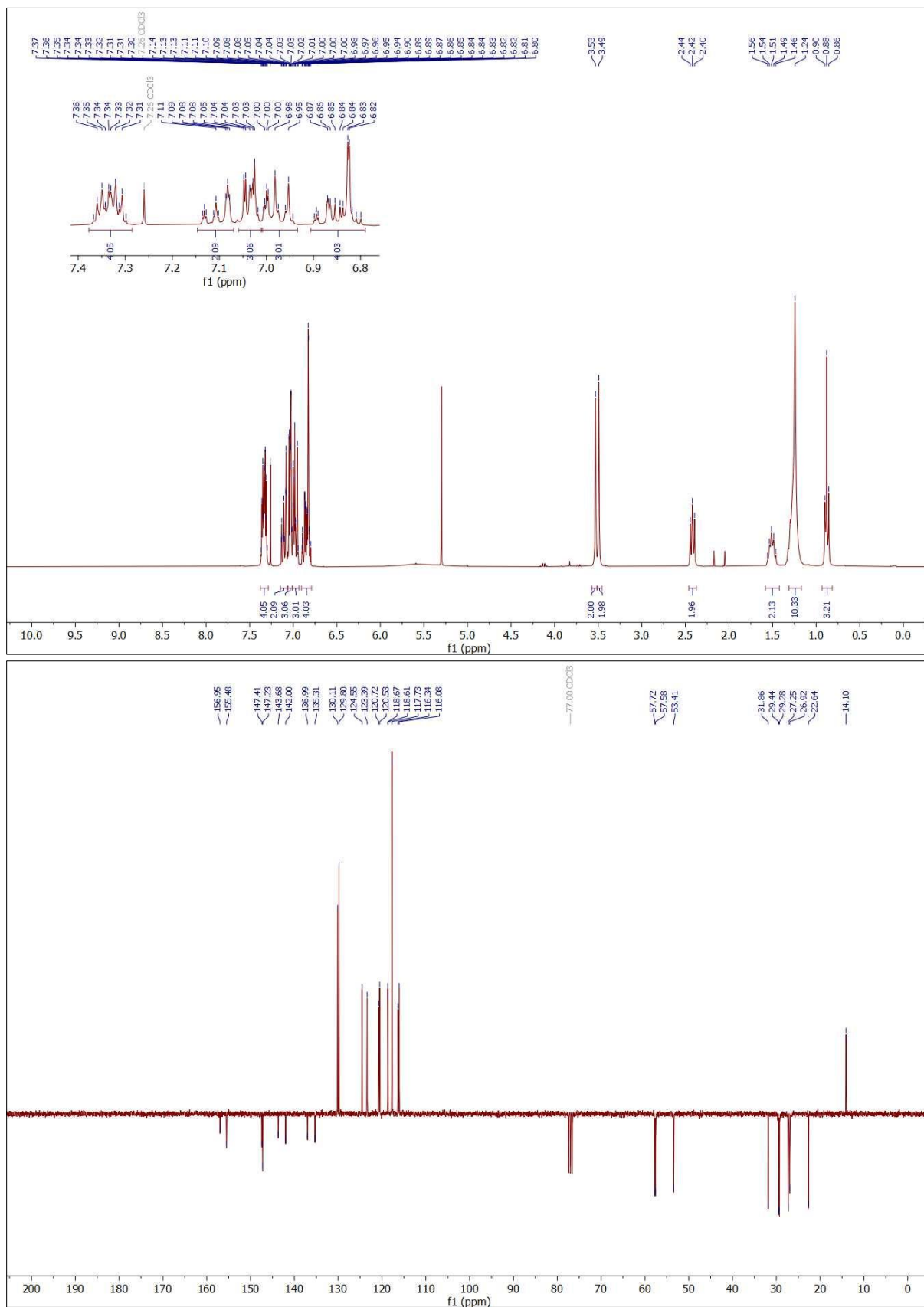
***N*-(4-(4-Chloro-2-methoxyphenoxy)benzyl)-*N*-(4-phenoxybenzyl)octan-1-amine (19).**



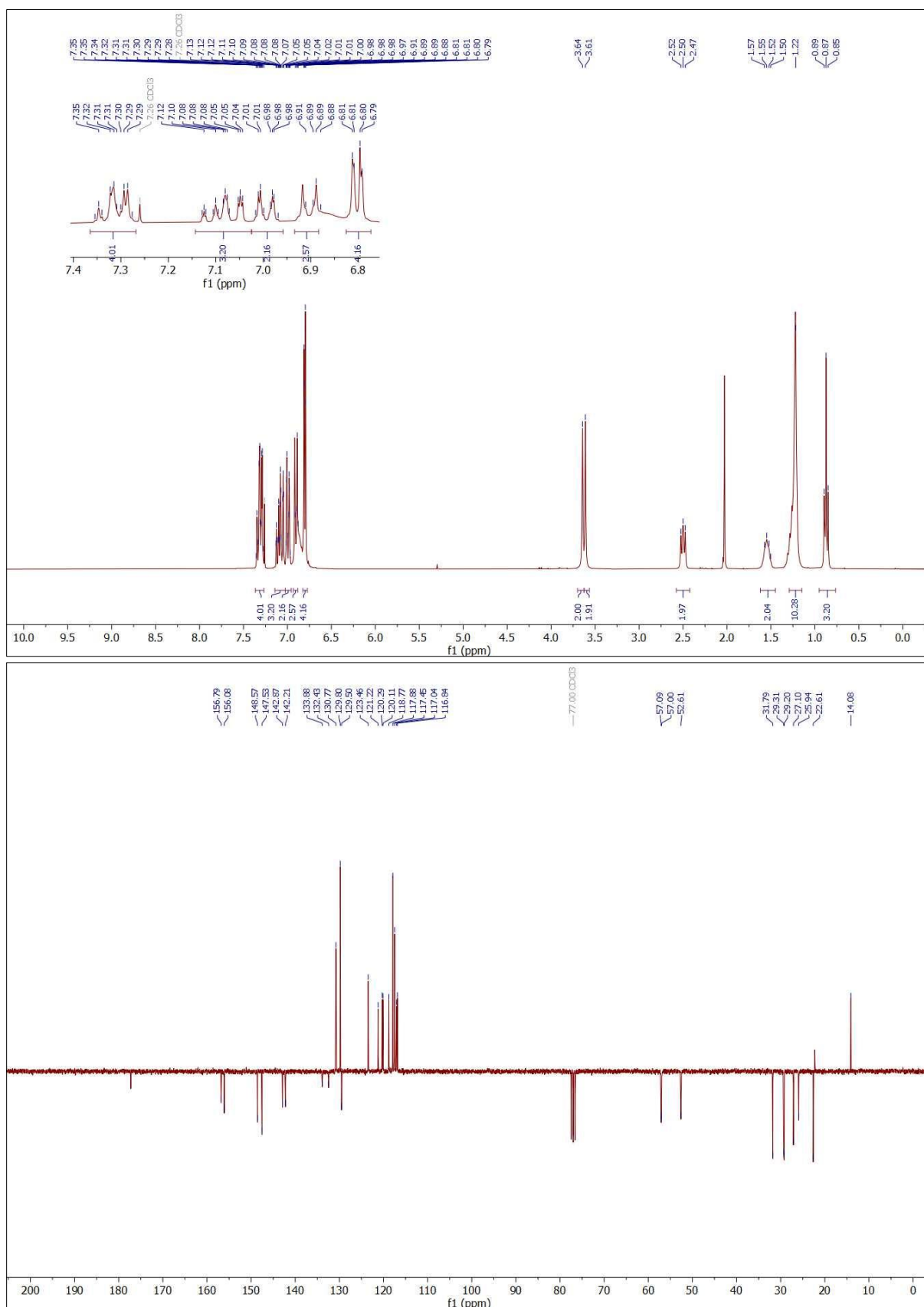
***N*-(3-methoxy-4-phenoxybenzyl)-*N*-(4-phenoxybenzyl)octan-1-amine (20).**



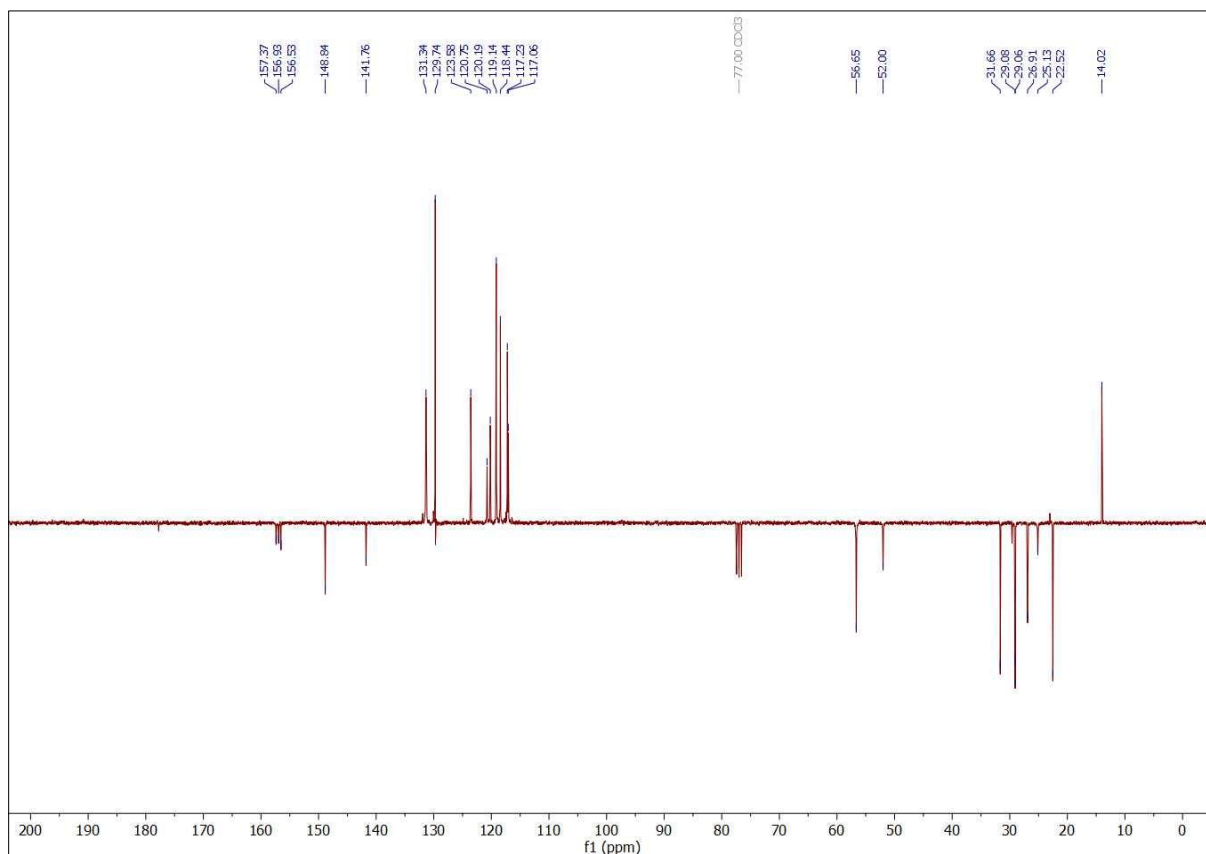
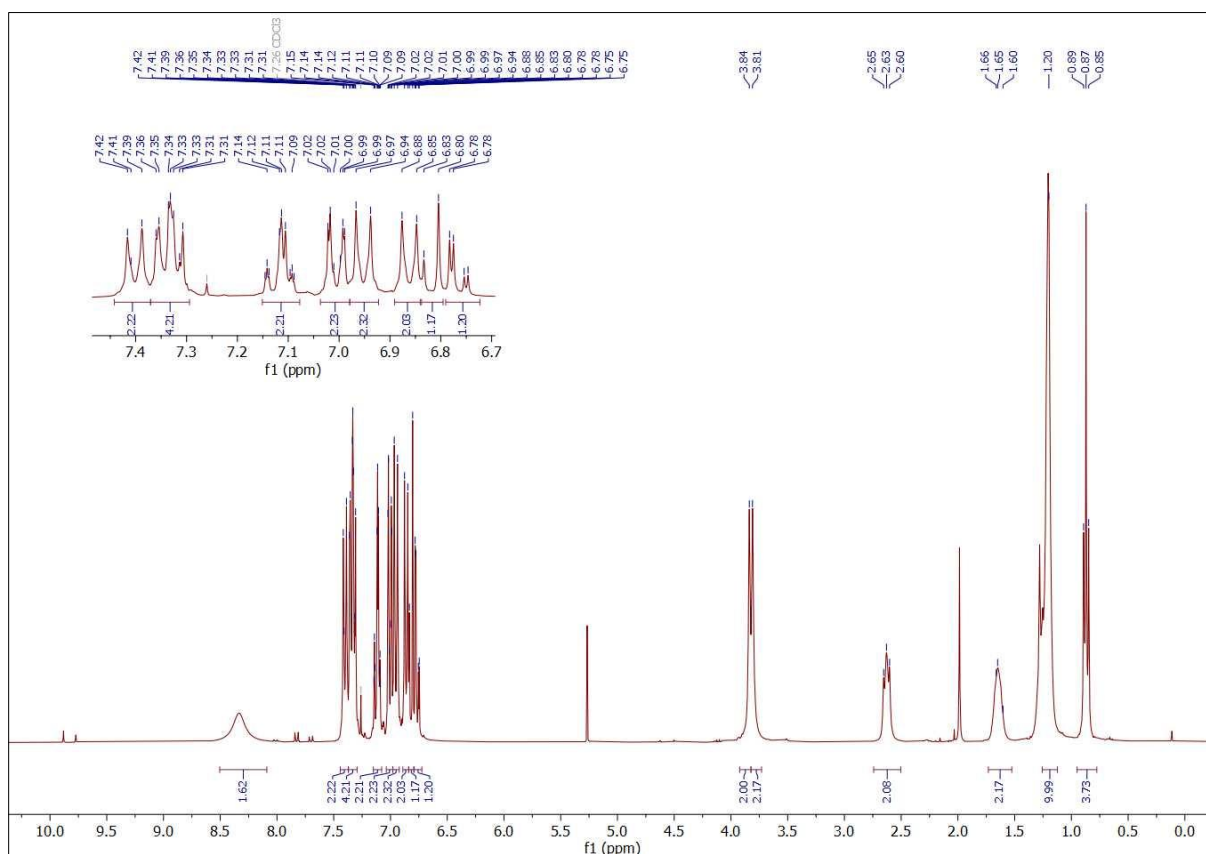
5-(((4-(2-Hydroxyphenoxy)benzyl)(octyl)amino)methyl)-2-phenoxyphenol (21).



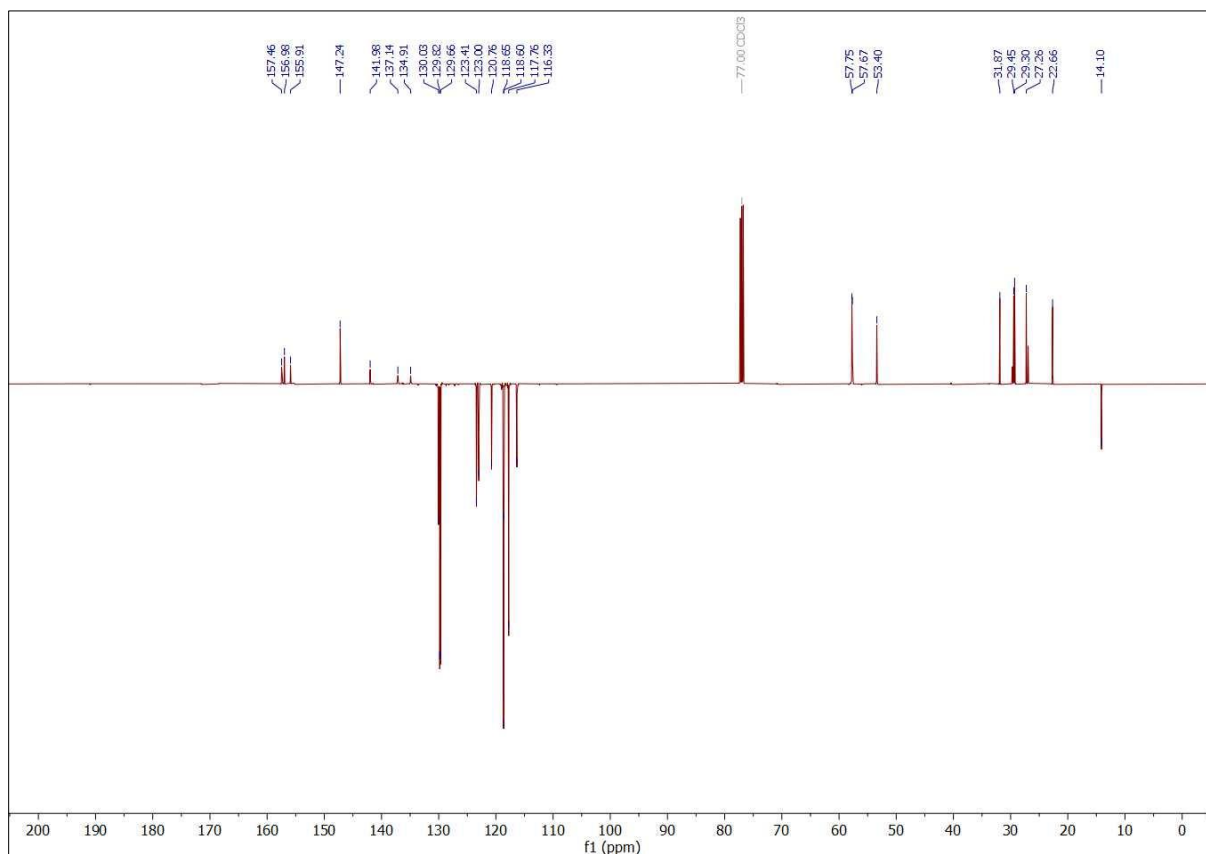
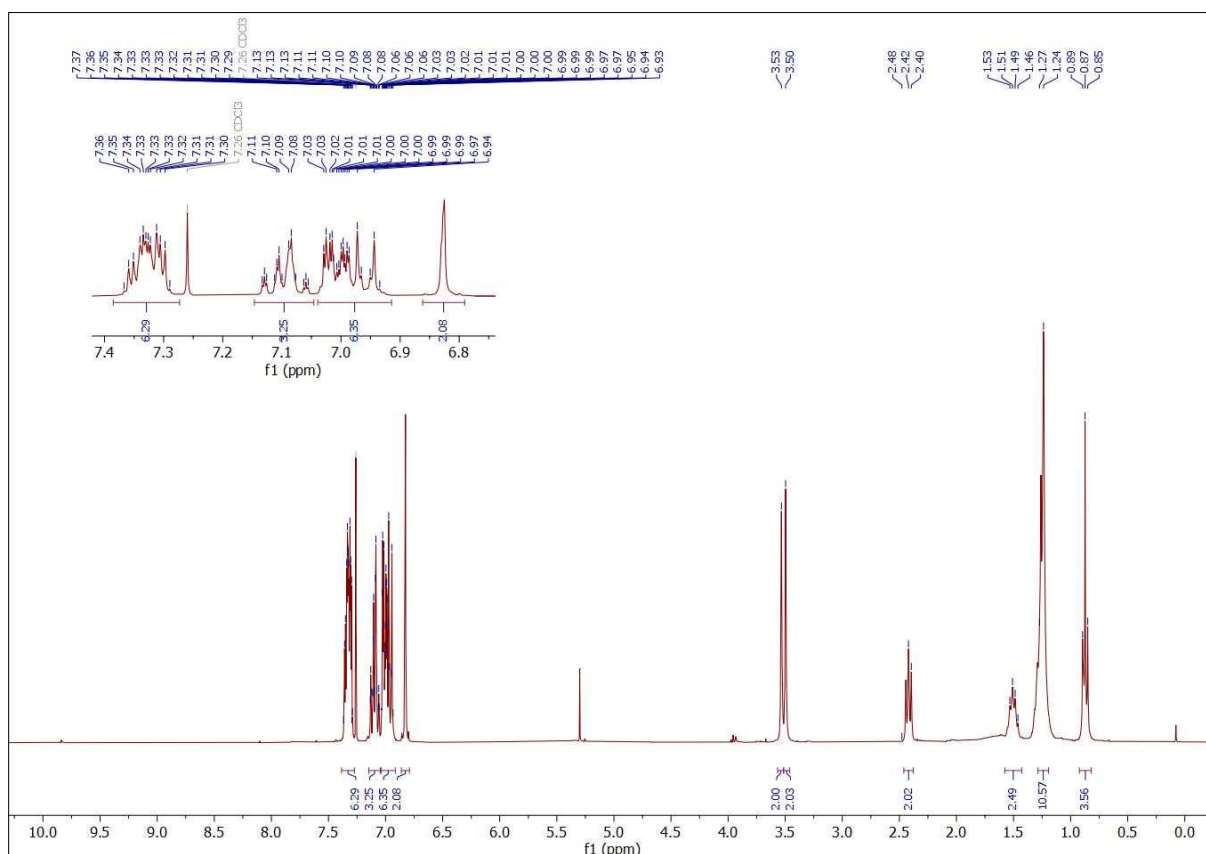
5-Chloro-2-(4-(((3-hydroxy-4-phenoxybenzyl)(octyl)amino)methyl)phenoxy)phenol (22).



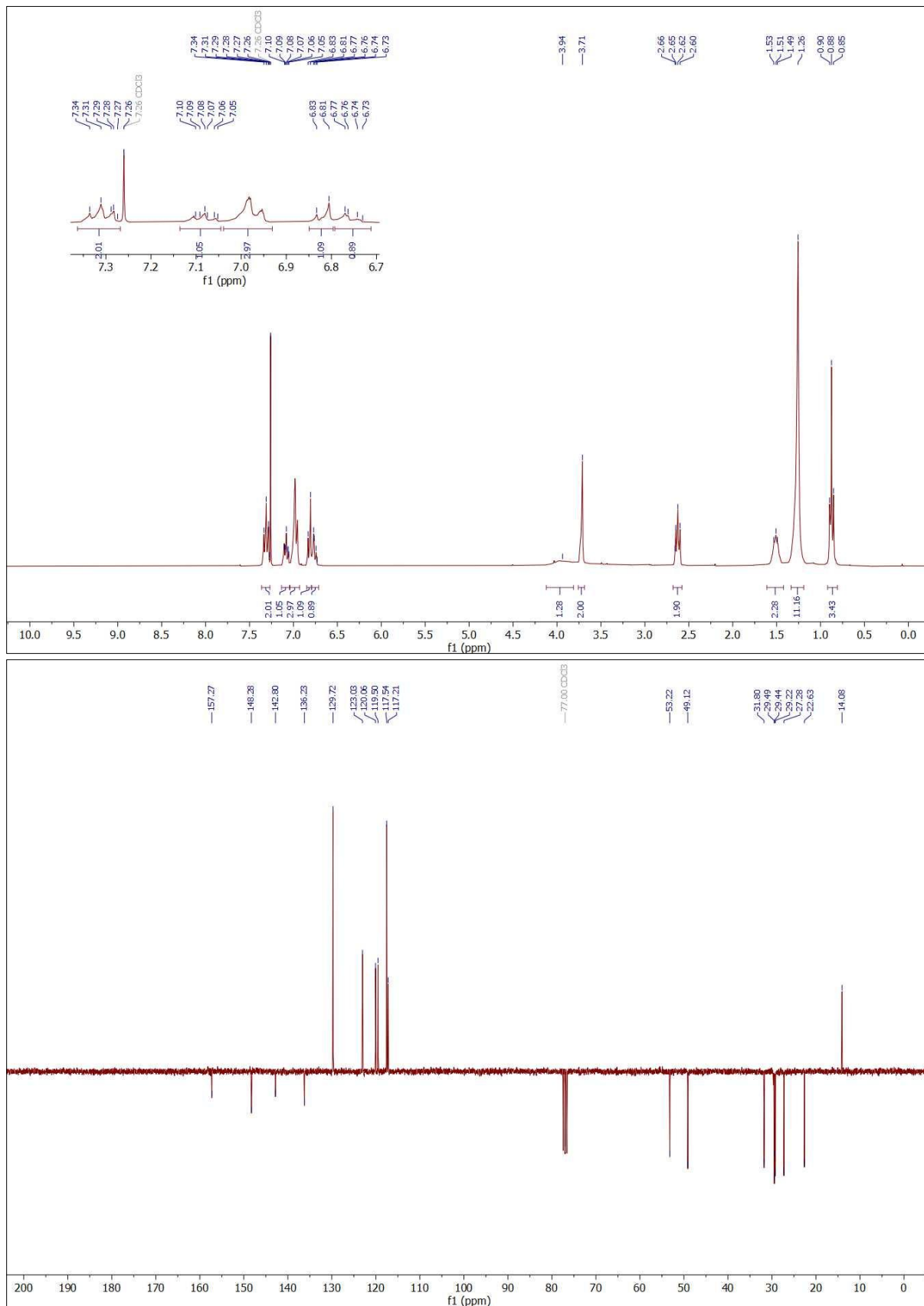
5-Chloro-2-(4-((octyl(4-phenoxybenzyl)amino)methyl)phenoxy)phenol (23).



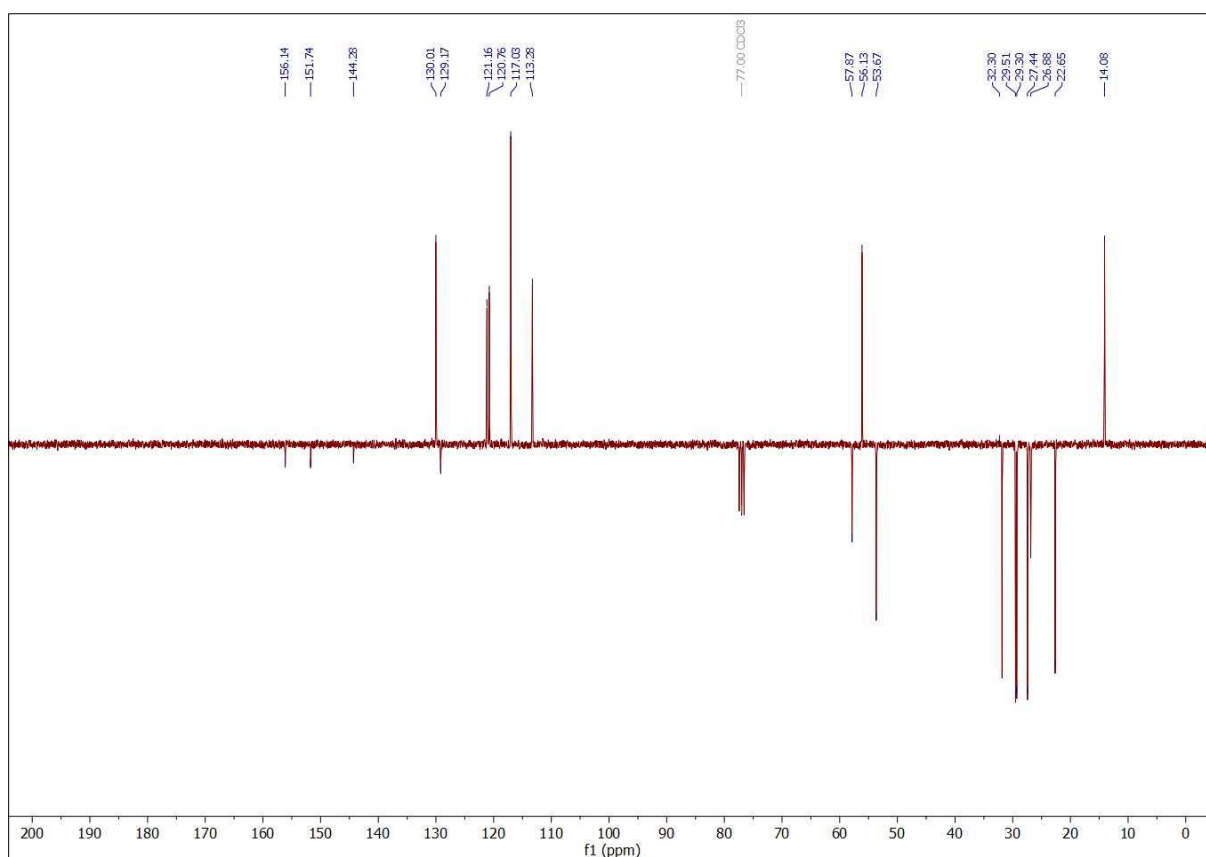
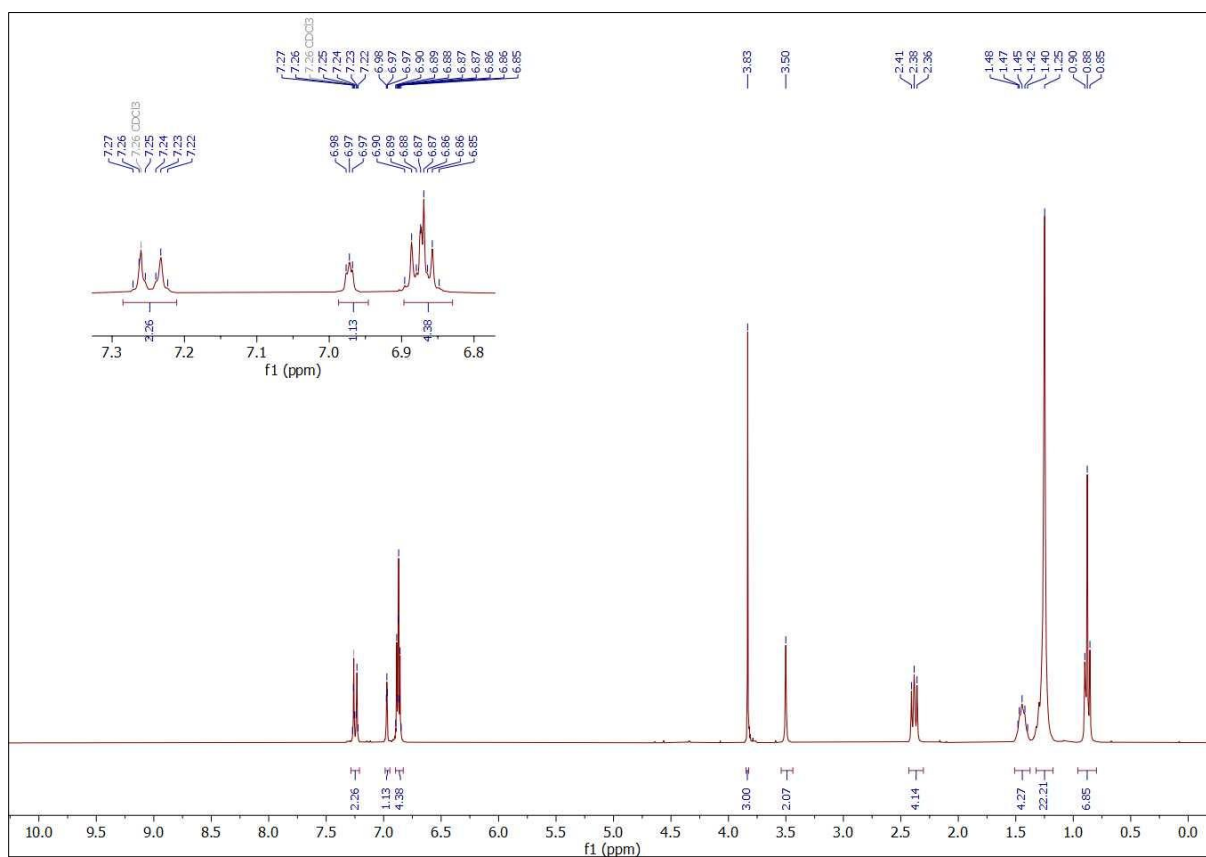
5-((octyl(4-phenoxybenzyl)amino)methyl)-2-phenoxyphenol (24).



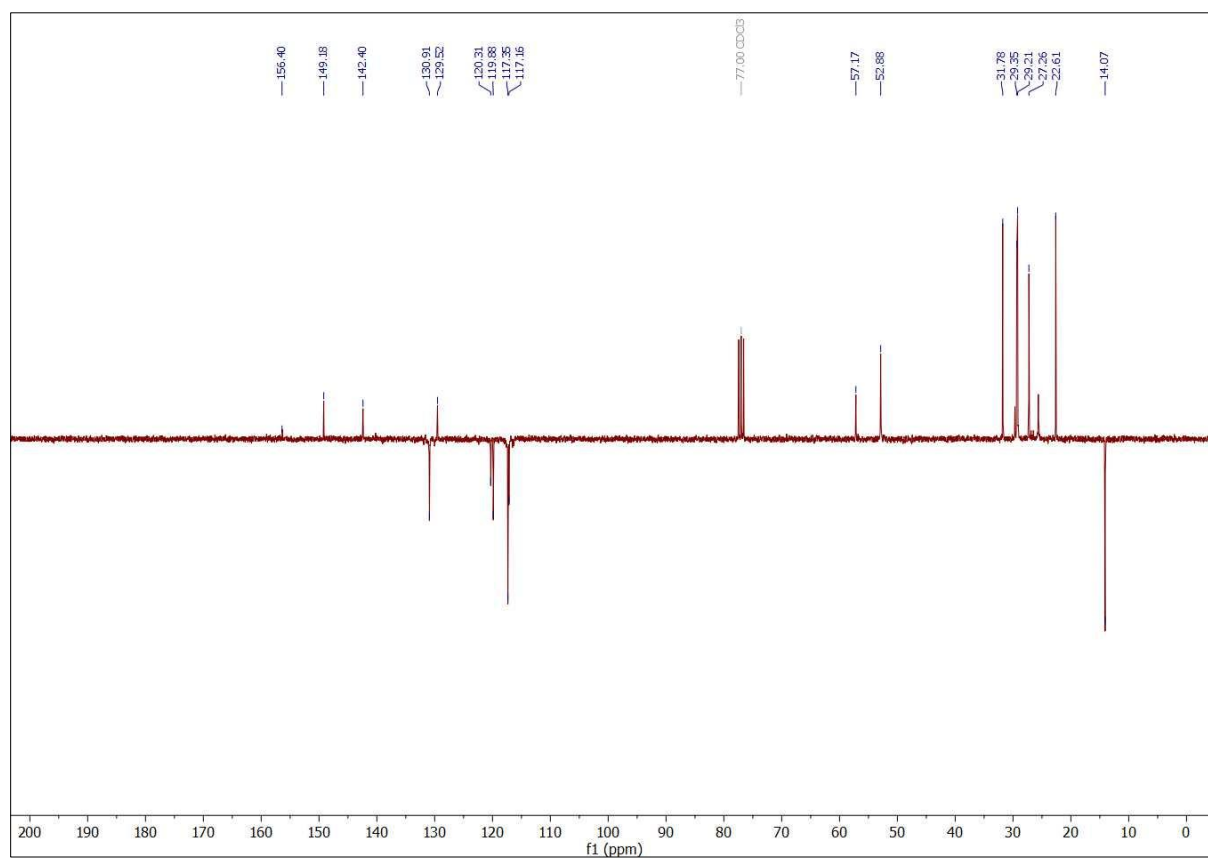
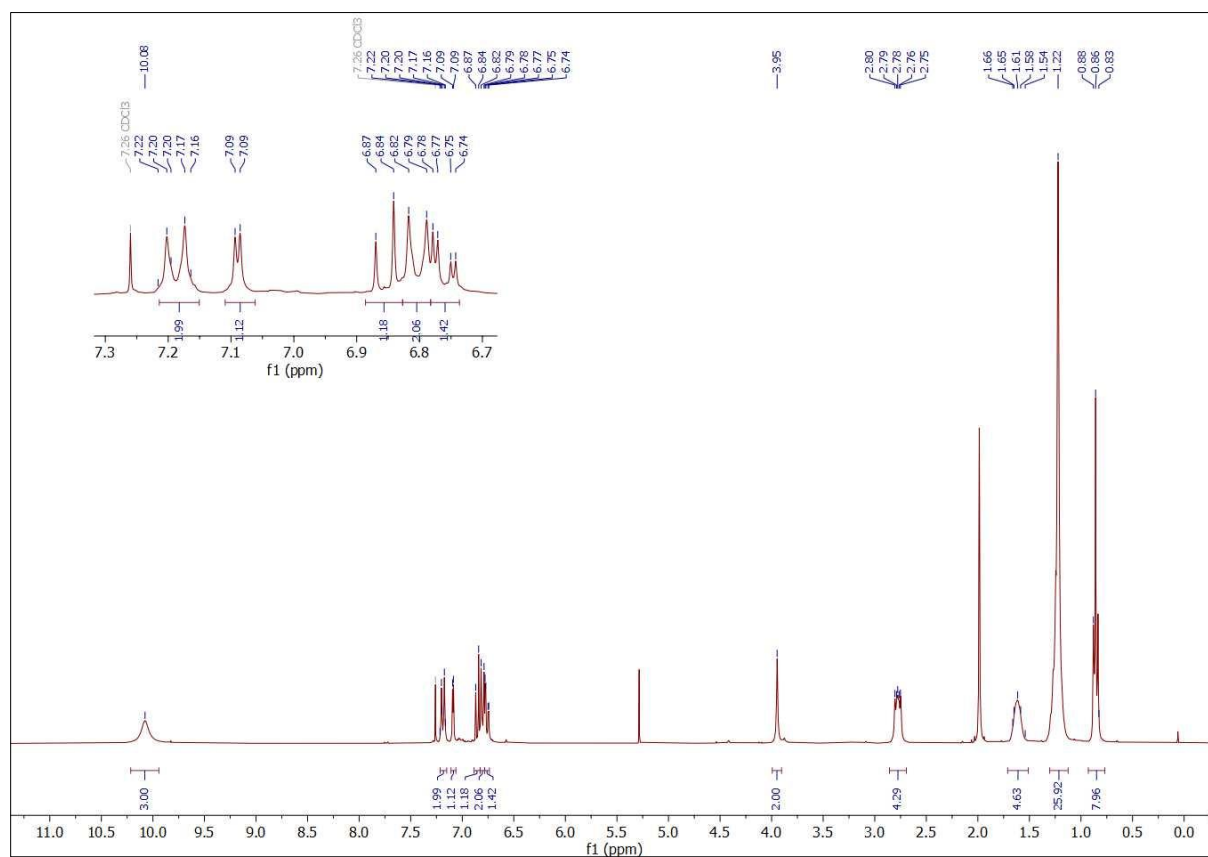
5-((Octylamino)methyl)-2-phenoxyphenol (25).



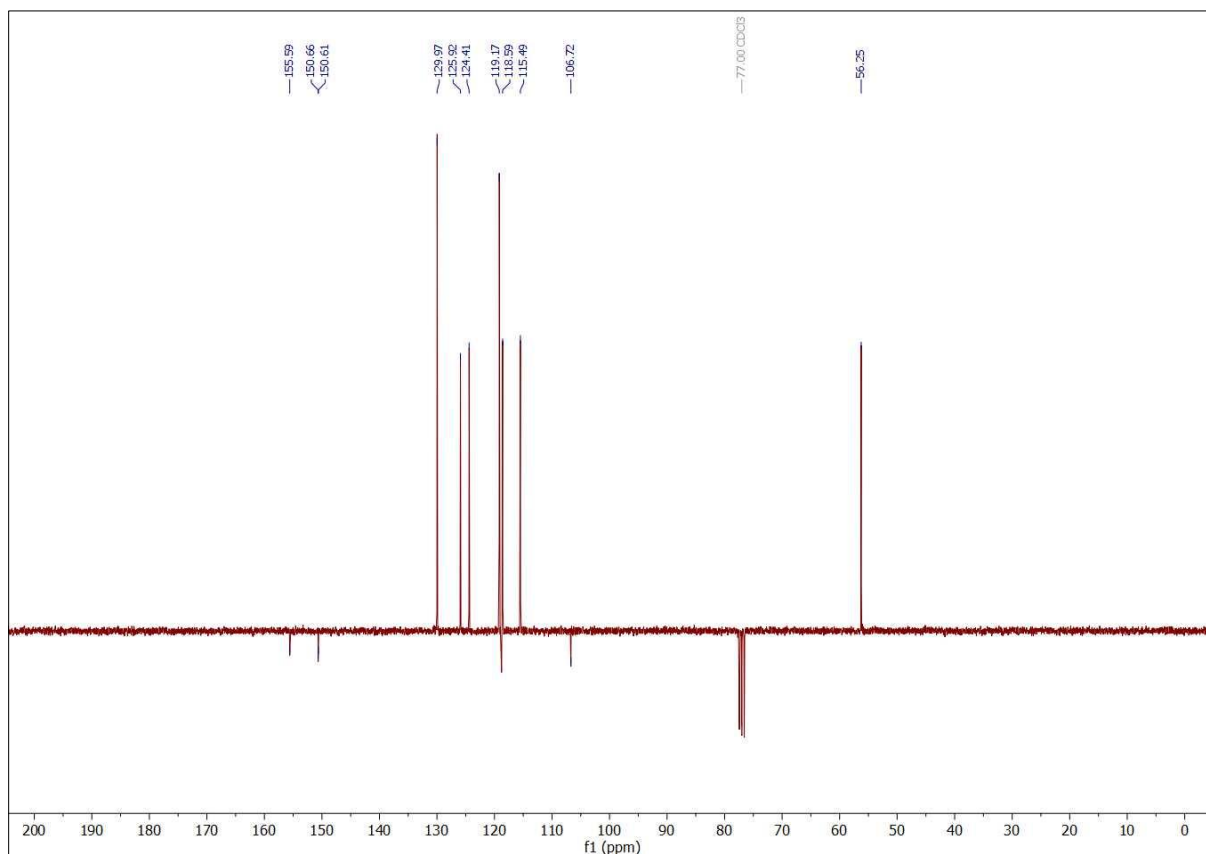
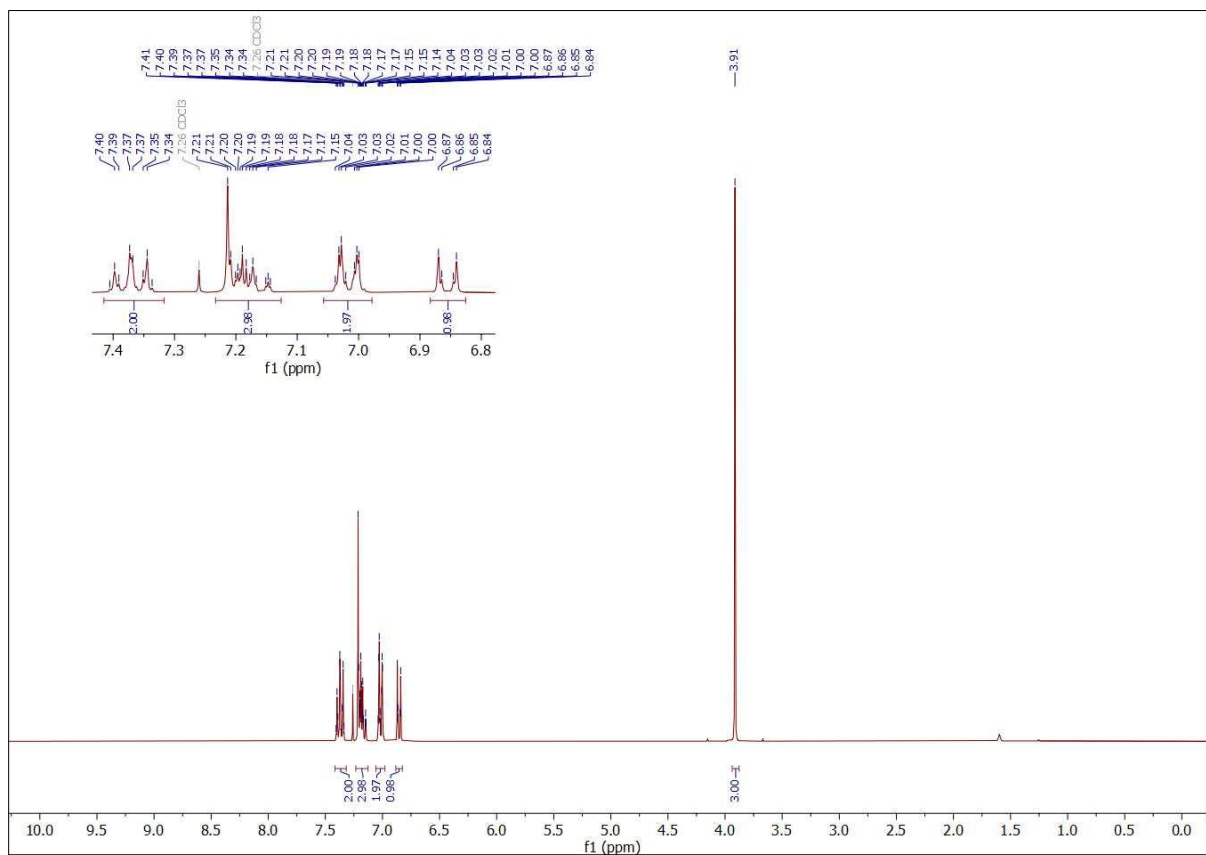
***N*-(4-(4-Chloro-2-methoxyphenoxy)benzyl)-*N*-octyloctan-1-amine (26).**



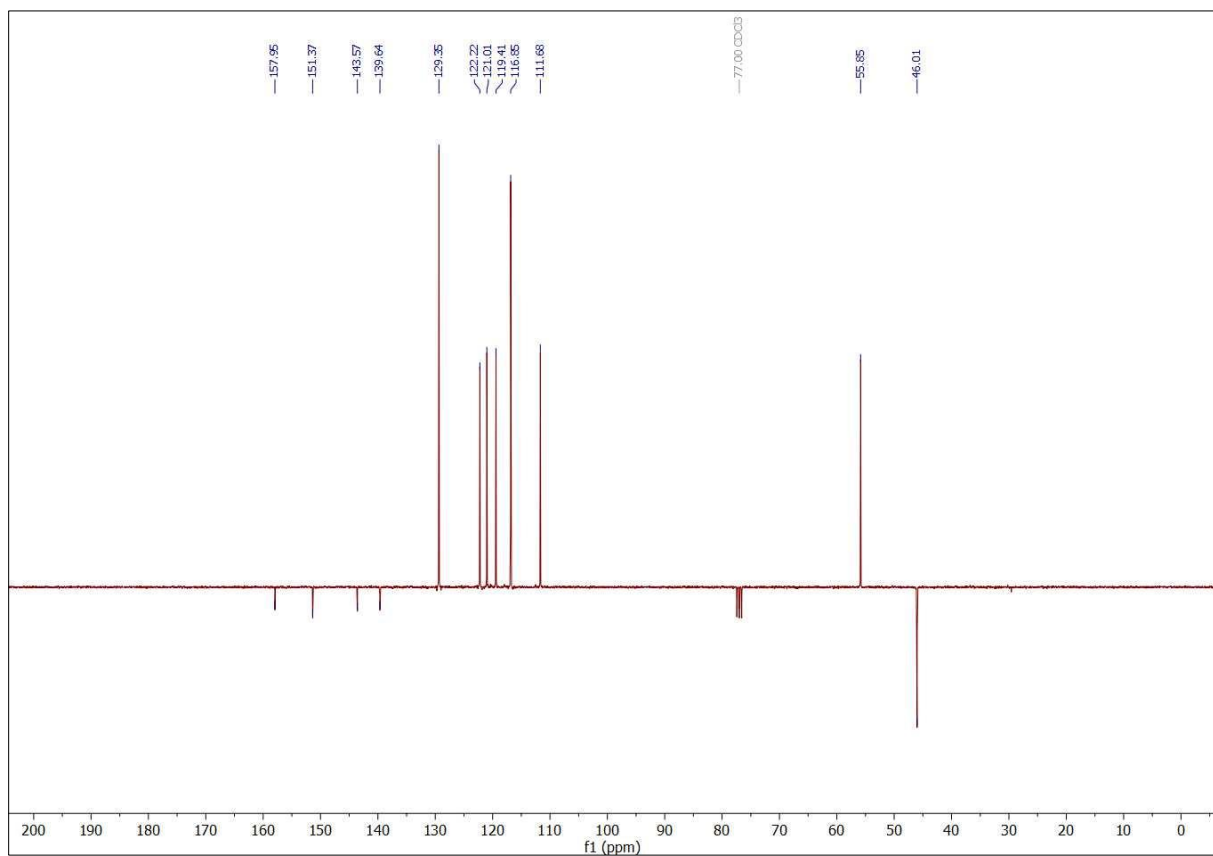
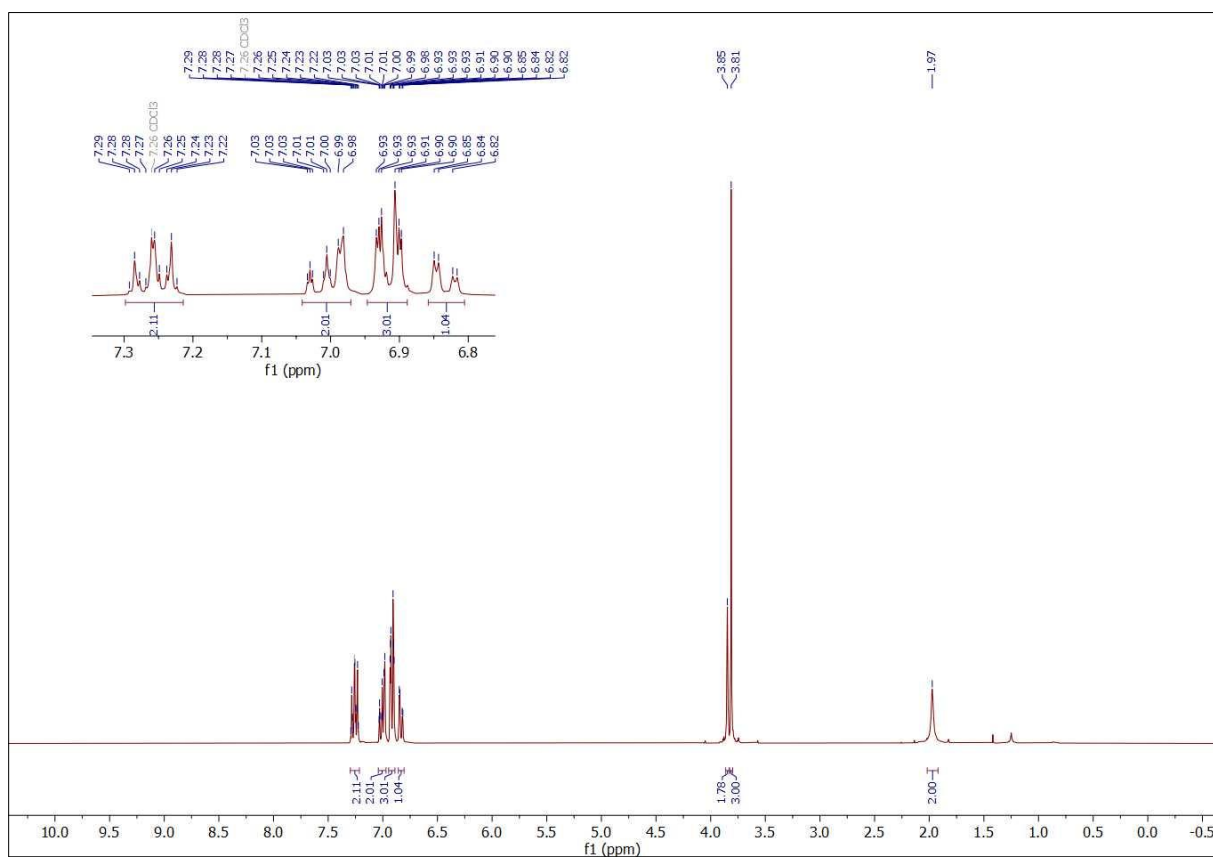
5-Chloro-2-(4-((diethylamino)methyl)phenoxy)phenol (27).



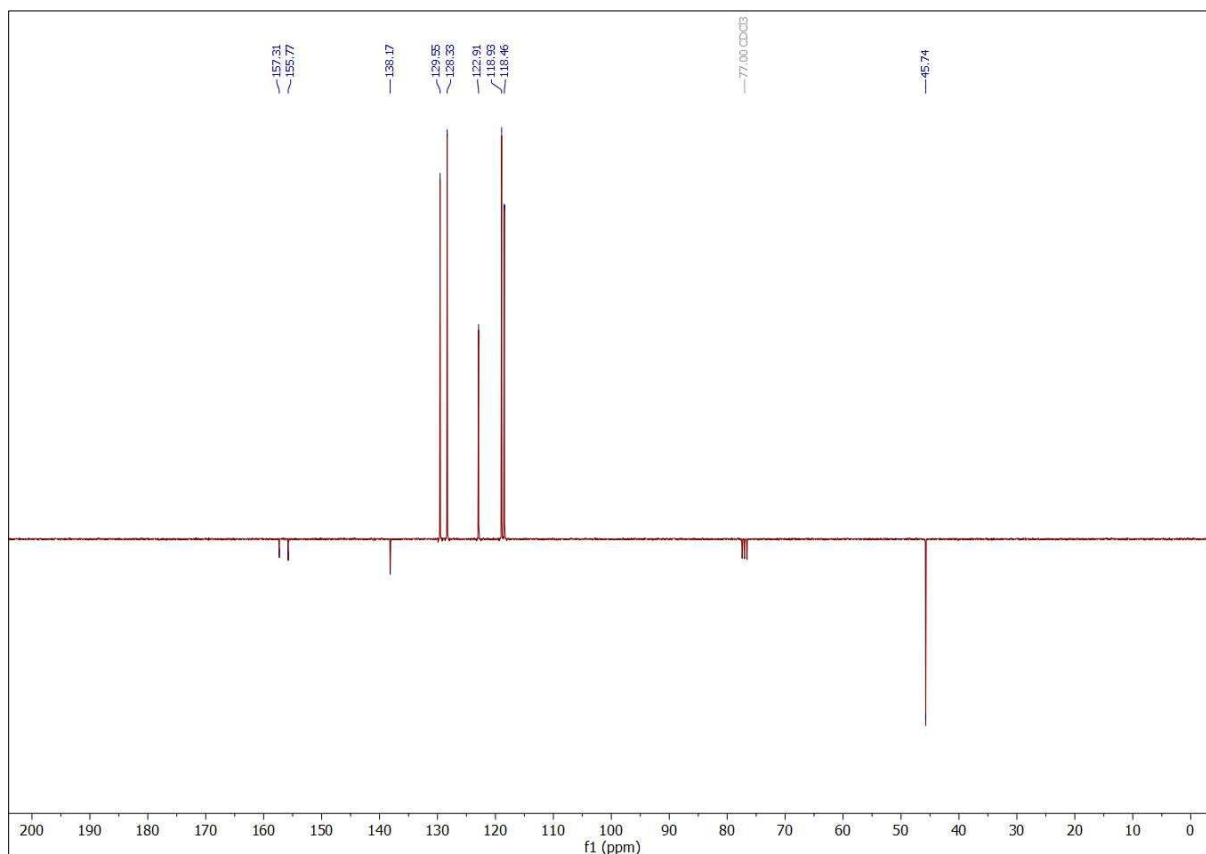
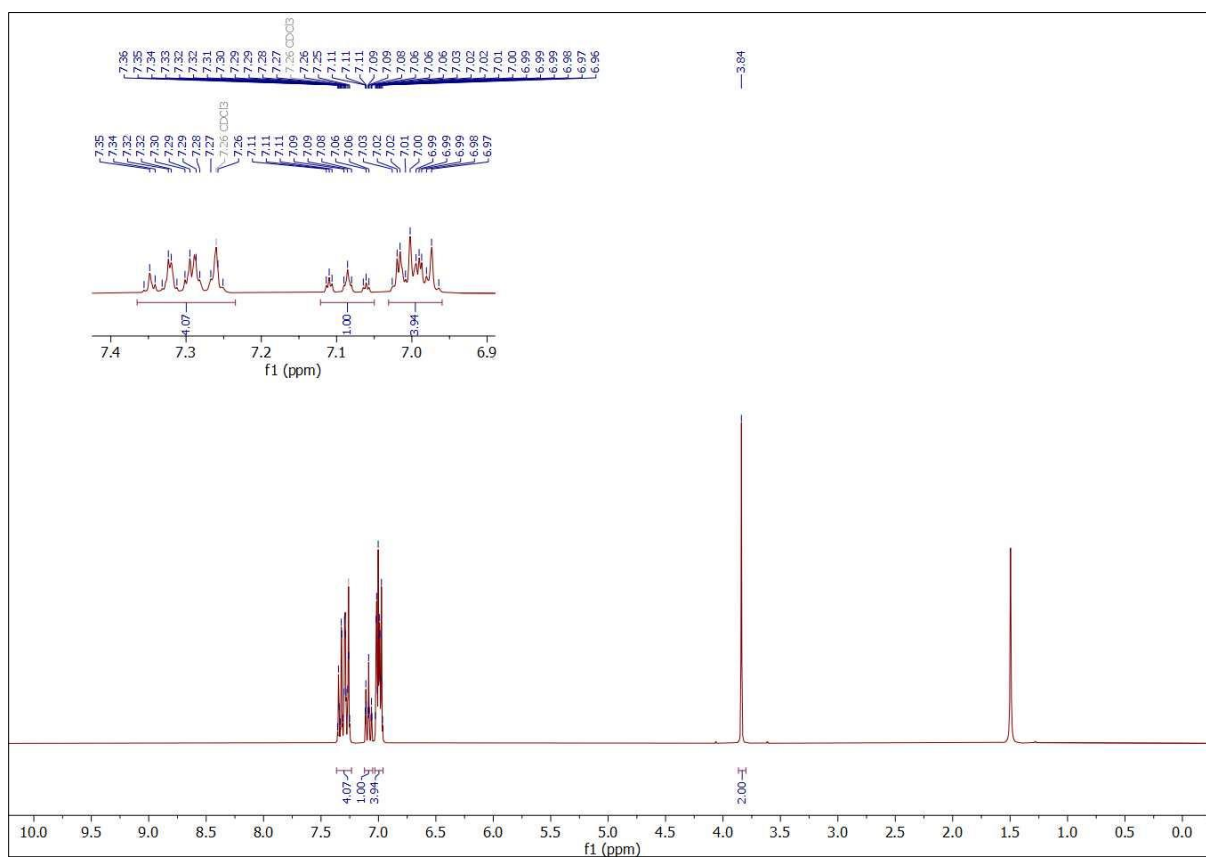
3-Methoxy-4-phenoxybenzotrile (28).



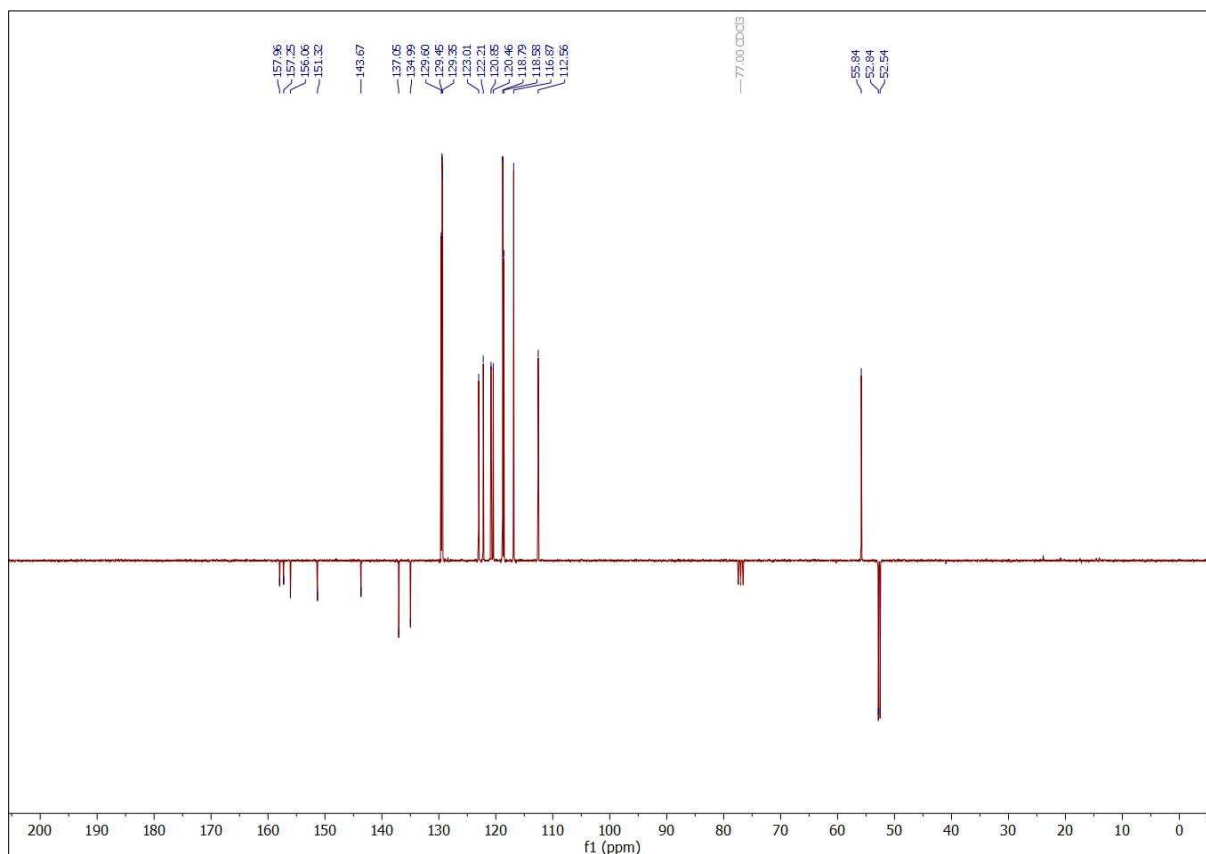
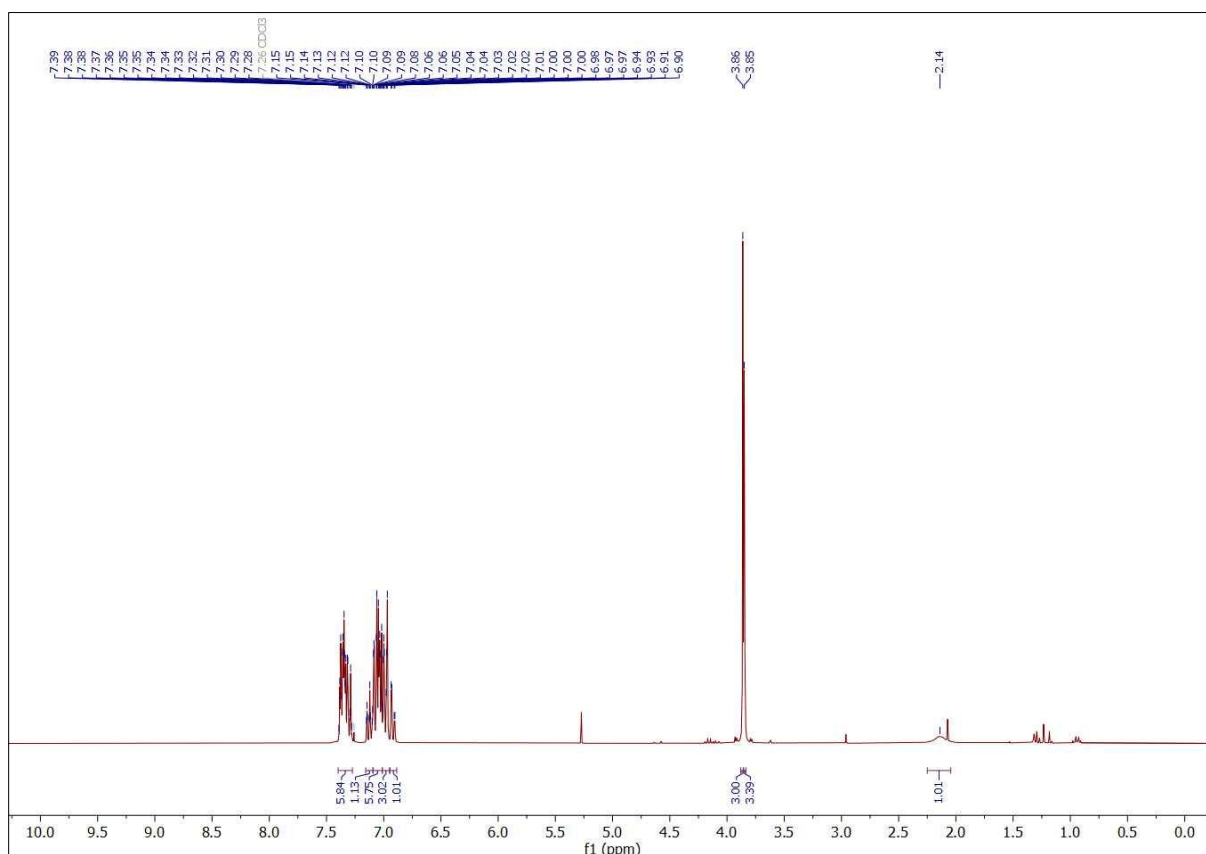
(3-Methoxy-4-phenoxyphenyl)methanamine (29).



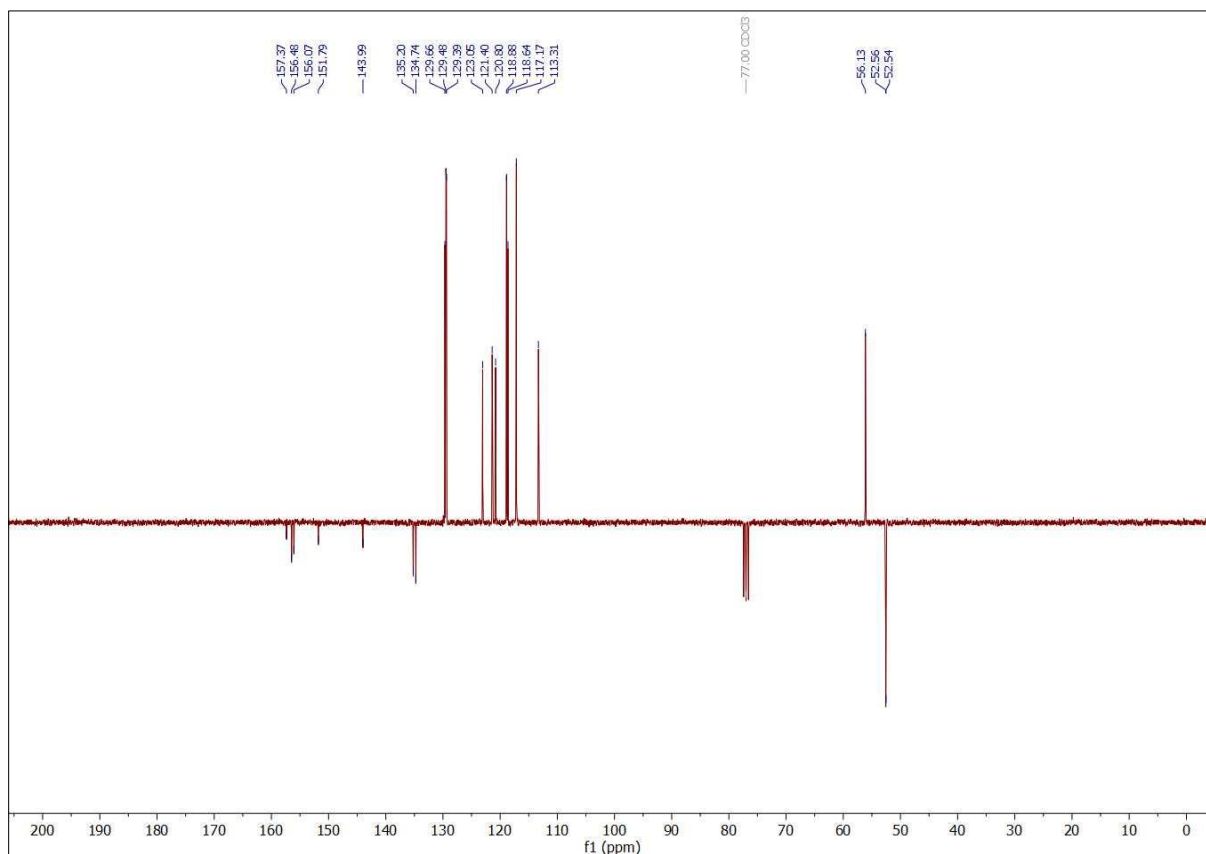
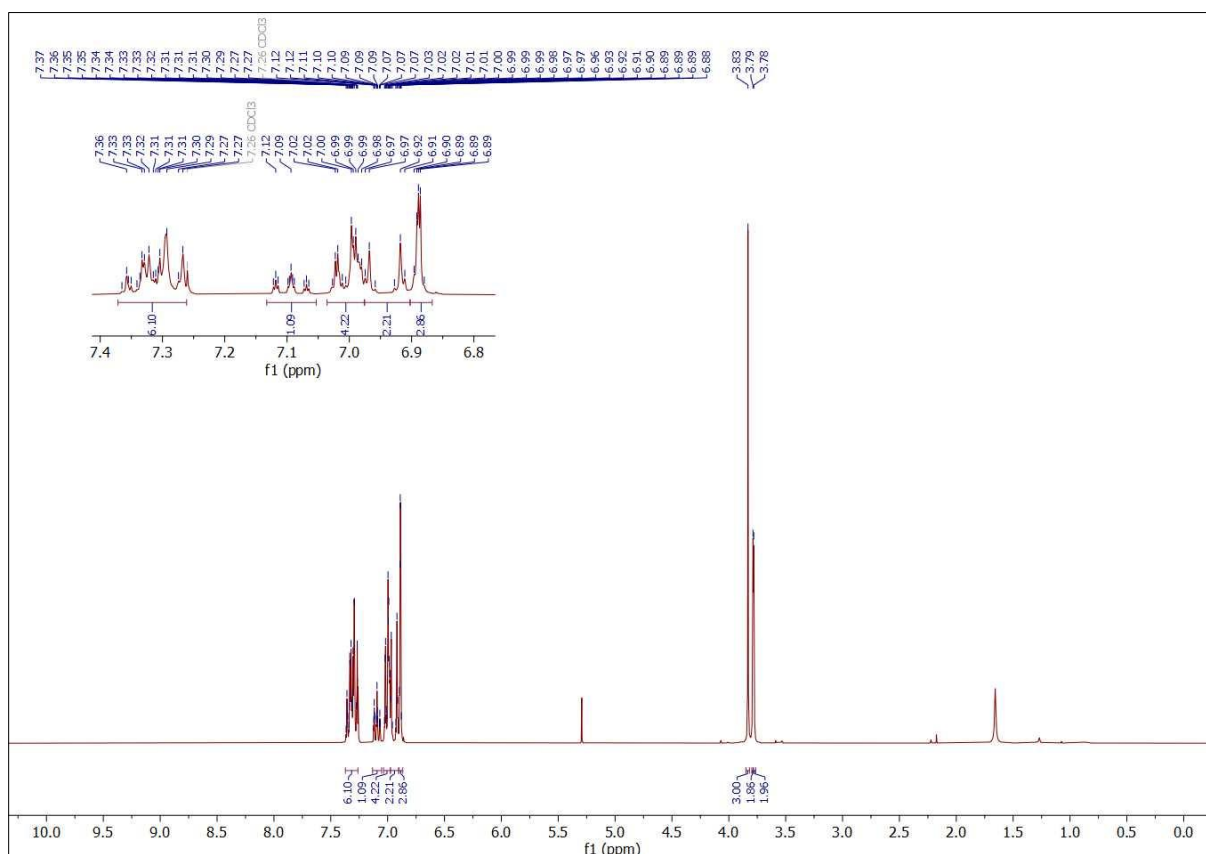
(4-Phenoxyphenyl)methanamine (30).



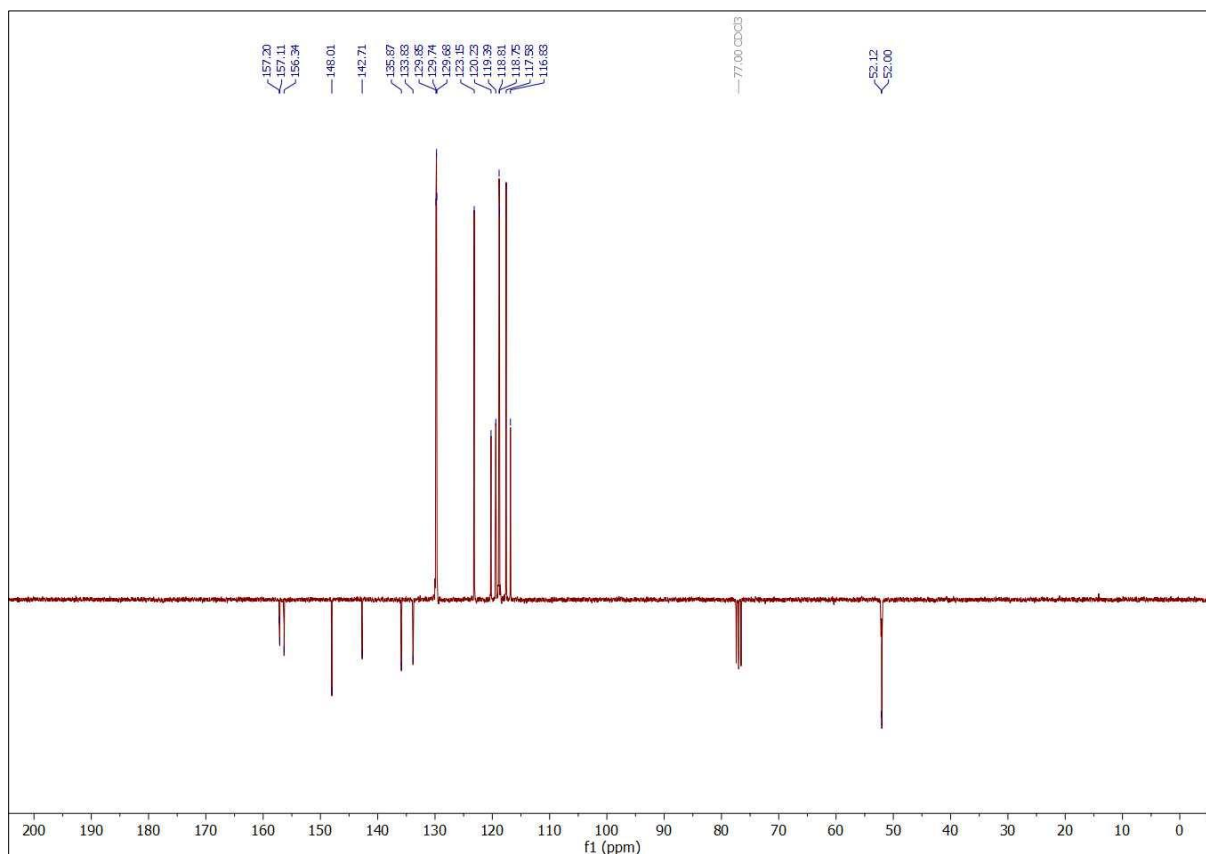
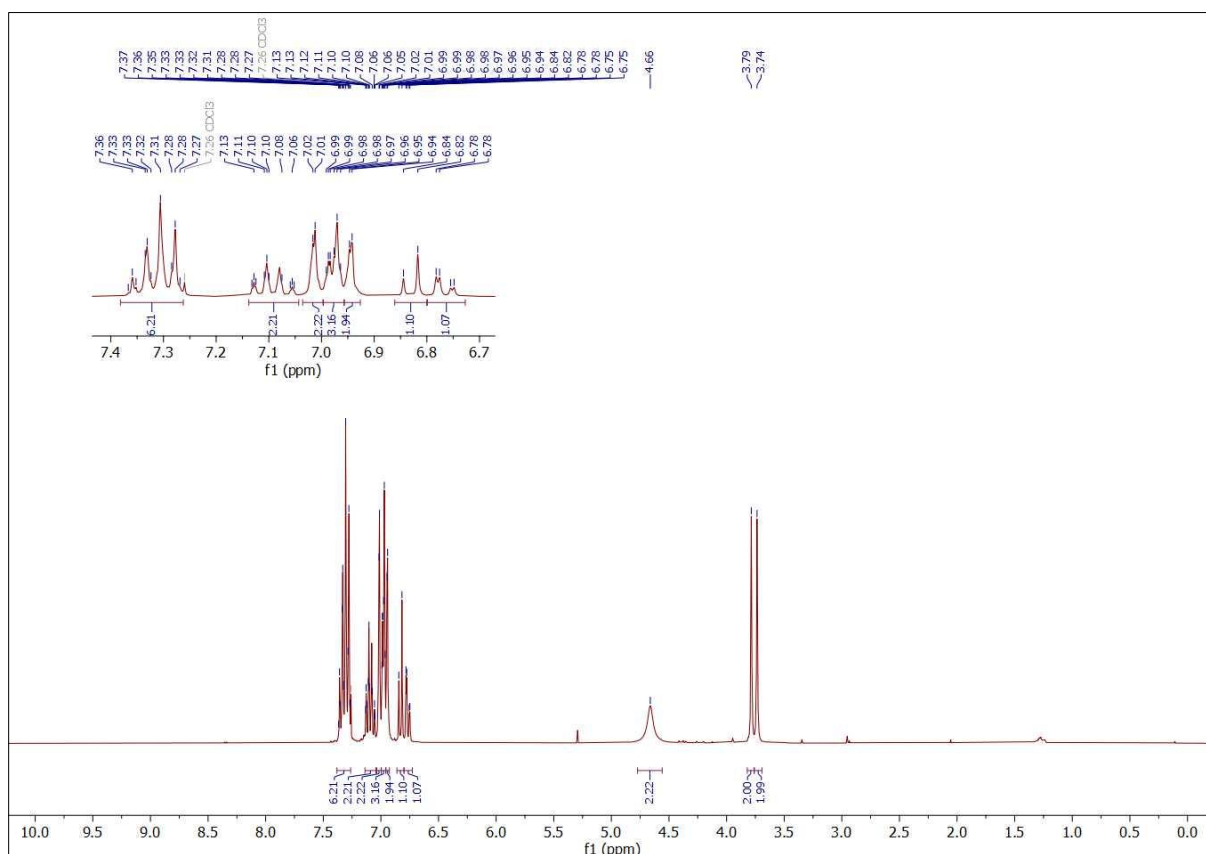
***N*-(3-Methoxy-4-phenoxybenzyl)-1-(4-phenoxyphenyl)methanamine (31).**



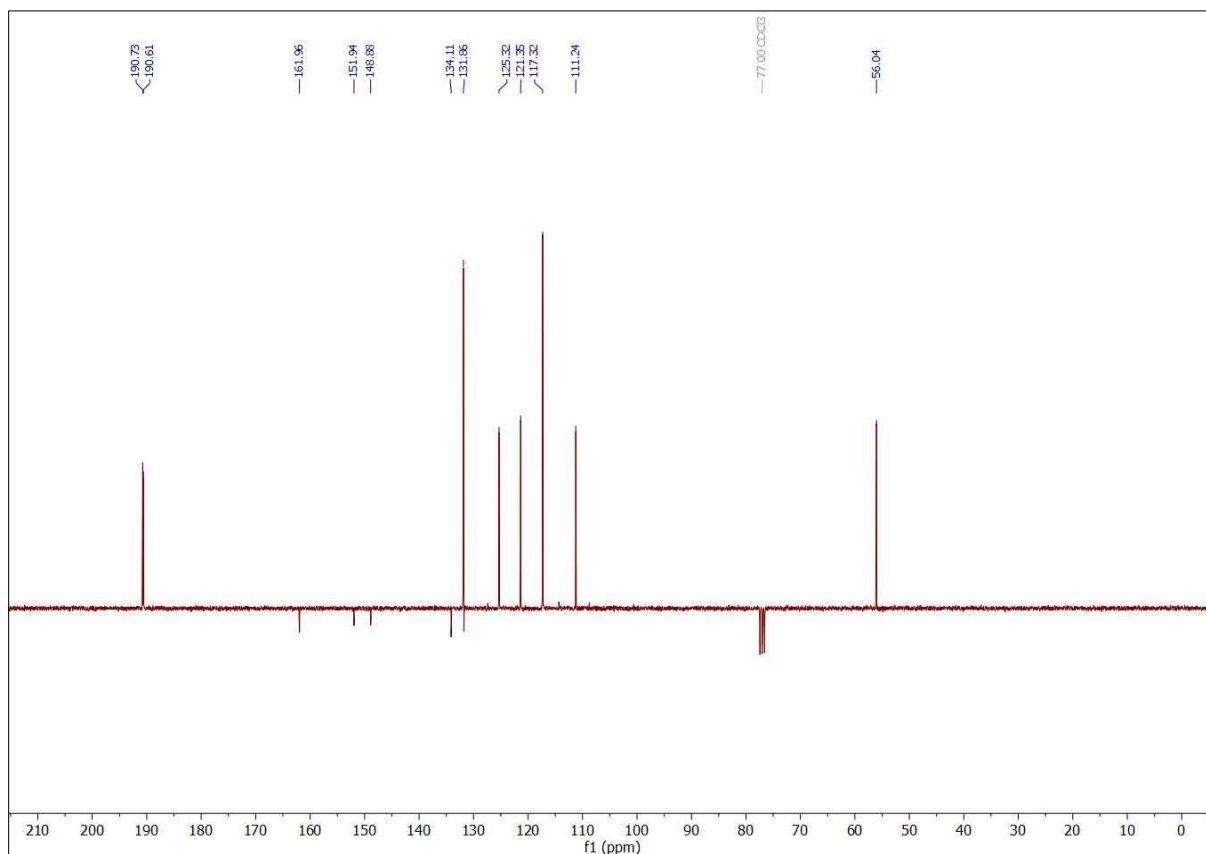
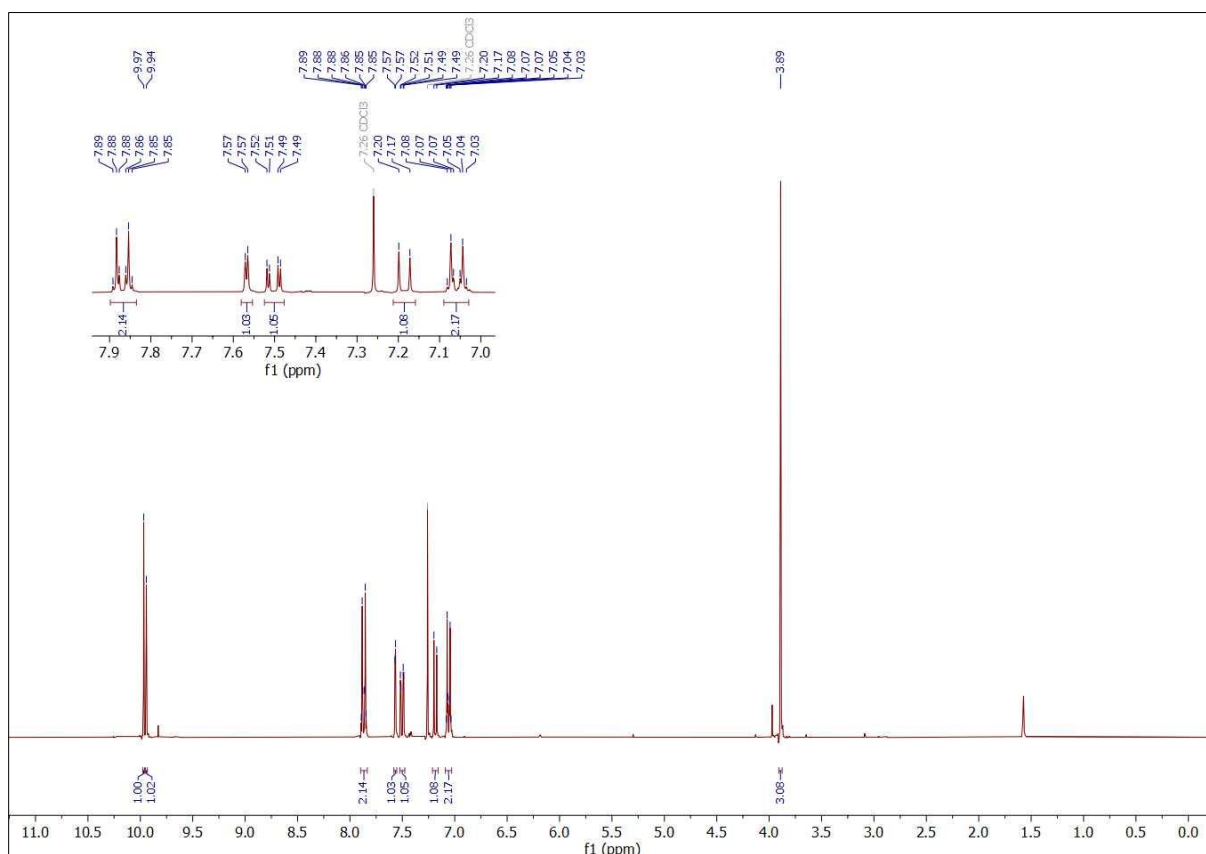
N-(4-(4-Chloro-2-methoxyphenoxy)benzyl)-1-(4-phenoxyphenyl)methanamine (32).



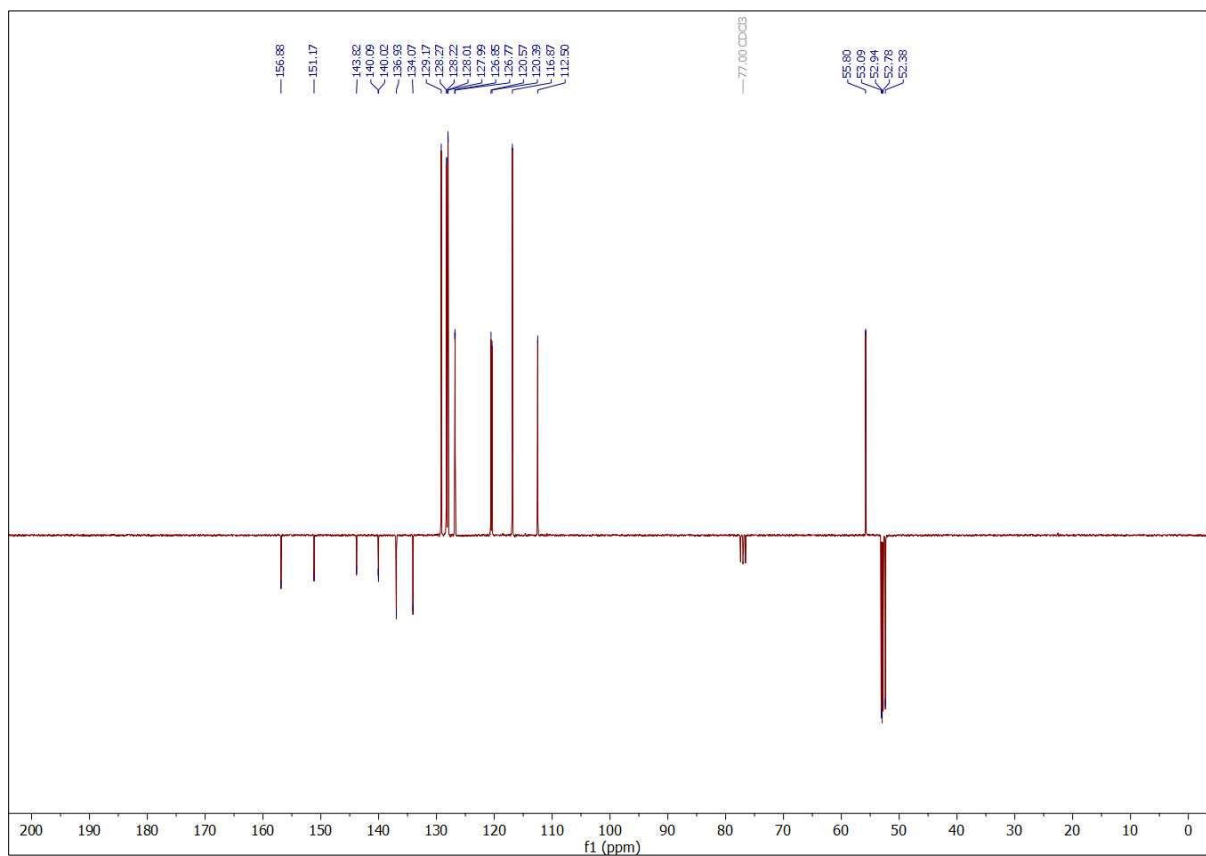
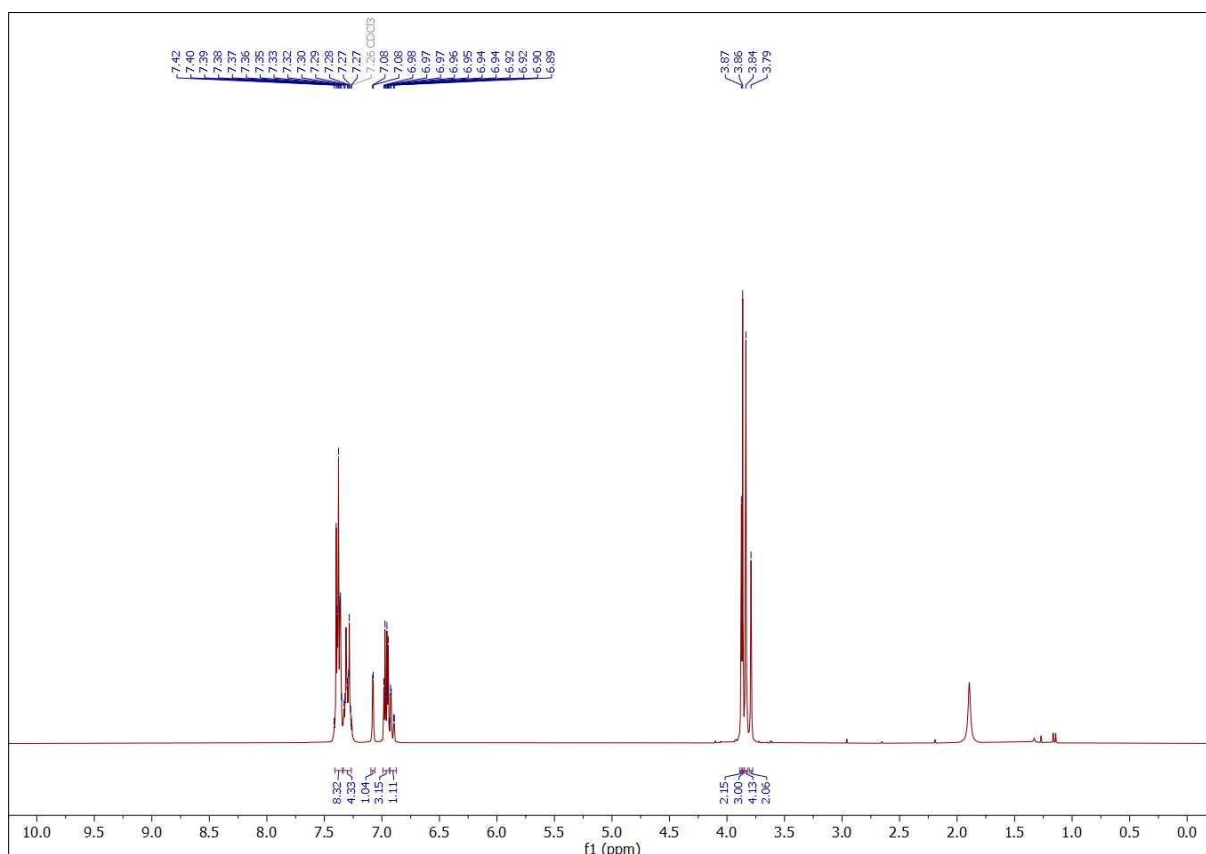
2-Phenoxy-5-(((4-phenoxybenzyl)amino)methyl)phenol (33).



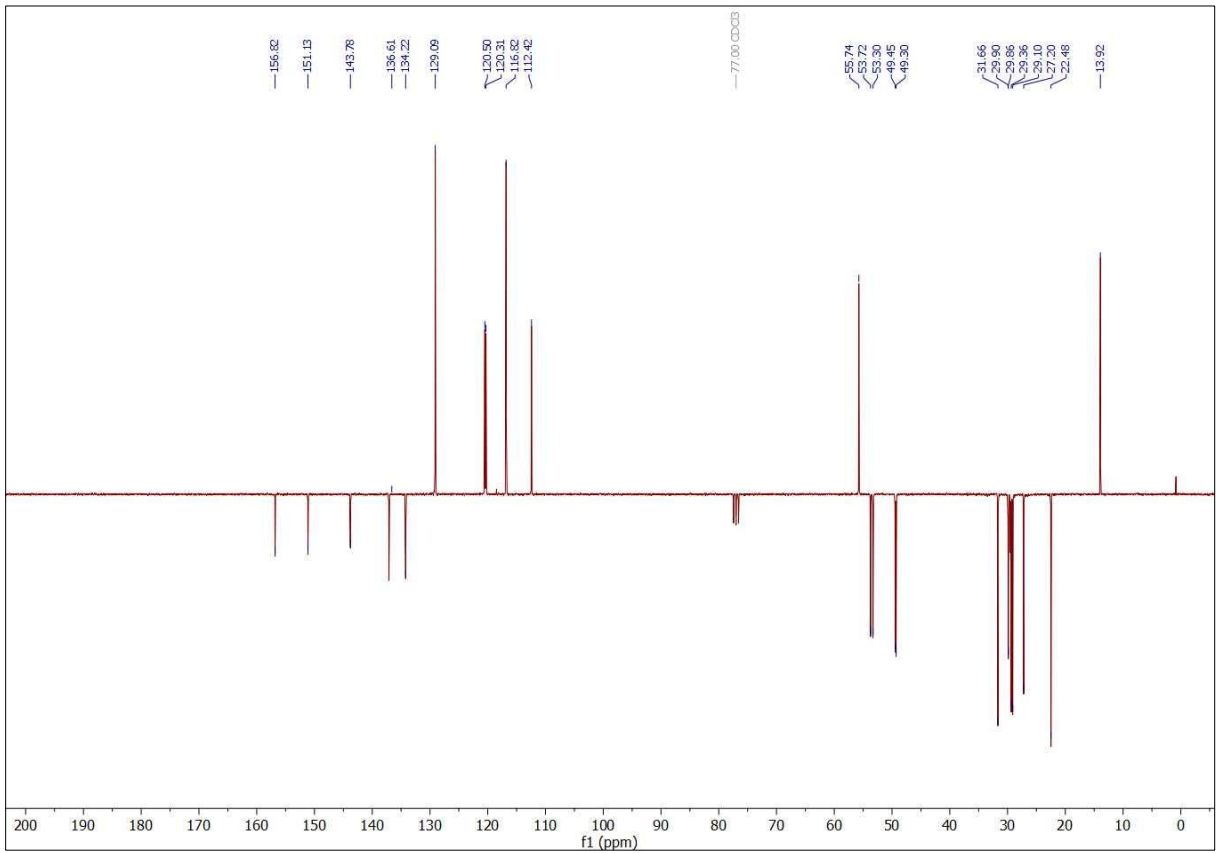
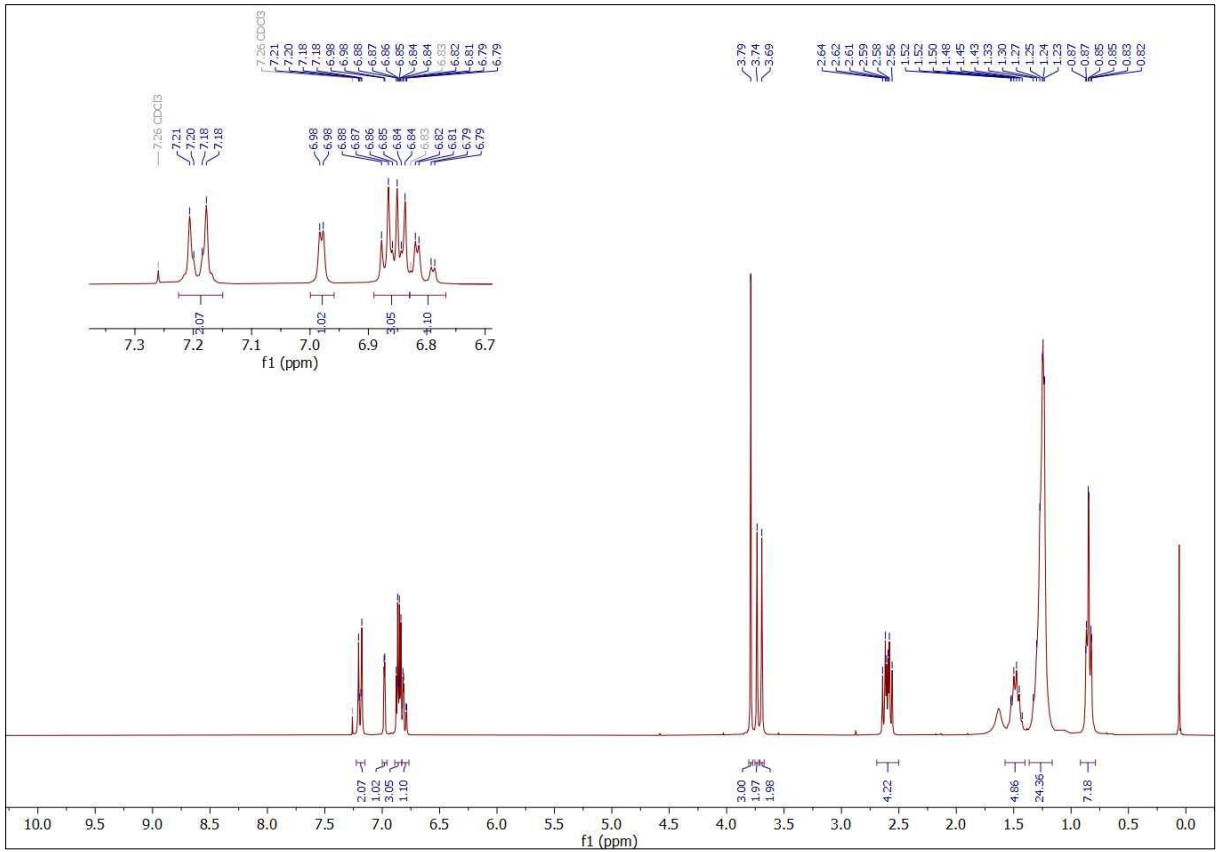
4-(4-Formylphenoxy)-3-methoxybenzaldehyde (35).



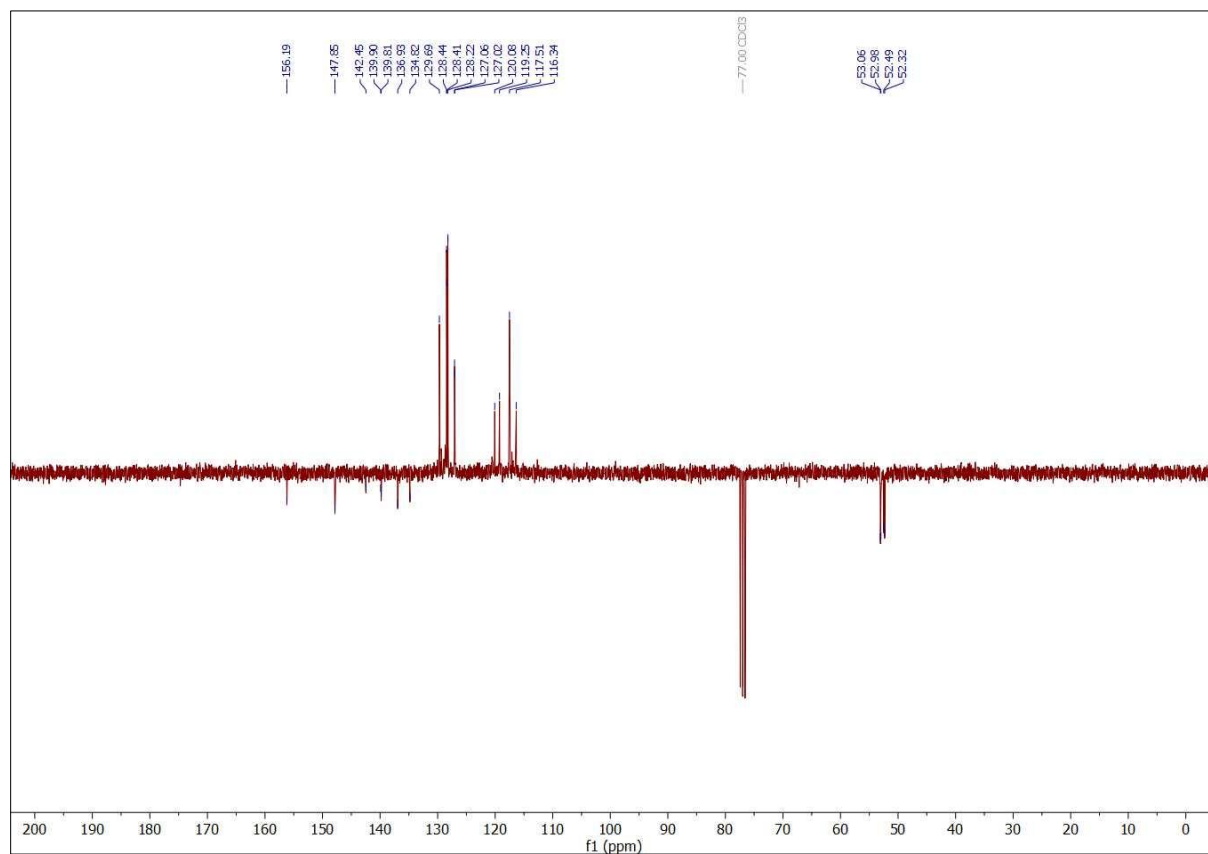
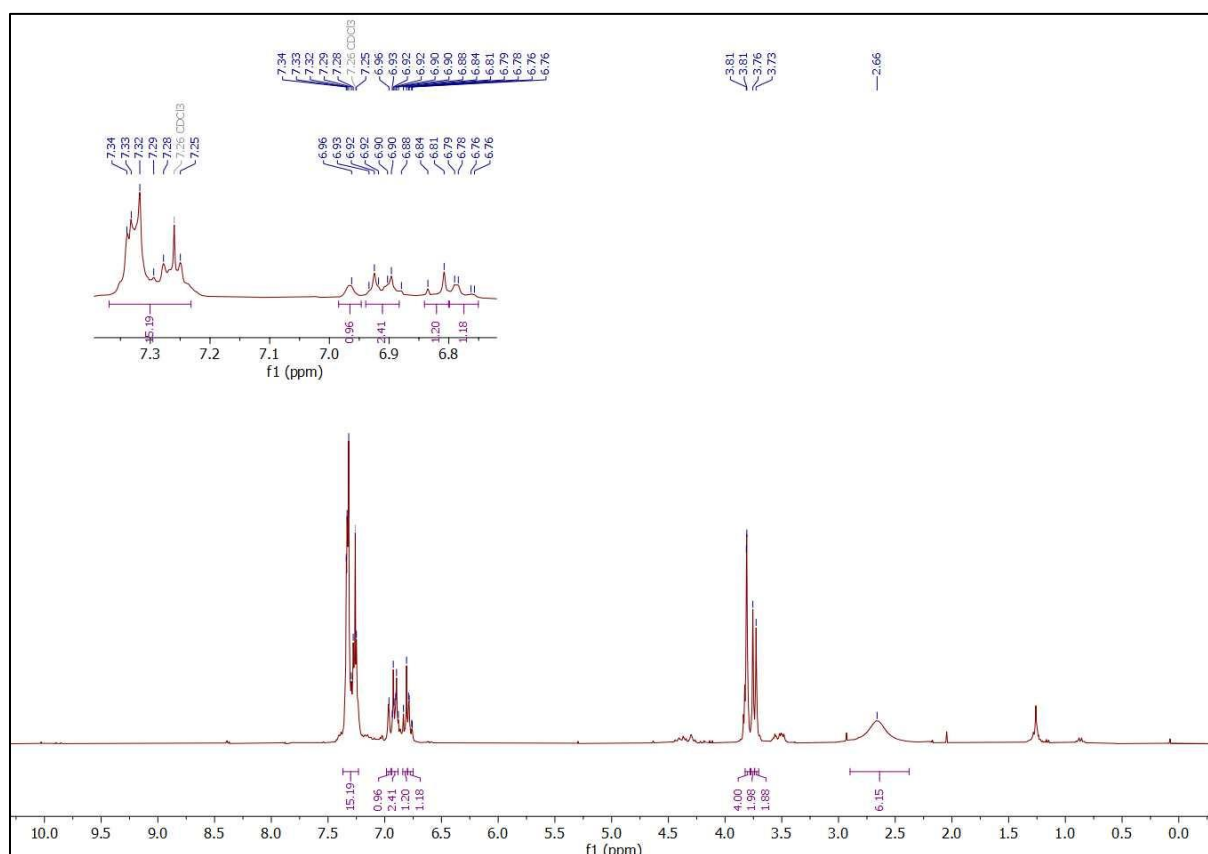
N-Benzyl-1-(4-(4-((benzylamino)methyl)-2-methoxyphenoxy)phenyl)methanamine (36).



***N*-(4-(2-Methoxy-4-((octylamino)methyl)phenoxy)octan-1-amine (37).**



5-((benzylamino)methyl)-2-(4-((benzylamino)methyl)phenoxy)phenol (38).



5-((octylamino)methyl)-2-(4-((octylamino)methyl)phenoxy)phenol (39).

